



UNIVERSITÄT
BAYREUTH

Department of Agroecosystem Research

Water use efficiency of rainfed and paddy rice ecosystem: Disentangling agronomic and ecosystem water use of rice

Dissertation to attain the academic degree of Doctor of Natural Science
(Dr. rer. nat.) of the Bayreuth Graduate School for Mathematical and
Natural Sciences of the University of Bayreuth

Submitted by
Bhone Nay-Htoon
Born 3rd April 1987 in Monywa, Myanmar

Bayreuth, 2016

This doctoral thesis was prepared at the department of Agroecosystem research, University of Bayreuth from September 2012 to June 2015 and was supervised by Prof. Dr. Christiane Werner.

This is a full reprint of the dissertation submitted to obtain the academic degree of Doctoral of Natural Sciences (Dr. rer. nat.) and approved by the Bayreuth Graduate School of Mathematical and Natural Sciences (BayNAT) of the University of Bayreuth.

Date of submission: July 30, 2015

Date of defense: January 26, 2016

Acting director: Prof. Dr. Stephan Kümmel

Doctoral Committee:

- (1) Prof. Dr. Christiane Werner (1st reviewer)
- (2) Prof. Dr. Christoph Thomas (2nd reviewer)
- (3) Prof. Dr. Thomas Köllner (Chairman)
- (4) Prof. Dr. Gerhard Gebauer

Summary

In the light of increasing pressure on limited fresh water resources, growing population and increasing greenhouse gas emission, maximizing crop water use becomes an important topic. Rice is a staple food for a large number of peoples and a crop with higher water demand. Water use efficiency of rice (*Oryza sativa* L) was studied from different viewpoints and at different spatiotemporal scales, which can markedly influence the information gain on different processes. Here, water use efficiency was assessed from a physiological, agronomic or ecosystem perspective, as well as at spatiotemporal scales comprising leaf level or ecosystem processes. The study sheds light on variations of different definitions and interpretation of water use efficiencies.

The work was carried out in two different rice ecosystems; rainfed rice and paddy rice, in Gwangju, South Korea. A variety of techniques were applied in this thesis to study different water use efficiency terms: the leaf gas exchange measurement, stable carbon isotope ($\delta^{13}C$) analysis, ecosystem gas exchange measurement (evapotranspiration and net carbon exchange), partitioning hourly to day-time evapotranspiration fluxes by stable water isotope ($\delta^{18}O$) approach, as well as partitioning daily to seasonal evapotranspiration (ET) fluxes by model simulation.

Stable water isotope ($\delta^{18}O$) based ET partitioning showed a significant role of the contribution of transpiration fluxes in the total water fluxes of rice ecosystem. Both $\delta^{18}O$ partitioning and partitioning by a modified Penman Monteith ET model ($56PM$) gave a similar trends of the contribution of transpiration to evapotranspiration (T/ET). Water fluxes from rainfed rice were mainly dominated by transpiration ($T/ET = 0.65$), while that of paddy rice was mainly driven by evaporation ($T/ET = 0.42$).

Comparing the water use efficiency of rainfed and paddy rice at different temporal and spatial scales indicated that physiologically defined water use efficiencies (i.e., leaf level intrinsic water use efficiency (A/g_s) and instantaneous water use efficiency (A/T) cannot represent the biomass related water use efficiencies (i.e., $WUE_{c_Abg/Tc}$ and WUE_{agro}). Physiologically defined WUE s, which include intrinsic WUE , instantaneous WUE and ecosystem WUE , of rainfed rice was higher than that of paddy rice. On the other hand, productivity based WUE s, which include biomass production per transpiration and grain yield per transpiration, paddy rice was higher than that of rainfed rice. Similar results were obtained when calculating integrated intrinsic

water use efficiency based on canopy integrated bulk leaves $\Delta^{13}C$ analysis. Thus, rainfed rice was more efficient, transpiring less water per assimilated carbon. On the other hand, considering productivity based *WUEs*, which include biomass production per transpiration and grain yield per transpiration, paddy rice was higher than that of rainfed rice, which was also reflected in its higher leaf area index (*LAI*) and slight, though not significant, higher grain yield.

At larger scales, partitioning the gross fluxes allows to disentangle the determining processes: considering total evapotranspirative water loss, which were 42.16 % lower rainfed rice, it had higher agronomic water use efficiency (55.42 %), in spite of only slightly lower grain yield compared to paddy rice. However, after partitioning the evapotranspiration into productive water loss (transpiration) and unproductive water loss (evaporation), transpiration efficiency, which is the ratio of grain yield per transpiration, was not different between paddy and rainfed rice. Thus, lower agronomic water use efficiency of paddy rice was in concert with its higher unproductive water losses. According to the seasonal trends of daily evapotranspiration fluxes, most of the unproductive water losses in paddy rice occurred before the crop development stage with low canopy cover. After the end of the crop development stage, evapotranspiration fluxes in both rainfed and paddy rice were similar, although slightly higher in paddy rice. Thus, minimizing the evaporation losses during the early crop growth stages of paddy rice system could increase the agronomic water use efficiency of paddy rice.

From the ecosystem point of view, if ecosystem water use efficiency is defined as the ratio of gross primary production to evapotranspiration, rainfed rice also had higher ecosystem water use efficiency (61.67 % higher) than paddy rice. Gross primary production is an important parameter to access the productivity (i.e., carbon gain), however, carbon loss through the ecosystem respiration process should not be neglected. Thus, when the respiratory carbon fluxes were taken into account (i.e., net ecosystem carbon exchange), ecosystem water use efficiency of both rainfed and paddy rice changed dramatically, pointing the role of ecosystem respiratory losses in the definition of ecosystem water use efficiency.

Comparing the agronomic and ecosystem water use efficiency of rainfed and paddy rice showed that rainfed rice had higher agronomic and ecosystem water use efficiency. However, higher water use efficiency of rainfed rice ecosystem comes at the expense of a slightly lower crop productivity and higher respiratory CO_2 loss mainly from the soils, which provides a source for greenhouse gas to the atmosphere.

Zusammenfassung

Der Optimierung der Wassernutzung von Nutzpflanzen kommt insbesondere im Hinblick auf den steigenden Druck auf bereits begrenzte Frischwasserressourcen, wachsender globaler Bevölkerung und zunehmender Treibhausgas Emissionen, eine immer stärkere Bedeutung zu. Reis ist ein Grundnahrungsmittel für einen großen Teil der globalen Bevölkerung und weist eine vergleichsweise hohe Wassernutzung auf. Die Wassernutzungseffizienz von Reis (*Oryza sativa* L) wurde bereits aus verschiedenen Blickwinkeln und auf unterschiedlichen räumlichen und zeitlichen Skalen untersucht, welche erheblichen Einfluss auf die gewonnenen Informationen nehmen kann. In dieser Arbeit, wurde die Wassernutzungseffizienz von Reis unter physiologischem, agronomischem und ökosystemarem Gesichtspunkt untersucht, zudem wurden verschiedene zeitliche und räumliche Skalen, von der Blatt- bis zu Ökosystemebene, untersucht. Dabei werden insbesondere die Unterschiede der verschiedenen Definitionen und Interpretationen von Wassernutzungseffizienz beleuchtet.

Die vorliegende Arbeit wurde in Gwangju Süd Korea, in zwei verschiedenen Reis Anbausystemen durchgeführt, Nass- sowie Trockenreis (regengespeist). Zur Untersuchung unterschiedlicher Wassernutzungseffizienz Definitionen wurden in dieser Studie zahlreiche Techniken angewendet: Gaswechselfmessungen auf einzelblatt und Bestandesebene zur Erhebung der Assimilation, Nettokohlenstoffaustausch sowie Transpiration und Evapotranspiration, Analyse stabiler Kohlenstoffisotope ($\delta^{13}C$) sowie die Auftrennung der Evapotranspiration (ET) in Bodenevaporation und Transpiration von stündlicher bis saisonaler Skala mittels stabiler Sauerstoffisotopen Analyse ($\delta^{18}O$) und model Simulationen.

Die Separierung der Evapotranspiration basierend auf stabiler Sauerstoffisotopen Analyse ergab eine signifikante Rolle des Transpirationsflusses für die Gesamtwasserabgabe des Ökosystems. Weiterhin stimmten beide verwendete Methoden, $\delta^{18}O$ Partitionierung und Modellierung basierend auf dem Penman Monteith Modell ($56PM$) weitestgehend überein. Insgesamt dominierten im Trockenreis Feld die Wasserverluste über Transpiration ($T/ET = 0.65$), während im Nassreis Feld die Bodenevaporation dominierte ($T/ET = 0.42$).

Vergleicht an die Wassernutzungseffizienz von Trocken- und Nassreis auf unterschiedlichen zeitlichen und räumlichen Skalen, konnte festgestellt werden, dass physiologisch definierte Wassernutzungseffizienzen (z.B. Blatt intrinsische WUE (A/g_s) und instantane WUE (A/T) nicht mit Biomasse abhängigen $WUEs$ vergleichbar sind (z.B. $WUE_{c_Abg/Tc}$ and WUE_{agro}).

Physiologisch definierte *WUEs*, wie intrinsische *WUE*, instantane und Ökosystem *WUE*, waren sämtlich höher in Trockenreis verglichen mit Nassreis. Andererseits, konnte Nassreis höhere *WUEs* basierend auf agronomischer Definition aufweisen, wie z.B. Biomasse Produktion pro Transpiration oder Kornertrag pro Transpiration. Ähnliche Ergebnisse wurden bei der Berechnung Kronen integrierter intrinsischer Wassernutzungseffizienz basierend auf stabiler Kohlenstoffisotopen Analyse ($\Delta^{13}C$) von Gesamtblattmasse erzielt. Trockenreis war demnach effizienter in seiner Wassernutzung, ausgehend von weniger Transpiration pro assimiliertem Kohlenstoff, während Nassreis insgesamt einen leicht höheren Ertrag aufwies und agronomisch definiert die höhere Effizienz aufwies.

Auf größerer Skala erlaubt die Auftrennung der Netto Kohlenstoff- und Wasserflüsse ein Verständnis der zu Grunde liegenden Prozesse: ausgehend von dem Gesamtwasserverlust des Systems (*ET*), der 42.16 % niedriger war, wies Trockenreis eine deutlich höhere Wassernutzungseffizienz als Nassreis auf (55.42 %), trotz des leicht niedrigeren Ertrags. Betrachtet man allerdings produktive und unproduktive Wasserverluste getrennt, so konnte gezeigt werden, dass die Transpirationseffizienz von Nass- und Trockenreis (GPP/T) sich nicht voneinander unterscheiden und die niedrigere agronomische Wassernutzungseffizienz auf Bestandesebene durch die hohen evaporativen Wasserverluste bedingt wurden. Der Großteil des unproduktiven Wasserverlusts im Nassreisfeld erfolgte dem saisonalen Evapotranspirationsverlauf zu Folge vor der Hauptwachstumsphase bei niedriger Kronendeckung. Im Gegensatz dazu, war die Evapotranspiration im Nass- und Trockenreis zum Ende der Vegetationsperiode, bei geschlossener Krone, ähnlich und nur wenig höher im Nassreis. Eine Minimierung der Evaporationsverluste während der frühen Entwicklungsphase des Nassreissystems könnte demnach zu einem deutlichen Anstieg der agronomischen Wassernutzungseffizienz von Nassreis führen.

Aus ökosystemarer Sichtweise, *WUE* definiert als GPP/ET , konnte ebenfalls gezeigt werden, dass die Wassernutzungseffizienz höher im Trockenreisfeld war (61.67 % höher). *GPP* ist ein wichtiger Parameter um Produktivität (Kohlenstofffixierung) zu ermitteln, allerdings muss dabei bedacht werden, dass auch die Atmung eines Ökosystems nicht vernachlässigt werden darf. Bei Einbeziehung der Ökosystem Atmung, $WUE=NEE/ET$, wies Nassreis eine höhere Wassernutzungseffizienz auf, da das Trockenreis Feld deutlich höhere Respirationsflüsse zeigte als das Nassreis Feld. Dies zeigt die Bedeutung auch der Ökosystem Atmung für die ökosystemisch definierte Wassernutzungseffizienz.

Vergleicht man agronomisch und ökosystemare Wassernutzungseffizienz von Trocken- und Nassreis, konnte gezeigt werden, dass Trockenreis höhere *WUEs* nach beiden Definitionen aufwies. Dies geht allerdings zu Lasten leicht geringeren Ertrages und höherer Respirationstranspirationsverluste, hauptsächlich durch Bodenatmung, welche eine Rolle für Treibhausgasproduktion spielen.

Acknowledgements

I do thanks to all who helped me throughout this exciting PhD life.

First, my special thanks go to Prof. Dr. Christiane Werner, my supervisor. I am indebted to her for her personal and scientific supports. She let me experience the “REAL” PhD life and make my stay in Bayreuth meaningful.

I do thanks to Prof. Dr. John Tenhunen for letting me be part of the TERRECO family. This study could not be done without his enthusiasm on the research, moral supports and leadership.

Many thanks to my mentors and advisors, Prof. Dr. Gerhard Gabauer, Prof. Dr. Jonghan Ko, Dr. Maren Dubbert, for their guidance, critiques, ideas and comments concerning the field experiment, research design and data analysis and many more.

Without the help of Prof. Ko and without his UAV, our field experiment in Gwangju is impossible. His supports on NDVI data analysis and crop modelling are also acknowledged.

Special thanks go to the “R guys” who helped me out with R-programming and Statistics. Thanks a lot, David, Gwanyong, Hamada and Kwanghun. Your suggestions and comments are valuable.

I am very thankful to our lab technicians, Margarete Wartinger and Ilse Thaufelder for their supports in the lab. I also thanks to Sandra Thomas, Sabine Glauer and Dr. Bärbel Heindl-Tenhunen for their helps with administrative works.

I do thanks to all of TERRECO members and friends for creating a lovely and exciting working atmosphere. TERRECO Stammtish, Karaoke and Wallenfels nights are unforgettable! Special thanks go to Xue Wei and Steve, who work, discuss and have fun together! Thanks a lot for the friendship and supports!

I am grateful to Seung Hyun, Seungtaek, Toncheng, Mijeong, Jinsil, Yongdoo, Fabian, Niko and Yannic, for their helps in the field.

Finally, I do thanks to my parents who always support me and always believe in me. Thanks, Mom and Dad!

Bhone Nay-Htoon

July, 2015, Bayreuth

Grant information

This study was supported by Deutsche Forschungsgemeinschaft (DFG), as an activity of the Bayreuth Center for Ecology and Environmental Research (BayCEER) in the context of the International Research and Training Group TERRECO: Complex Terrain and Ecological Heterogeneity (GRK 1565/1) at the University of Bayreuth, Germany and by the Korean Research Foundation (KRF) at Kangwon National University, Chuncheon, South Korea.

Contents

Summary	i
Zusammenfassung	iii
Acknowledgements	vi
Grant information	vii
Contents	viii
List of Figures	xi
List of Tables	xv
Symbols and Abbreviations	xvii
Definitions of different water use efficiencies	xxii
I.	Introduction	1
1.1	Rice production under global change	1
1.1.1	Rice (<i>Oryza sativa</i> L.).....	1
1.1.2	Rice and global change	2
1.2	Water use efficiency	7
1.3	Productive and unproductive water use partitioning evapotranspiration.....	11
1.4	Objectives	14
1.5	Outline of the thesis	15
II.	Materials and Methods	18
2.1	Study site.....	18
2.2	Environmental variables	20
2.3	Crop growth and development.....	21
2.3.1	<i>LAI</i> and biomass measurements.....	21
2.3.2	High resolution remote sensing for <i>NDVI</i> of rice fields	22
2.3.4	Estimation of daily <i>NDVI</i> , <i>LAI</i> and crop yield.....	23
2.4	Canopy gas exchange measurements.....	23
2.5	Estimation of evapotranspiration of rice field	24
2.6	Estimation of daily carbon exchange of rice field	25

2.7	Partitioning evapotranspiration.....	26
2.7.1	Partitioning diurnal <i>ET</i> fluxes by $\delta^{18}O$ isotopes	26
2.7.2	Daily <i>ET</i> partitioning	29
2.8	Crop water use efficiency of rice	30
2.8.1	Leaf water use efficiency	31
2.8.2	Ecosystem and canopy water use efficiency.....	32
2.8.3	Agronomic water use efficiency	32
2.9	Statistical Analysis.....	33
III.	Environmental condition and crop growth	37
3.1	Meteorological conditions of the study site	37
3.1.1	General meteorological conditions	37
3.2	Crop growth and development of rainfed and paddy rice.....	39
3.2.1	<i>LAI</i> , plant height and biomass development	39
3.2.2	Crop yield and Yield components.....	42
3.3	Summary	43
IV.	Model development for evapotranspiration	44
4.1.	Estimation of evapotranspiration	44
4.1.1	Reference crop <i>ET</i> (<i>ET₀</i>).....	45
4.1.2	Performance of different <i>ET₀</i> models	49
4.2	Crop coefficients	50
4.2.1	Basal crop coefficient (<i>K_{cb}</i>): The <i>FAO</i> recommended <i>K_{cb}</i>	50
4.2.2	Basal crop coefficient (<i>K_{cb}</i>): <i>NDVI</i> derived <i>K_{cb}</i>	52
4.2.3	Evaporation coefficient: <i>K_e</i>	52
4.2.4	Crop coefficients of rainfed and paddy rice.....	54
4.3	Evapotranspiration estimation by three different models	57
4.4	Summary	60
V.	Partitioning evapotranspiration	61
5.1	Partitioning seasonal <i>ET</i> by modelling approach.....	61
5.1.1	Estimation of daily canopy transpiration	61
5.1.2	Partitioning daily evapotranspiration.....	62

5.2 Partitioning daytime ET by $\delta^{18}O_{ET}$ approach.....	67
5.2.1 $\delta^{18}O$ of precipitation	67
5.2.2 Volumetric soil water content, soil temperature and $\delta^{18}O$ of soil water.....	68
5.2.3 Measured $\delta^{18}O_{ET}$, modelling $\delta^{18}O_E$, $\delta^{18}O_T$ and partitioning ET	71
5.3 Comparing $\delta^{18}O$ and PM derived fraction of T to ET (T/ET).....	74
5.4 Summary	75
VI. Water use efficiency of rainfed and paddy rice.....	76
6.1. Water use efficiency from the physiological point of view	76
6.1.1 Short term Leaf water use efficiency (WUE_l).....	76
6.1.2 Integrated leaf water use efficiency	79
6.1.3 Integrated canopy water use efficiency (WUE_{c-intg})	82
6.2 Agronomic water use efficiency	84
6.3 Ecosystem water use efficiency	85
6.3.1 Carbon and water exchange in rainfed and paddy rice	85
6.3.2 Ecosystem water use efficiency of rainfed and paddy rice.....	87
6.4 Summary	91
VII. Discussion and outlook	92
7.1 Evapotranspiration estimation methods	92
7.2 Partitioning Evapotranspiration	94
7.3 Water use efficiency concepts	97
Definition of ecosystem water use efficiency (WUE_{eco}).....	98
7.4 More crop per drops.....	99
References.....	104
List of publication.....	124
Curriculum Vitae	126
Versicherungen und Erklärungen	127

List of Figures

Figure I-1 Rice production area (Source: International Rice Research Institute [IRRI], 2014) 2

Figure I-2 Physical and economic water scarcity worldwide (Physical Water scarcity: water resources development is approaching or has exceeded sustainable limits; Approaching to physical water scarcity: these areas will experience physical water scarcity in the near future; Economic water scarcity: these areas are suffering water scarcity due to human, financial and institutional limitations although natural water resources are abundant relative to water use; Little or no water scarcity: Abundant water resources relative to use) (Source: Comprehensive Assessment of Water Management in Agriculture, 2007)..... 4

Figure I-3 Water use efficiency at different temporal and spatial scale. WUE_i is intrinsic water use efficiency; A is photosynthetic CO_2 assimilation; g_s is stomatal conductance; T is transpiration, WUE_c is canopy water use efficiency; A_c is canopy photosynthetic CO_2 assimilation; T_c is canopy transpiration; TBM is total dry biomass; Biomass is dried biomass of interest; $Yield$ is the yield of biomass of interest, i.e., grain yield in the case of rice; ET is evapotranspiration; NEE is net ecosystem CO_2 exchange; GPP is gross primary CO_2 exchange. When a WUE equation is written directly on the dashed line, that WUE equation is commonly used to calculate for both temporal and spatial scales directly above and below the dashed line (Adapted from Kuglitsch et al., 2008). 8

Figure I-4 CO_2 exchange in a vegetation system. NEE is net ecosystem CO_2 exchange which is the net flux of respiratory and photosynthetic CO_2 exchange; R_{eco} is ecosystem respiration which is the net flux of plant and soil respiration; GPP is gross primary production or the photosynthetic CO_2 assimilation of the vegetation system..... 11

Figure I-5 $\delta^{18}O$ values of water pool and fluxes in the Soil-Plant-Atmosphere Continuum. δ_p is $\delta^{18}O$ of precipitation; δ_s is $\delta^{18}O$ of soil water; δ_γ is $\delta^{18}O$ of ground water; δ_E is $\delta^{18}O$ of soil evaporation; $\delta_{L,b}$ is $\delta^{18}O$ of bulk leaf water; δ_x is $\delta^{18}O$ of xylem water; δ_T is $\delta^{18}O$ of transpiration and δ_v is $\delta^{18}O$ of atmospheric water vapor (Zhang et al., 2010)..... 13

Figure II-1 Study site location: (a) Location of Gwangju; (b) Experimental site location in the Chonnam National University research farm, Gwangju, South Korea. ($35^\circ 10' N$, $126^\circ 53' E$, alt. 33m). 18

Figure II-2 Planting of paddy and rainfed rice: (a) Germination of paddy rice in the nursery trays; (b) Ready to be transplanted paddy rice seedlings in the nursery; (c) Manual puddling and leveling before the transplanting of paddy rice; (d) Machine transplanting of paddy rice; (e) Gap filling in the paddy rice field after the machine transplanting; (f) Single row direct

seeder used for rainfed rice seeding; (g) direct seeding of rainfed rice; (h) pre-emergence herbicide application in the rainfed rice field20

Figure II-3 Remote sensing with Unmanned Aerial Vehicle. (a) Miniature Multiple Camera Array (Mini MCA) with 450, 550, 650, 800, 830, and 880 nm bands and 10 cm ground resolution at 300 m altitude; (b) mini MCA mounted on the UAV; (c and d) real time quality control of the remote sensing pictures; (e) Calibration plates (black, gray and white); (f) NDVI data sampling points (yellow for rainfed rice and green squares for paddy rice) and remote sensing data evaluation points (soil (light orange circle), crop (white circle), cement (gold circle) and asphalt (dark orange circle)).....22

Figure III-1 Meteorological conditions during monsoon 2013. (a) daily averages of wind speed (ms^{-1}) and relative humidity (%); (b) daily averages of air temperature ($^{\circ}\text{C}$) and radiation ($\text{Mj m}^{-2} \text{d}^{-1}$); (c) daily total rainfall (mmd^{-1}) and daily average volumetric soil water content at 5cm depth ($\text{m}^3 \text{m}^{-3}$). *Note:* Volumetric soil water content data is not available starting from the day of year 221 as the volumetric soil water sensors were uninstalled from the site of study, to ship back to Bayreuth.38

Figure III-2 Seasonal leaf area index, crop growth and development of (a) rainfed and (b) paddy rice. Crop growth stages were classified according to International Rice Research Institute (IRRI) and Food and Agricultural Organization (FAO). IRRI classified rice crop growth as vegetative, reproductive and maturity stages while FAO classified Initial stage (IS), Crop development (CD), Mid-Season (MS) and Late-Season (LS) stages. Numbers above the pictures were day of year of photo-shoot.....41

Figure III-3 Biomass distribution of rainfed and paddy rice. Biomass sampling was done during the late season stage. ($n=3 - 8, \pm\text{SD}$).....42

Figure IV-1 NDVI derived basal crop coefficient (K_{cb}) of paddy and rainfed rice at different crop growth stages: (a) rainfed rice; (b) paddy rice; $0.5 \times 0.5 \text{ m}^2$ ground resolution.55

Figure IV-2 Daily crop coefficients of paddy and rainfed rice: (a) Transpiration coefficient or basal crop coefficient, K_{cb} ; (b) Evaporation coefficient, K_e56

Figure IV-3 Comparison of measured ET versus estimated ET by different estimation methods. ($n=6$). The models used for panel a-h are provided in table 4.3, together with statistics.58

Figure V-1 Canopy transpiration of rainfed and paddy rice modelled by the original PM (Monteith 1956) (net radiation intercepted by canopy as radiation input) and the FAO 56 dual crop coefficient ($K_{cb} \times ET_0$) (Allen, 1998).61

Figure V-2 Daily evapotranspiration (black line), canopy transpiration (green dashed line) and evaporation (blue dotted line) of rainfed rice (a) and paddy rice (b). (n=3, \pm SD)..... 63

Figure V-3 Daily precipitation (dark blue columns), $\delta^{18}O$ of rainwater (light blue cycle) and extracted soil water (white triangle), (n=3 - 8, mean values \pm SD) (b) Daytime VPD (dotted line) and soil water content (thick blue line). 68

Figure V-4 Profile of volumetric soil water content at different depths, 5, 10, 30, 60 cm (SWC, blue line with blue circle, n=3, mean values \pm SD), soil temperature (T_{soil} , dotted line with red circle, n=3, mean values \pm SD and soil $\delta^{18}O$ ($\delta^{18}O_s$, black line with black circle, n=3, mean values \pm SD) of rainfed rice field on DOY 172, 182, 192, 202, 206 and 218. 70

Figure V-5 CRDS based measured $\delta^{18}O$ of baresoil plot, $\delta^{18}O_E$ against modelled $\delta^{18}O_E$. $\delta^{18}O_E$ measurements were carried out on DOY 177, 193, 199, 207, and 220, at 12:00, 14:00 and 18:00 hours. Modled $\delta^{18}O_E$ was calculated based on measured $\delta^{18}O$ of soil water at 5 cm ($\delta^{18}O_s$), measured $\delta^{18}O$ of ambient air ($\delta^{18}O_a$), soil temperature at 5 cm, air temperature, relative humidity and soil water content data of the day of interest. 72

Figure V-6 CRDS based measured ET , $\delta^{18}O_{ET}$ (a,e,i,m,q,u, white cycle = $\delta^{18}O_{ET}$, blue diamond = ET , n=3, mean values \pm SD), modelled $\delta^{18}O_E$ and $\delta^{18}O_T$ (b,f,j,n,r,v, black line = $\delta^{18}O_E$, dashed line = $\delta^{18}O_T$), diurnal contribution of T to ET (f_t) (c,g,k,o,s,w). Each panel represents to day of year 172, 182, 192, 202, 205 and 218 respectively..... 73

Figure V-7 T/ET of rainfed rice derived by stable water isotope approach (dark green circles) and 56PM approach (line). T/ET ($\delta^{18}O$) was the average f_t calculated for 12:00, 14:00 and 18:00 hour of the respective day (n=3 \pm SD, be noted that the value is the mean of 3 different measurement times of the day) while T/ET (56PM) was the daily T/ET 74

Figure VI-1 Instantaneous water use efficiency ($inWUE$) of rainfed and paddy rice (n=3 to 6 \pm SD for each growth stages). The instantaneous water use efficiency was calculated as the ratio of maximum assimilation to transpiration (A_{max}/T). A_{max} was the maximum assimilation and T was the transpiration of the uppermost rice leaf. Both A_{max} and T were measured under 1500 $\mu\text{molm}^{-2}\text{s}^{-1}$ PAR and 400 μmolmol^{-1} CO₂ and A_{max} (black for paddy and white for rainfed rice) and T (straight line for paddy and dashed line for rainfed rice) were provided in the small panel..... 77

Figure VI-2 Correlations between (a) Maximum assimilation (A_{max}) and stomatal conductance to H₂O (g_s) of rainfed (black circles) and paddy rice (white circles) measured at the uppermost flag leaves under the controlled environment 1500 $\mu\text{molm}^{-2}\text{s}^{-1}$ PAR, 400 PPM CO₂; (b) Maximum assimilation (A_{max}) and Transpiration (T) of rainfed (black circles) and paddy rice (white circles) leaves; (c) Instantaneous WUE ($inWUE$) and V_{cmax}/g_s . All the measurements were done during Initial, Crop development, Mid-season and Late season stages. 79

Figure VI-3 $\delta^{13}C$ carbon isotope discrimination ($\Delta^{13}C$) of rainfed and paddy rice aboveground biomass harvested at different growth stages: (a) $\Delta^{13}C$ discrimination of rainfed rice (white circle) and paddy rice (black circle) correlated to the sum of the precipitation recorded within 10 days before the leaf biomass harvest (b) $\Delta^{13}C$ of rainfed rice (white circle) and paddy rice (black circle) followed the same seasonal trend although rainfed rice had lower carbon isotope discrimination (n=3 - 12, \pm SD).....81

Figure VI-4 Growth stage integrated intrinsic water use efficiency ($WUE_{i-\delta^{13}C}$, light green for rainfed and dark green for paddy rice) and instantaneous water use efficiency ($inWUE_{\delta^{13}C}$, white for rainfed and black for paddy rice). Growth stage integrated WUE_i was calculated based on measured $\Delta^{13}C$ isotope values of bulk leaves harvested at different growth stages. Growth stage integrated $inWUE$ was calculated by multiplying the $\Delta^{13}C$ derived integrated WUE_i with growth stage average atmospheric VPD (n=3 to 12 \pm SD).....82

Figure VI-5 Growth stage integrated canopy water use efficiency ($WUE_{c-Abg/Tc}$) of rainfed rice (white) and paddy rice (black); n=3 - 6 \pm SD. $WUE_{c-Abg/Tc}$ was calculated as the ratio of dry weight of above ground biomass harvested at a specific growth stage to the integrated daily canopy transpiration of the same growth stage.....83

Figure VI-6 Agronomic water use efficiency ($WUE_{agro} = Grain\ yield/ET$) and transpiration use efficiency ($TE = Grain\ yield/T$) of rainfed and paddy rice. Both T and ET were calculated as the sum of daily T , and ET of the whole crop season (i.e., 120 days) (n= 12, \pm SD)85

Figure VI-7 Daily carbon fluxes of paddy and rainfed rice: (a) paddy rice; (b) rainfed rice (simulated gross primary production, blue line; measured gross primary production, white circle; simulated ecosystem respiration, red dashed-line; measured ecosystem respiration, white triangle; simulated net ecosystem exchange, black dotted line; chamber measured net ecosystem exchange, black circle); n=3 \pm SD.87

Figure VI-8 Comparing ecosystem water use efficiency of rainfed and paddy rice to highlight the importance of evaporation and ecosystem respiration in the definition of WUE_{eco} ; n=12 \pm SD88

Figure VII-1 $\delta^{18}O$ values of source water (rain) and fluxes in the Soil-Plant-Atmosphere Continuum of the rainfed rice field. $\delta^{18}O_{rain}$ is $\delta^{18}O$ of precipitation; $\delta^{18}O_{soil}$ is $\delta^{18}O$ of soil water; $\delta^{18}O_E$ is $\delta^{18}O$ of soil evaporation; $\delta^{18}O_L$ is $\delta^{18}O$ of bulk leaf water; $\delta^{18}O_T$ is $\delta^{18}O$ of transpiration and δ_v is $\delta^{18}O$ of atmospheric water vapor97

Figure VII-2 Spatial and temporal variation of the different $WUEs$ of rainfed and paddy rice98

Figure VII-3 Seasonal carbon and water balance of paddy and rainfed rice. Measured and simulated daily gross primary production (*GPP*), net ecosystem exchange (*NEE*), ecosystem respiration (*R_{eco}*), evapotranspiration (*ET*), transpiration (*T*) and grain yields were used in this schematic representation. All flux data and grain yield are mean values (flux data: $n=3 \pm SD$; grain yield: $n=6 \pm SD$). Crop growing season was 120 days (sowing to harvest)..... 100

List of Tables

Table I-1 Some of the conventional and water saving rice production systems and their crop management practices 6

Table II-1 Soil chemical and physical properties of study area, Chonnam National University research farm, Gwangju, S. Korea. 19

Table II-2 Field measurements campaigns carried out in 2013. 34

Table II-3 Different water use efficiency calculation methods applied in this study 35

Table II-4 Different water use efficiency calculation methods applied in this study (Continued) 36

Table III-1 Measured mean leaf area index and plant height of rainfed and paddy rice ($n=6 \pm SD$) 39

Table III-2 Statistics for yield components and grain yield of rainfed and paddy rice ($n=3$ to $8, \pm SD$). Wilcoxon-Mann-Whitney Rank Sum test was performed to test the differences between rainfed and paddy rice. *W* and *p* are test statistics of Wilcoxon-Mann-Whitney Rank Sum test. 43

Table IV-1 Correlation coefficient between conventional reference crop evapotranspiration (*ET₀*, grass as reference crop) models and *ET₀* model modified specifically for rice (healthy, well-irrigated rice as reference crop). *R²* is determination of coefficients, *SE* is standard error, *SD* is standard deviation, *p* (t-test) is level of significant of the test, *ET₀* ratio is the ratio of rice crop *ET₀* and grass reference crop *ET₀*, and Ranking is model performance ranked according to the ratio of *m56PM_{mrc} ET₀* to other *ET₀*..... 50

Table IV-2 The *FAO56* recommended basal crop coefficients (*K_{cb}*) and adjusted *K_{cb}* by climatic conditions at the site of study by equation 4.2.1..... 51

Table IV-3 Comparison of different crop *ET* estimation methods. *Mk*, *PT*, *56PM*, *m56PM₈₀*, *m56PM₁₀₀*, *m56PM₁₂₀* are conventional reference crop *ET* (*ET₀*, grass as reference crop) estimation methods while *m56PM_{mrc}* is reference crop *ET* of rice (*ET₀*, healthy and well-watered rice as reference crop). *K_{cb_FAO}* is the *FAO* recommended hypothetical basal crop coefficients (Provided in section (4.2.1), Table (4.2) while *K_{cb_NDVI}* is *NDVI* derived basal crop coefficient. *R²* is determination of coefficients, *RMSE* is root mean square error, *p* (t-test) is level of significant of the test, *CV* (*RMSE*) is coefficient of variation determined by *RMSE*, *ME* (*N_{seff}*) is model efficiency and *Score* is the score of model performance ranked based on *ME* and *R²*.....59

Table V-1 Environmental variables controlling crop evapotranspiration of rainfed rice. Spearman rank order correlation was performed by using chamber measured *ET* and environmental variables.....65

Table V-2 Factors controlling crop evapotranspiration of paddy rice. Spearman rank order correlation was performed by using chamber measured *ET* and environmental variables.....66

Table VI-1 Summary statistics of the components of different spatiotemporal water use efficiencies of rainfed and paddy rice. Wilcoxon-Mann-Whitney Rank Sum test was performed to compare different *WUE* components of rainfed and paddy rice. All of the values except the values labeled as “Field scale” and “Growing Season” are the overall crop growth season means. Values labeled as “Field scale” and “Growing Season” are the integrated values over the growing season.....89

Table VI-2 Comparison of different spatiotemporal water use efficiencies of rainfed and paddy rice. Wilcoxon-Mann-Whitney Rank Sum test was performed to compare different *WUEs* of rainfed and paddy rice.....90

Table VII-1 Partitioning evapotranspiration of rainfed and paddy rice by different methods....
.....95

Symbols and Abbreviations

Symbols	Meanings
1000-grain-weight	total grain weight of 1000 oven-dried rice grains
<i>56PM</i>	Penman-Monteith ET model modified by the Food and Agriculture Organization of the United Nation
$\delta^{18}O_e$	stable water isotope signature of leaf water at the evaporating sites
$\Delta^{13}C$	Carbon isotope discrimination; the change in relative abundance of ^{13}C between an educt and product
Δ	slope of the saturation vapor pressure temperature relationship
α	empirical constant of the Priestley and Taylor evapotranspiration model, which is equal to 1.26
α^+	equilibrium fractionation factor
α^k	kinetic fractionation factor
$\delta^{13}C$	ratio of stable carbon isotope $^{13}C:^{12}C$
$\delta^{18}O_E$	$\delta^{18}O$ signatures of soil evaporation
$\delta^{18}O_{ET}$	$\delta^{18}O$ signatures of evapotranspiration
$\delta^{18}O_{rain}$	$\delta^{18}O$ signatures of precipitation (rain)
$\delta^{18}O_{soil}$	$\delta^{18}O$ signatures of soil water
$\delta^{18}O_T$	$\delta^{18}O$ signatures of plant transpiration
δ_{in}	$\delta^{18}O$ signatures at ambient air
δ_{out}	$\delta^{18}O$ signatures at outlet of the chamber
γ	psychrometric constant
λ	latent heat of vaporization of water vapor
θ	volumetric soil water content
ρ	mean air density at constant pressure
<i>A</i>	photosynthetic CO ₂ assimilation
<i>ABM</i>	above ground biomass
<i>A_{max}</i>	maximum photosynthetic CO ₂ assimilation

<i>AWD</i>	alternate wetting and drying rice production practice
<i>C_a</i>	atmospheric CO ₂ concentration
<i>CD</i>	crop development stage
<i>CEC</i>	cation ion exchange capacity
<i>C_i</i>	sub-stomatal CO ₂ concentration
<i>CRDS</i>	Cavity Ring-Down Spectrometer
<i>D_{e, i-1}</i>	cumulative depth of evaporation depletion from topsoil at the end of the day (<i>i-1</i>)
<i>e_s - e_a</i>	vapor pressure deficit of the air
<i>ET</i>	evapotranspiration
<i>ET₀</i>	evapotranspiration of a reference crop, which is a well-managed and watered grass or alfalfa
<i>FAO</i>	Food and Agriculture Organization of the United Nation
<i>FC</i>	field capacity
<i>fPAR</i>	fraction of incident to absorbed <i>PAR</i>
<i>G</i>	soil heat flux
<i>GISP</i>	Greenland Ice Sheet Precipitation, a laboratory standard for stable water isotope analysis
<i>GPP</i>	gross primary CO ₂ exchange.
<i>g_s</i>	stomatal conductance
<i>inWUE</i>	instantaneous water use efficiency as the ratio of photosynthetic carbon assimilation to transpiration
<i>inWUE_{δ¹³C}</i>	instantaneous water use efficiency calculated by $\delta^{13}C$ discrimination of bulk leaf ($\Delta^{13}C$ ‰) and atmospheric VPD
<i>k</i>	von Karman's constant (0.41)
<i>k'</i>	coefficient derived by exponential correlation of T/ET_0 and <i>LAI</i>
<i>k''</i>	coefficient derived by exponential correlation of <i>LAI</i> and <i>NDVI</i>
<i>K_c</i>	crop coefficient or evapotranspiration coefficient of FAO 56 single crop coefficient model
<i>K_{cmax}</i>	upper limit of evaporation and transpiration from a cropped surface
<i>K_e</i>	evaporation coefficient of FAO 56 dual crop coefficient model

K_r	soil evaporation reduction coefficient
LA	leaf area
LAI	leaf area per unit ground area
LS	late season stage
LUE	light use efficiency
$m56PM_{100}$	$56PM$ model modified by fixing the canopy resistance at 100 sm^{-1} instead of the original 70 sm^{-1} .
$m56PM_{120}$	$56PM$ model modified by fixing the canopy resistance at 120 sm^{-1} instead of the original 70 sm^{-1} .
$m56PM_{80}$	$56PM$ model modified by fixing the canopy resistance at 80 sm^{-1} instead of the original 70 sm^{-1} .
$m56PM_{mrc}$	$56PM$ model modified by applying the canopy resistance derived from measured leaf resistance.
Mk	Makkink (1957) evapotranspiration model
MS	mid-season stage
$NDVI$	normalized different vegetation index
$NDVI$	normalized different vegetation index
$NDVI_{max}$	maximum NDVI
$NDVI_{min}$	minimum NDVI
NEE	net ecosystem CO ₂ exchange
NIR	near-infra red wavelength
PAR	photosynthetic active radiation
pH	numeric scale used to specify the acidity or alkalinity of an aqueous solution
PT	Priestley and Taylor (1972) evapotranspiration model
R_a	isotope ratio of ambient water vapor.
r_a	aerodynamic resistance
r_c	canopy resistance
R_e	isotope ratio of soil water at the evaporating site which is the isotope ratio of extracted soil water.
R_E	ratio of heavy to light water isotope ($^{18}O/^{16}O$) of evaporated water vapor
R_{ecoref}	reference ecosystem respiration

<i>Red</i>	red wavelength
<i>REW</i>	readily evaporable water which is cumulative depth of depletion of evaporable water from the soil surface layer at the end of stage one
<i>r_l</i>	leaf resistance
<i>R_n</i>	net radiation
<i>R_s</i>	solar radiation
<i>R_{soil}</i>	soil respiration
<i>SDM</i>	standard delivery module
<i>SLAP</i>	Standard Light Antarctic Precipitation, a laboratory standard for stable water isotope analysis
<i>SWC</i>	volumetric soil water content
<i>T</i>	transpiration
<i>T/ET</i>	ratio of transpiration to evapotranspiration
<i>T_{air}</i>	air temperature
<i>TBM</i>	total biomass
<i>T_c</i>	canopy transpiration
<i>TEW</i>	maximum depth of water that can evaporated from the soil when topsoil is completely wet
<i>T_{soil}</i>	soil temperature
<i>u₂</i>	wind speed
<i>V_{cmax}</i>	maximum carboxylation capacity
<i>VSMOW</i>	Vienna Standard Mean Ocean Water, a laboratory standard for stable water isotope analysis
<i>W_{in}</i>	H ₂ O concentration at ambient air
<i>W_{out}</i>	H ₂ O concentration at outlet of the chamber
<i>WP</i>	wilting point
<i>WUE</i>	water use efficiency
<i>WUE_{agro}</i>	agronomic water use efficiency
<i>WUE_{c-Abg/Tc}</i>	growth stage integrated canopy water use efficiency, the ratio of dry weight of above ground biomass harvested at a specific growth stage to the integrated daily canopy transpiration of the same growth stage.

WUE_{eco}	ecosystem water use efficiency which is the ratio of net or gross ecosystem CO ₂ fluxes to evapotranspiration
WUE_i	intrinsic water use efficiency as the ratio of the leaf photosynthesis to stomatal conductance
$WUE_{i-\delta^{13}C}$	intrinsic water use efficiency calculated by $\delta^{13}C$ discrimination of bulk leaf ($\Delta^{13}C$ ‰)
Z_e	depth of surface soil layer
z_h	height of humidity measurements
z_m	height of wind speed measurement site
z_{oh}	roughness length governing the heat and vapor transfer
z_{om}	roughness length governing the momentum transfer

Definitions of different water use efficiencies

Leaf water use efficiency

Intrinsic water use efficiency (WUE_i)

The ratio of photosynthesis measured as CO₂ uptake (A) to stomatal conductance to water (g_s) is defined as the intrinsic WUE (WUE_i) (Osmond et al., 1980).

Instantaneous water use efficiency ($inWUE$)

The ratio of photosynthesis measured as CO₂ uptake (A) to rate of transpiration (T) is defined as the instantaneous WUE ($inWUE$) (Bierhuizen and Slatyer, 1965).

Agronomic water use efficiency (WUE_{agro})

Farmers and agronomists defined the agronomic water use efficiency as the ratio of the yield of harvested product to water applied to produce the crop, which could be precipitation and/or irrigation. (Condon et al., 2004) modified the agronomic water use efficiency definition by considering the physiological definitions (i.e., WUE_i or $inWUE$) and describing grain yield as the function of the amount of water used for crop production (i.e., evapotranspiration). Thus, WUE_{agro} is also defined as the ratio of grain yield to evapotranspiration and this definition was applied in this study.

Ecosystem water use efficiency (WUE_{eco})

WUE_{eco} is defined as the ratio of gross primary production (GPP) to evapotranspiration (ET)

Ecosystem WUE is also defined as the ratio of net ecosystem carbon exchange (NEE) to ET

(Beer et al., 2009; Kuglitsch et al., 2008).



1



Introduction

I. Introduction

1.1 Rice production under global change

1.1.1 Rice (*Oryza sativa* L.)

Rice (*Oryza sativa* L.) is a staple food for a large number of people and is the single largest food source for the poor. It is one of the only two domesticated and widely cultivated species of the genus *Oryza*, tribe *Oryzae* and family *Poaceae* and it is domesticated in Asia. However, the exact time and place of rice domestication is not clearly documented and has long been debated (Fuller et al., 2009; Gross and Zhao, 2014; Li Liu et al., 2007). Tracing the distribution of the Asian wild grass (*Oryza rufipogon*), which is most closely related to *O. sativa*, Ganges valley of northern India, some regions in China and Southeast Asian regions were roughly reported to be the very first places of *O. sativa* domestication (Huang et al., 2012; Kovach et al., 2007; Londo et al., 2006; Molina et al., 2011). Another species, *O. glaberrima* was domesticated in Africa after the Asian rice domestication. *O. glaberrima* is not as popular as *O. sativa* and has never been a staple food due to its lower grain productivity (Linares, 2002). *O. sativa* is the only commercial and widely cultivated rice on the Earth and is currently cultivated in Asia, tropical Latin American and Caribbean regions and Europe (Seck et al., 2012).

Rice is produced in a wide range of climatic and geographic locations, from the wettest Myanmar's Arakan coast (5,100 mm of growing season rainfall) to Al Hasa Oasis in Saudi Arabia (annual rainfall is less than 100 mm) (Mohanty et al., 2013). Approximately 158 million hectares of rice farms in more than a hundred countries produce 700 million tons grain (470 ton milled rice) annually (GRiSP (Global Rice Science Partnership), 2013). 90 % of rice is produced in Asia (Kudo et al., 2014; Yan et al., 2003) while the rest are produced in Africa and Latin America. Most of rice production in Asia and Africa are small-scale subsistence production systems compared to Latin American countries (GRiSP [Global Rice Science Partnership], 2013). Depending on the climatic and geographic locations, rice was produced by different crop management practices, especially, water management practices. It is primarily grown on the vast areas of flat, low-laying river basins and deltas of Asia, which are flooded

at different depths. However, upland rice, rainfed rice and other water saving rice production practices can be found in water scarce regions.

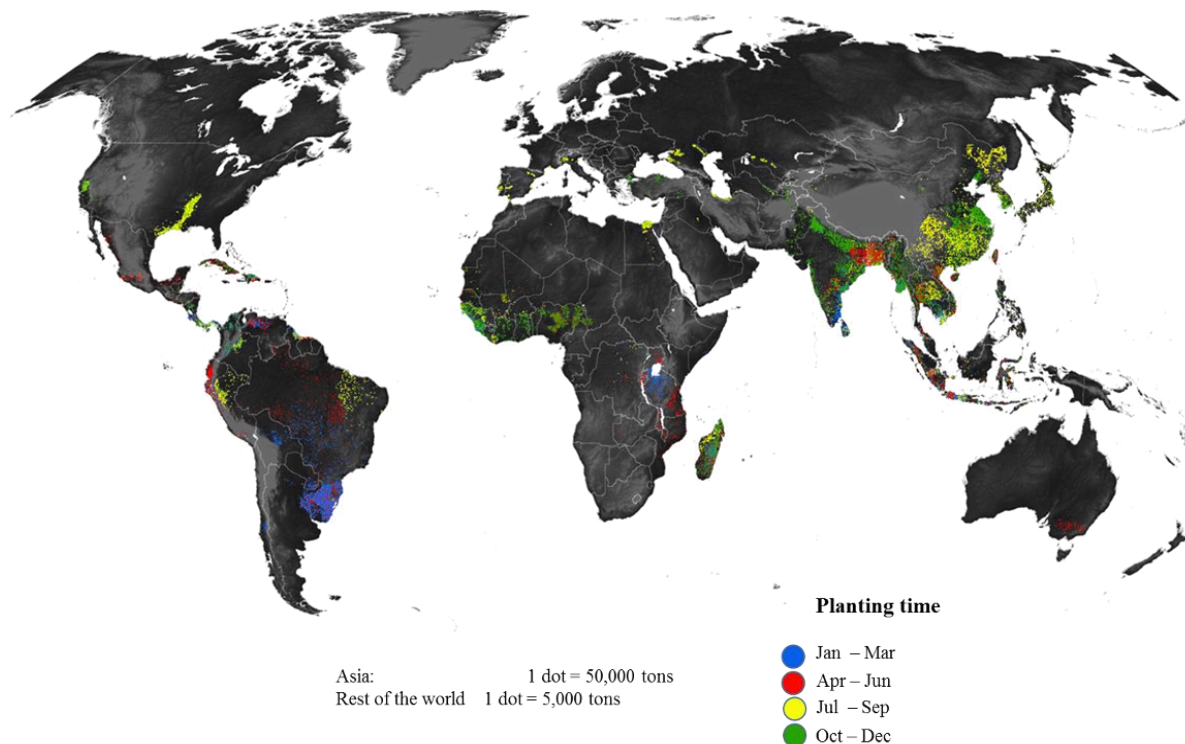


Figure I-1 Rice production area (Source: International Rice Research Institute [IRRI], 2014)

1.1.2 Rice and global change

Intergovernmental Panel on Climate Change [IPCC] projected that the atmospheric CO₂ concentration may increase up to 730 – 1020 ppm by 2100 and the global average temperature may rise roughly up to 0.2 °C per decade (Meehl and Stocker, 2007). Moreover, change in precipitation patterns, especially, higher chance of increasing intense and heavy episodic rainfall associated with longer relatively dry periods in between are predicted (Meehl and Stocker, 2007). These predicted climatic changes may have significant impacts on crop yield via change in crop evapotranspiration, crop growth and development (Lobell and Field, 2007; Lobell et al., 2011; Long et al., 2006; Ray et al., 2015). Increase or decrease in rice grain yield

under projected climate changes, is region specific and depends a lot on regional precipitation and temperature pattern (Iizumi et al., 2011; Ko et al., 2014; Lobell et al., 2011; Peng et al., 2004; Ray et al., 2015).

At the same time, it is reported that global average yield improvements of rice are slower (only 0.9 to 1.6 percent annually) than required rates to satisfy the global demand (Fischer et al., 2014; Grafton et al., 2015; Ray et al., 2013). According to the projected population growth, the current agricultural production system needs to produce 50 % more food to supply the needs of projected 9 billion population by 2050 (Alexandratos and Bruinsma, 2012) and thus, needs to double the current crop production. Expansion of crop production area and intensive use of existing croplands could be an option to increase the crop production (Godfray et al., 2010; Ray et al., 2013) although possible environmental impacts such as greenhouse gas emission (CH_4 , N_2O) could lead to other challenges.

However, water resource availability is another limitation to expand or intensify current agricultural production, especially the rice production. Roughly, 90% of global rice production area is located in Asia and 80% of it is cultivated under conventional flooded conditions (Bhattacharyya et al., 2014; Nie et al., 2012). Almost 30% of world's fresh water was withdrawn by about 80 million hectares of irrigated rice worldwide (Bouman et al., 2007) and most of global rice producing countries are suffering economic (water scarcity due to human, institutional and financial capital limited access to water) and physical water scarcity (water supply does not meet water demand) (*Figure I-2*). Along with the fresh water resources limitation, conventional flooded rice is also notorious for its high methane (CH_4) emission and urged for a suitable adaptation measures (Hussain et al., 2014; Kudo et al., 2014; Smith et al., 2007). Therefore, several water saving rice production techniques are introduced, which also aim at adapting and mitigating the CH_4 emission (Bouman et al., 2005; Pittelkow et al., 2013; Zou et al., 2005).

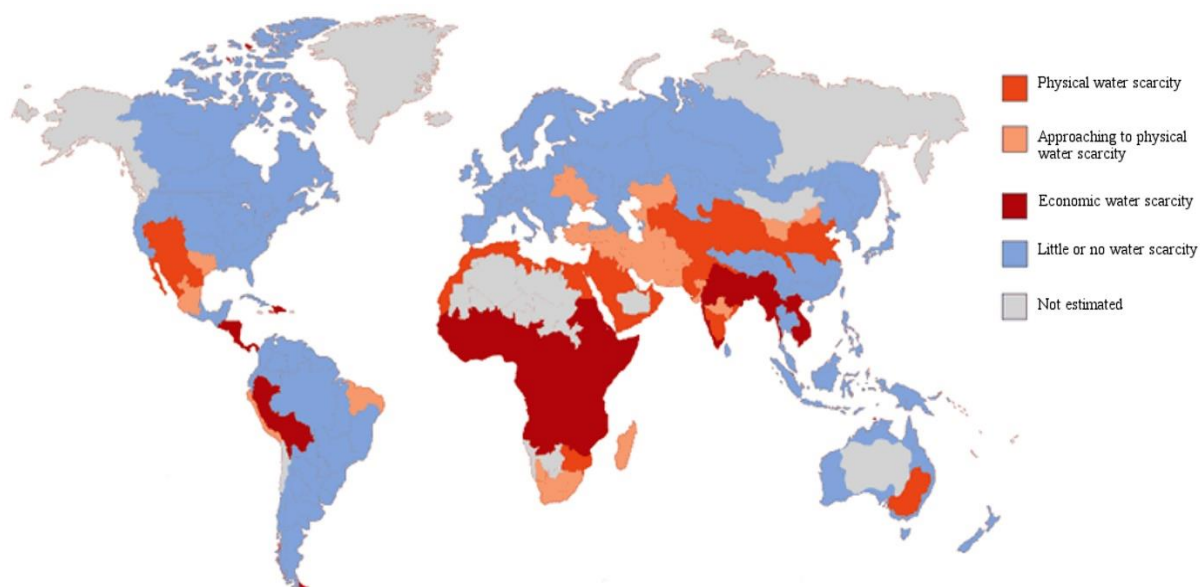


Figure I-2 Physical and economic water scarcity worldwide (Physical Water scarcity: water resources development is approaching or has exceeded sustainable limits; Approaching to physical water scarcity: these areas will experience physical water scarcity in the near future; Economic water scarcity: these areas are suffering water scarcity due to human, financial and institutional limitations although natural water resources are abundant relative to water use; Little or no water scarcity: Abundant water resources relative to use) (Source: Comprehensive Assessment of Water Management in Agriculture, 2007)

Among the introduced water saving rice production techniques, aerobic rice (no flooded standing water) and alternate wetting and drying (*AWD*) were reported to have high water productivity with less technical complexity (Farooq et al., 2009). Aerobic rice is grown in well drained and non-puddled soil with no standing water (Bouman et al., 2005). The production and management methods of aerobic rice resembles to that of conventional rainfed upland rice or other irrigated but non-flooded upland crops such as maize, barley and wheat. Aerobic rice production can save 60 to 90% of water compared to conventional flooded paddy rice but with up to 20-30 % yield reduction (Mostafa and Fujimoto, 2014; Tuong and Bouman, 2003) *AWD* can be described as an irrigation management system since it is a rotation of flooded and non-flooded period. Depending on the frequency, duration and timing of flooding and drying cycles, the degree of water stress during the drying period, water productivity and crop yield of *AWD* system varies (Chapagain et al., 2011). However, the decreased crop yield under water limited conditions, which could lead to reduced economic profitability, are reported in all of water saving rice production systems, although rice is a crop which can be grown under different

water availabilities, ranging from flooded to non-flooded (Bouman and Tuong, 2001; International Rice Research Institute [IRRI], 2002).

Table I-1 Some of the conventional and water saving rice production systems and their crop management practices

Rice system	Typical crop management	Geography	Water input	Water needs	Remark
Paddy rice (Deep water)	Flooded and needs a special deep water rice variety	Natural wetlands with deep water	Natural flood	-	Conventional
Paddy rice (Irrigated)	Flooded with irrigated water	Almost everywhere rice can be planted	Rain + Irrigation	High	Conventional
Paddy rice (Rainfed lowland)	Rain water is ponded following the land preparation and rice is transplanted in the rain water pond.	Tropical and subtropical regions with high intensity of rainfall	Rain water	Medium	Conventional
Paddy rice (Alternate Wetting and Drying)	Irrigation is supply intermittently depending on soil water status and crop water demand	Almost everywhere rice can be planted but regions with well-functioning irrigation facilities	Rain+ Irrigation	Less	Water saving paddy rice
Rainfed rice / Aerobic rice	No standing flooded water	Almost everywhere rice can be planted but favorable to the regions with high intensity of rainfall.	Rain water	Super less	Water saving rice as well as conventional practice

1.2 Water use efficiency

As defined in most efficiency concepts, water use efficiency (*WUE*) is a simple balance between the gain (kg of biomass produced or unit CO₂ assimilated) and the cost (unit water transpired to produce the biomass or to assimilated CO₂). Along with the increasing pressure on limited fresh water resources, growing population and increasing atmospheric CO₂ concentration, plant physiologists, hydrologists, agronomics and ecologists draw attention to maximizing crop water use. Thus, *WUE* is studied at different spatial (from leaf to whole plant to farm to ecosystem) and temporal (from minutes to months to crop growing seasons to years) scales (*Figure I-3*) (Blum, 2009; Bouman et al., 2005; Kuglitsch et al., 2008; Pittelkow et al., 2013; Zou et al., 2005).

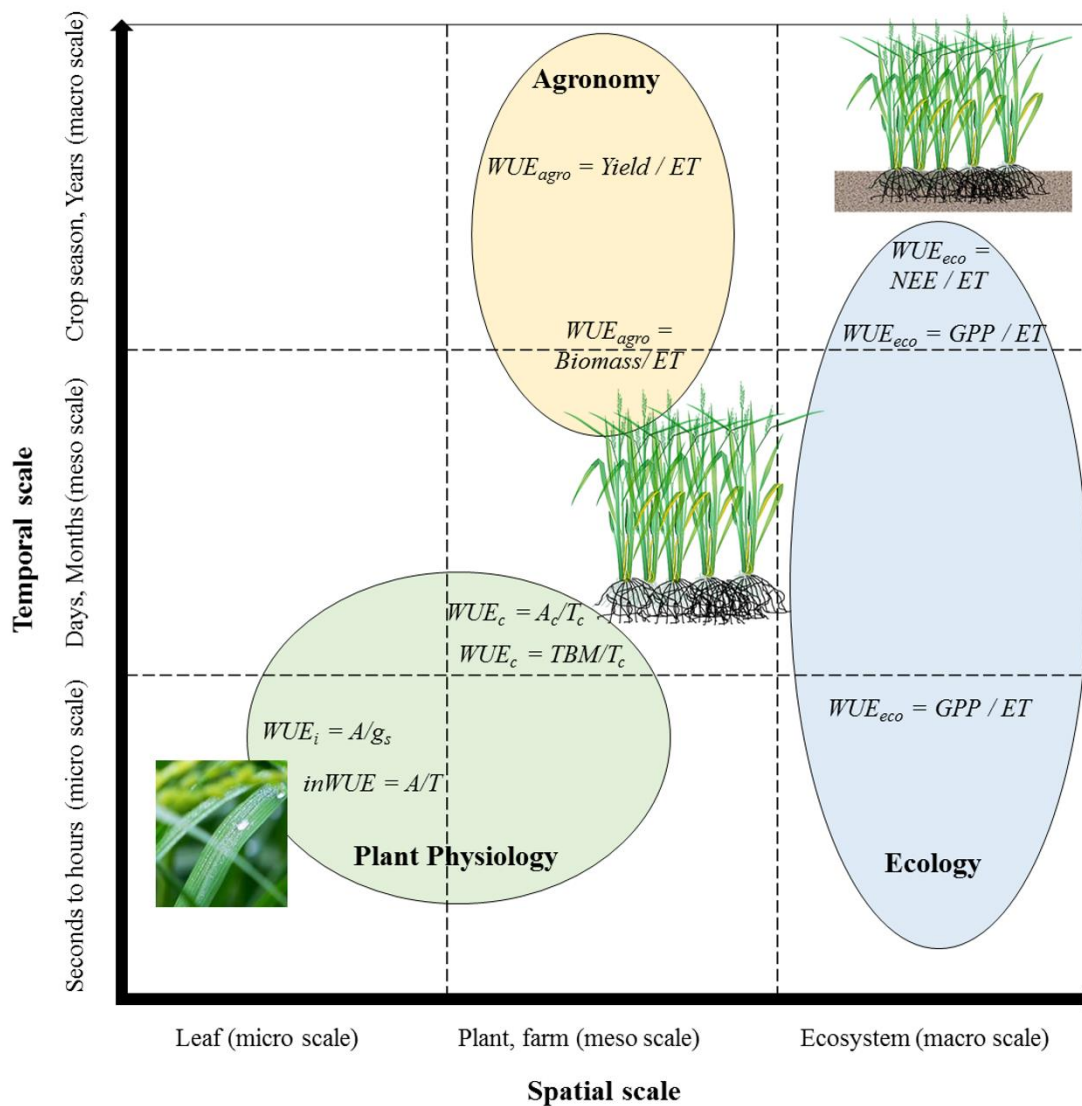


Figure I-3 Water use efficiency at different temporal and spatial scale. WUE_i is intrinsic water use efficiency; A is photosynthetic CO_2 assimilation; g_s is stomatal conductance; T is transpiration, WUE_c is canopy water use efficiency; A_c is canopy photosynthetic CO_2 assimilation; T_c is canopy transpiration; TBM is total dry biomass; Biomass is dried biomass of interest; $Yield$ is the yield of biomass of interest, i.e., grain yield in the case of rice; ET is evapotranspiration; NEE is net ecosystem CO_2 exchange; GPP is gross primary CO_2 exchange. When a WUE equation is written directly on the dashed line, that WUE equation is commonly used to calculate for both temporal and spatial scales directly above and below the dashed line (Adapted from Kuglitsch et al., 2008).

At leaf scale, WUE is measured as both short and long time scales. Short temporal scale leaf WUE measurements can be done by instantaneous gas exchange measurements. Long temporal scale measurements can be done by carbon isotope ($\delta^{13}C$) analysis of the soluble sugar of the leaf or the accumulated leaf dry mass. Short temporal scale leaf WUE is estimated by relating the rate of photosynthetic CO_2 assimilation (A) to either stomatal conductance (g_s) or leaf transpiration (T) (Bierhuizen and Slatyer, 1965; Farquhar and Richards, 1984; Fischer and Turner, 1978; Osmond et al., 1980). The ratio of A to g_s is defined as intrinsic WUE (WUE_i) and the ratio of A to T is defined as instantaneous WUE ($inWUE$). Long temporal scale leaf WUE can be measured by $\delta^{13}C$ analysis of accumulated dry mass since $\delta^{13}C$ discrimination ($\Delta^{13}C$) of leaf dry mass is determined by the ratio of sub-stomatal CO_2 concentration (C_i) and atmospheric CO_2 concentration (C_a), which is determined relationship between photosynthetic CO_2 assimilation (A) and stomatal conductance (g_s) (Farquhar and Richards, 1984; Farquhar et al., 1989; Werner et al., 2011). Among this three leaf $WUEs$, A/g_s and $\Delta^{13}C$ – the intrinsic WUE (WUE_i) is mostly applied to determine WUE independent to specific environmental conditions. Since the regulation of A/g_s is genetic dependent but independent to environmental effects such as atmospheric evaporative demands, A/g_s and $\Delta^{13}C$ is commonly applied in crop varietal screening (Bierhuizen and Slatyer, 1965; Condon et al., 2004; Gago et al., 2014; Galmés et al., 2011; Rizza et al., 2012). On the other hand, $inWUE$ (A/T) is widely applied to access the leaf WUE changes under different environmental conditions since T depends on the degree of stomatal opening (g_s) and leaf to air vapor pressure deficit (VPD). $inWUE$ is used to access the time integral (minutes, hours to day) change in leaf WUE , i.e., accumulated carbon gain and transpiration water loss during a certain time period ranging from minutes to day (Medrano et al., 2012, 2009; Morison et al., 2008; Rizza et al., 2012). Studying A/g_s and A/T at the same

time under different environmental conditions such as water limited and non-water limited condition can help to understand the genetic and environmental controls over crop water use.

Although many water use efficient crop varieties are screened based on the leaf water use efficiency analysis by leaf gas exchange or $\Delta^{13}C$ measurements, it is reported that water use efficiency of a certain crop is hard to define based on leaf scale measurements (Blum, 2009, 2011). The degree of day light interception by different leaves in a canopy varies depending on the location of the leaf and thus photosynthetic CO_2 assimilation of leaves in a canopy vary significantly (Flexas et al., 2010; Medrano et al., 2012). Hence, water use efficiency of leaves in a canopy may vary depending on their specific locations in the canopy and higher leaf water use efficiency does not necessarily mean higher canopy WUE (WUE_c).

WUE_c is the balance of total biomass production or net CO_2 assimilation and transpiration water loss of the whole plant canopy and it can be estimated as the ratio of daily-integrated canopy CO_2 assimilation to canopy transpiration. Daily integrated WUE_c can be calculated as the ratio of chamber measured canopy CO_2 assimilation rate to canopy transpiration (Linderson et al., 2012).

The main target of agricultural crop production is the final harvestable yield of the biomass of interest, i.e., grain in the case of cereals and boll in the case of cotton. Thus, water use efficiency of a crop is also measured as the ratio of crop yield to evapotranspiration ($\text{Grain yield} / ET$) and is termed agronomic WUE (WUE_{agro}) (Mo et al., 2009; Pereira et al., 2012; Tallec et al., 2013). Although leaf and canopy WUE is calculated as the ratio of carbon or biomass gain per transpiration, WUE_{agro} often apply evapotranspiration (the sum of water loss by soil evaporation and plant transpiration) as well as transpiration as the denominators depending on the interest of study (Blum, 2009).

Improving the crop water use efficiency of a certain agroecosystem by changing crop management practices is widely practiced or recommended in many countries with water resource limitations. On the other hand, it is also essential to consider the possible ecosystem impacts due to the change in agricultural practices since an agroecosystem is a complex network of multiple ecosystem components. All of the system components of an agroecosystem are linked to each other and a change in one system component could lead to change in another, affecting the sustainability of the agroecosystem (Sakai et al., 2004). Even a slight and short time fluctuation of flooded water level in a paddy rice field can alter the carbon and water cycle over the rice field (Alberto et al., 2009; Kudo et al., 2014; Miyata et al., 2000; Nishimura et al.,

2015; Thanawong et al., 2014). For the larger spatial and temporal scales, change in crop, tillage, cultivation and management practices affects the seasonal change in PAR-albedo, evapotranspiration, carbon uptake and sequestration, emissions and net carbon fluxes (Gordon et al., 2008; Luo et al., 2010; Pielke et al., 2007; Sakai et al., 2004; West and Marland, 2002). Thus, from a minor to major changes in a certain agroecosystem not only affects the crop production but also affects the ecosystem functions of the agroecosystem. Therefore, branding a crop variety or a crop production practice as a highly water use efficient variety or practices based on the water use efficiency quantified according to the genetic, leaf and crop physiological performance might not enough for the agroecosystem sustainability. It is also important to see the possible ecosystem impacts due to the changes in physiological and agronomic water use.

WUE of cultivated and natural vegetation are also studied at ecosystem scale from an ecological point of view. Since plants are playing an important role in balancing ecosystem carbon and water cycle through the photosynthesis and transpiration process (*Figure I.4*), the influence of vegetation land cover on global scale ecosystem carbon and water balance is prominent (Kuglitsch et al., 2008). Thus, ecosystem *WUE* (WUE_{eco}) of vegetation is studied as the ratio of ecosystem carbon assimilation of the vegetation to evapotranspiration or transpiration. When calculating WUE_{eco} , both gross ecosystem carbon exchange (*GPP*) (i.e., ecosystem carbon fluxes excluding respiratory carbon losses) and net ecosystem carbon exchange (*NEE*) (i.e., ecosystem carbon fluxes including respiratory carbon losses) are used as nominators (Beer et al., 2009; Dubbert et al., 2014b; Hu et al., 2009; Kuglitsch et al., 2008; Reichstein et al., 2005).

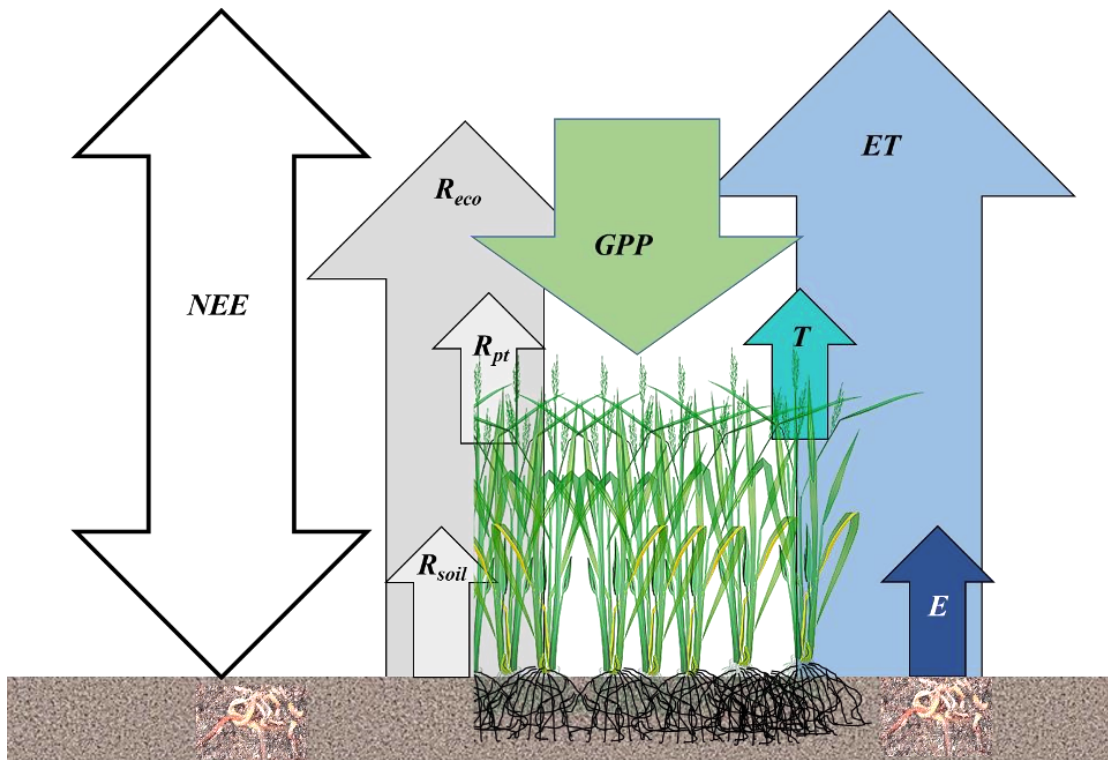


Figure I-4 CO₂ exchange in a vegetation system. *NEE* is net ecosystem CO₂ exchange which is the net flux of respiratory and photosynthetic CO₂ exchange; *R_{eco}* is ecosystem respiration which is the net flux of plant and soil respiration; *GPP* is gross primary production or the photosynthetic CO₂ assimilation of the vegetation system.

1.3 Productive and unproductive water use partitioning evapotranspiration

Plant transpiration is the water used during the photosynthesis process and it is regarded as productive water use. On the other hand, soil evaporative water loss, which is not associated to biomass production, is regarded as the non-productive water. Therefore, in comparing the water use efficiencies of two different rice ecosystems (rainfed and paddy rice), it will be useful to compare the productive and unproductive water use of both systems (Agam et al., 2012; Van Halsema and Vincent, 2012). Moreover, it will need to partition the unproductive soil evaporation and productive plant transpiration.

Attempts to partition transpiration and evaporation of both agricultural systems and natural vegetation systems were done as early as 1959. A good example of simple partitioning approaches is eliminating soil evaporation by covering ground surface (Harrold et al., 1959;

Peters and Russell, 1959; Shaw, 1959). Model based partitioning (Ritchie, 1972; Shuttleworth and Wallace, 1985; Tanner and Jury, 1976), micro-lysimeter based methods (Boast and Robertson, 1982; Walker, 1984), Sap flow measurements based partitioning (Čermák et al., 1973; Cohen et al., 1993; Cohen et al., 1981; Sakuratani, 1981) and the stable water isotope based partitioning method (Cuntz et al., 2007; Dubbert et al., 2014b, 2013; Wang and Yakir, 2000; Yakir and Sternberg, 2000) are popular and advanced partitioning approaches. Each approach has their own benefits and drawbacks. Regardless of differences in spatial and temporal scales; differences in modelling procedures; partitioning ET by different ET flux modelling approaches apply the same energy and/or water balance theories and need similar data input. However, stable water isotope ($\delta^{18}O$) based ET partitioning is a bit different to aforementioned modelling approaches since this approach partition ET based on the distinct isotopic composition of transpired water vapor ($\delta^{18}O_T$) to soil evaporated water vapor ($\delta^{18}O_E$). Due to its direct partitioning of ET by tracing distinct $\delta^{18}O$ signals of E and T , it is regarded as a direct partitioning method (Kool et al., 2014)

Many ET partitioning studies were done on agricultural crops and some on natural vegetation and over 50 publications were published (Kool et al., 2014). However, there is few on partitioning ET fluxes in the rice ecosystems. In this study, $\delta^{18}O$ isotope based direct partitioning method was applied to partition daytime canopy ET fluxes and compared to the PM (Monteith, 1965) and $FAO 56$ dual crop coefficient ($56PM$) based partitioning methods.

Stable oxygen isotope ($\delta^{18}O$) is used as a tracer to trace the water movement in the ecosystem because the $\delta^{18}O$ composition of water in the soil, vegetation and atmosphere are unique to each other (Yakir and Sternberg, 2000). $\delta^{18}O$ of soil evaporated vapor is depleted compared to source water, which is rain water in the case of no additional irrigation, at evaporating site due to the kinetic and equilibrium fractionations (Allison et al., 1983; Barnes and Allison, 1984, 1983; Craig and Gordon, 1965) under isotopic unsteady state condition. However, the water vapor transpired from leaf is isotopically similar to that of soil water transported by the root, as isotopic fractionation does not occur during the root water uptake. Moreover, leaf water is mostly at an isotopic steady state due to the rapid turnover of water in the transpired leaf (Ehleringer and Dawson, 1992; Wang and Yakir, 2000). On the other hand, the steady state conditions (i.e., $\delta^{18}O$ of transpiration flux is equal to the $\delta^{18}O$ of xylem/source water) cannot be found under the transient atmospheric changes (Yakir and Sternberg, 2000) and non-steady state transpiration is depleted in $\delta^{18}O$ than the source water (Cuntz et al., 2007; Dongmann et

al., 1974; Dubbert et al., 2013). Nevertheless, ET can be partitioned by tracing the distinct water isotopic composition of soil-evaporated water vapor and plant transpired water vapor (Figure I-5).

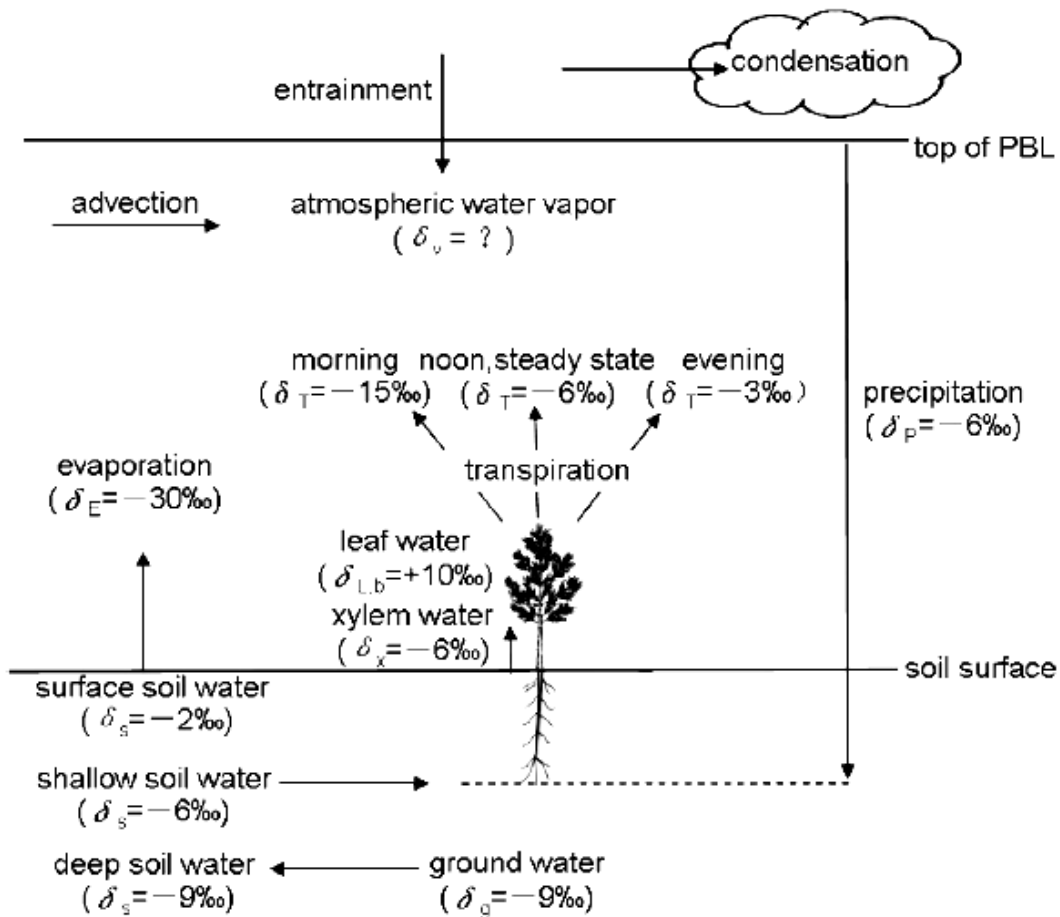


Figure I-5 $\delta^{18}O$ values of water pool and fluxes in the Soil-Plant-Atmosphere Continuum. δ_p is $\delta^{18}O$ of precipitation; δ_s is $\delta^{18}O$ of soil water; δ_g is $\delta^{18}O$ of ground water; δ_e is $\delta^{18}O$ of soil evaporation; $\delta_{L,b}$ is $\delta^{18}O$ of bulk leaf water; δ_x is $\delta^{18}O$ of xylem water; δ_T is $\delta^{18}O$ of transpiration and δ_v is $\delta^{18}O$ of atmospheric water vapor (Zhang et al., 2010)

1.4 Objectives

Water saving rice production techniques are introduced to adapt water scarcity and to mitigate methane (CH₄) emission (Dijkstra et al., 2012; van Groenigen et al., 2012, 2011; Yao et al., 2014; Zou et al., 2005). Contrastingly, agricultural land-use changes such as shifting the conventional flooded paddy rice cultivation to the water saving rice-farming impacts further on the carbon and water exchange of rice ecosystems. (Alberto et al., 2013, 2009; Kudo et al., 2014; Nishimura et al., 2015, 2008; Pathak et al., 2005; Sakai et al., 2004; Wang et al., 2000; Wassmann et al., 2000). Even in conventional paddy rice system, intensity and timing of flooding and drainage regulation influences the seasonal carbon and water balance (Alberto et al., 2009; Kudo et al., 2014; Miyata et al., 2000; Nishimura et al., 2015; Thanawong et al., 2014). Although previous studies reported the differences in ecosystem carbon and water balance of paddy and rainfed rice (Alberto et al., 2009; Thanawong et al., 2014), quantification of the contribution and seasonal dynamics of the productive (plant transpiration and gross primary productivity) and unproductive (respiration and soil evaporation) components of ecosystem carbon and water exchange is still lacking. However, such information is very important to estimate the possible trade-offs of water saving and conventional paddy rice productions from the ecosystem and agronomic perspectives. In addition, it is necessary to contrast the water use efficiency of rice from different perspectives. Moreover, according to the previous works (Blum, 2009, 2011; Condon et al., 2004; Galmés et al., 2011; Huang et al., 2010; Luo, 2010; Medrano et al., 2015; Tuong and Bhuiyan, 1999; VanLoocke et al., 2012), the leaf scale water use efficiency of a certain crop could not represent well to the canopy or agronomic water use efficiency. And the variation between agronomic and ecosystem water use efficiency of some crops are also described (for example, Tallec et al., 2013 and Zeri et al., 2013). Therefore, it is hard to define an agronomic practice and an agroecosystem as a water use efficient practice or ecosystem based on the results of a certain water use efficiency analysis. Thus, this study on water use efficiency of rice by comparing non-flooded rainfed rice and conventional flooded paddy rice was carried out with a general aim: *to examine the spatiotemporal variation of water use efficiency of rainfed and paddy rice ecosystem.*

To fulfill the general aim of this study, the following specific objectives are laid out:

1. To estimate the daily evapotranspiration of rainfed and paddy rice by integrating the Food and Agriculture Organization of the United Nations modified Penman-Monteith model (*56PM*) and high resolution spatial vegetation indexes

2. To quantify the productive water use (Transpiration) and unproductive water loss (Evaporation) of two different rice ecosystems and identify the role of productive water use (Transpiration), unproductive water loss (Evaporation) as well as respiratory carbon loss in the definition of ecosystem and agronomic water use efficiencies
3. To contrast the limitations of widely applied small-scale water use efficiency indicators (i.e., leaf and short temporal scales) for the representation of larger spatiotemporal scales water use efficiency (i.e., canopy, agronomic, ecosystem and longer temporal scales)

1.5 Outline of the thesis

This thesis is organized in eight chapters and water use efficiency of rainfed and paddy rice is distinguished at different scales, from the leaf to the ecosystem, from the hourly, daily to crop seasonal time scales. Different factors controlling different water use efficiency are also identified. Finally, based on the comparison of crop growth and development and water and carbon cycling of the rainfed and paddy rice systems, the needs to improve water use efficiency of rice in a profitable and sustainable way are highlighted. The organization of each chapters is summarized as follow:

Chapter 1: Introduction

This chapter introduces the background and context for the thesis. It introduces the rice production practices, gives a general overview of water use efficiency concepts and, the partitioning of productive and unproductive water use of the crop.

Chapter 2: Materials and Methods

Theoretical background and descriptions of materials and methods applied in the study are summarized in this chapter. Crop growth and development measurement, daily and seasonal evapotranspiration estimation and field measurements, partitioning of hourly, daily and seasonal evapotranspiration by modelling approach as well as stable water isotope ($\delta^{18}O$) approach and different water use efficiency estimation methods are described detail in this chapter.

Chapter 3: Environmental condition and crop growth

This chapter presents the environmental condition of the study area, daily and seasonal crop growth and development of rainfed and paddy rice. Crop growth and development of rainfed and paddy rice is described in terms of leaf area development, biomass distribution, grain yield and physiological factors controlling grain yield (i.e., yield components). Classification of crop growth and development stages of rainfed and paddy rice is illustrated in this chapter as well.

Chapter 4: Model development of evapotranspiration

Detailed model development and improvement of dual crop coefficient *56PM* (Penman Monteith model modified by Food and Agriculture Organization of the UN) is explained. The focus of this chapter is the development of ET model specifically for rice. The specific objective (1) is addressed in this chapter.

Chapter 5: Partitioning evapotranspiration

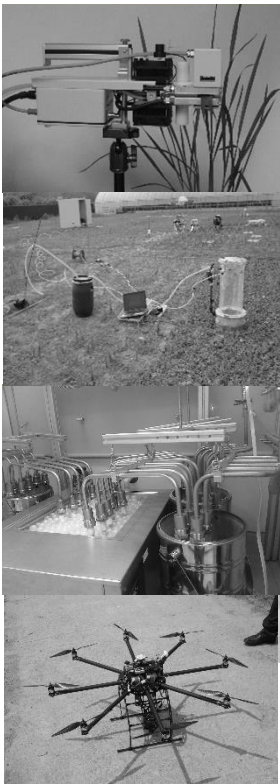
Comparing the water use efficiency of two different rice ecosystems, rainfed and paddy rice systems, specifically needs to compare productive and unproductive water use of the systems. In this chapter, partitioning evapotranspiration by an energy balance modelling approach, which is mostly applied in large scale partitioning studies, and stable water isotope ($\delta^{18}O$) partitioning approach, are compared. Daily contribution of productive water use (transpiration) and unproductive water loss (evaporation) to evapotranspiration is estimated for rainfed and paddy rice ecosystem. The specific objective (2) is addressed in this chapter.

Chapter 6: Water use efficiency of rainfed and paddy rice

As the main focus of this study, leaf, canopy, agronomic and ecosystem water use efficiency of rainfed and paddy rice are presented in this chapter. Factors controlling each water use efficiency term are explained and the needs to balance agronomic and ecosystem water use efficiency are pointed out. Moreover, ecosystem carbon and water exchange trade-offs of the rainfed and paddy rice ecosystem is highlighted by partitioning productive and unproductive water loss. The role of respiratory carbon loss in ecosystem water use efficiency concept and the inclusion of respiratory carbon loss in the calculation of ecosystem water use efficiency (i.e., $WUE_{eco} = Net\ Ecosystem\ CO_2\ Exchange / Evapotranspiration$) is evaluated. The specific objective (3) is addressed in this chapter.

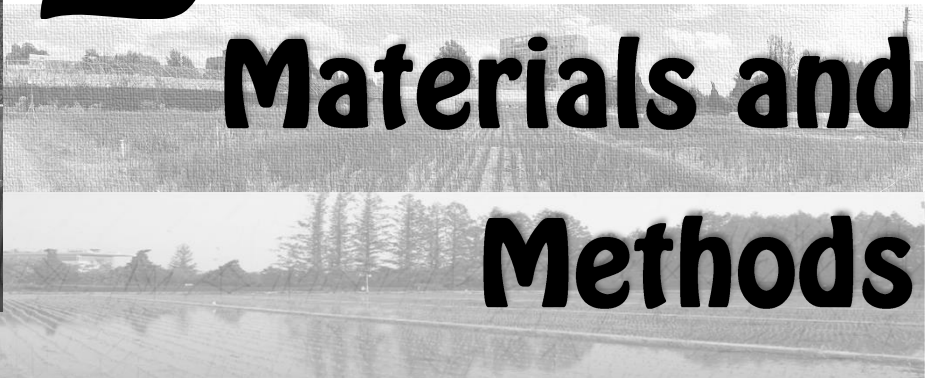
Chapter 7: Discussion and conclusion

This chapter is a general discussion and overview of the results presented in the chapters 3, 4, 5 and 6. Moreover, a list of conclusions in relation to the specific objectives and general aim of this thesis is provided in the end of the chapter.



2

Materials and Methods



II. Materials and Methods

2.1 Study site

The study was conducted in the Chonnam National University research farm, (35° 10' N, 126° 53' E, alt. 33m), Gwangju, Chonnam province, Republic of Korea (South Korea) (*Figure II.1*). Chonnam province is one of the major rice growing regions of South Korea, which has typical East Asian monsoon climate with an annual mean temperature of 13.8°C and annual mean precipitation of ~1391 mm during the past 30 years (1981–2010) (Choi et al., 2013). More than 60% of precipitation events occurred during the monsoon season (May to October). Both paddy and rainfed rice fields have similar soil properties with loamy texture and pH 6.5. Detailed soil properties are indicated in table (*II-1*).

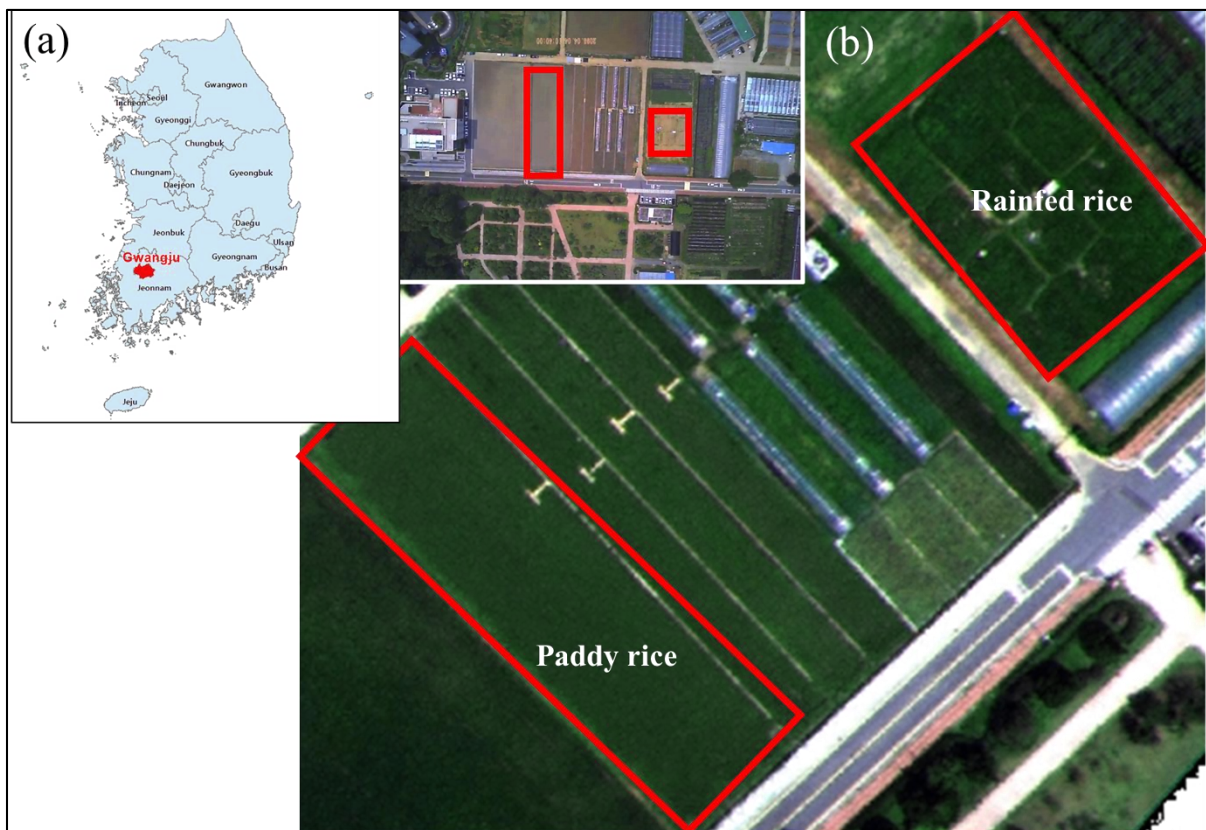


Figure II-1 Study site location: (a) Location of Gwangju; (b) Experimental site location in the Chonnam National University research farm, Gwangju, South Korea. (35° 10' N, 126° 53' E, alt. 33m).

Table II-1 Soil chemical and physical properties of study area, Chonnam National University research farm, Gwangju, S. Korea.

Parameters	Values
pH (1:5)*	6.5 (0.1)
Total organic carbon (Cgkg ⁻¹)	12.3 (0.5)
Total N (gKg ⁻¹)	1.0 (0.2)
Available P (mgP ₂ O ₅ kg ⁻¹)	13.1(0.7)
CEC (cmolkg ⁻¹)**	14.4 (0.4)
Texture	Loam (Sand: Silt: Clay= 40: 37: 23)

Note: * = Soil pH was analyzed from 1:5, soil:water suspension. ** Cation exchange capacity of soil. Values were mean values of six replicates and standard errors in Parentheses.

Rice (*Oryza sativa* L. subsp. *Japonica* cv. *unkwang*) was cultivated as rainfed dryland crop and flooded paddy crop. In both rainfed and paddy rice fields, N: P: K fertilizer (11:5:6) were applied at a rate of N = 115 kgha⁻¹ (80% as basal dosage and 20% during the tillering stage). P fertilizer (62 kgha⁻¹) was applied as a 100% basal dosage. K fertilizer (60 kgha⁻¹) was applied as 65% basal dosage and 35% during tillering). Rainfed rice was directly seeded on DOY 107 while paddy rice was transplanted on DOY 140. Before transplanting, paddy rice was germinated on the same date with rainfed rice seeding and raised in the nursery for about four weeks (*Figure II-2*). Both paddy and rainfed rice were planted at 10 cm of inter-plant spacing and 30 cm of inter-row spacing, at a seed-density of 50.48 kgha⁻¹. All field management practices of paddy rice and fertilizer dosages reflected the practices of farmers in the region. Paddy rice field was kept flooded starting from 5 days before transplanting until the heading stage (late July). Whenever the water level decreased below 5 cm above the soil surface, paddy rice field was regularly irrigated until the heading stage. Under rainfed condition, no additional irrigation was applied to natural precipitation. The experiment was conducted in a randomized complete block design with three replications. Field measurements campaigns were carried out on the days mentioned in *table (II-2)*.



Figure II-2 Planting of paddy and rainfed rice: (a) Germination of paddy rice in the nursery trays; (b) Ready to be transplanted paddy rice seedlings in the nursery; (c) Manual puddling and leveling before the transplanting of paddy rice; (d) Machine transplanting of paddy rice; (e) Gap filling in the paddy rice field after the machine transplanting; (f) Single row direct seeder used for rainfed rice seeding; (g) direct seeding of rainfed rice; (h) pre-emergence herbicide application in the rainfed rice field

2.2 Environmental variables

Weather data (global radiation, precipitation, air temperature, relative humidity and wind speed) were continuously collected at 2 m height with an automatic weather station every five minutes (Automated Weather Station, WS-GP1, Delta-T Devices Ltd., UK) and half hourly mean values were logged. Photosynthetic photon flux density (PPFD, LI-190, LI-COR, USA) was measured directly above the crop canopy (~20 cm above the canopy and inside the chamber). Air temperature (T_{air}) (at ~20 cm above the canopy) inside the chamber was also measured by custom-built temperature sensor. Soil temperature at root zone was manually measured along with gas exchange measurements using temperature probes (Conrad, Hirschau,

Germany). Soil temperature and volumetric water content (5TE and 10HS, respectively, Decagon, Washington, USA) were measured continuously at 5, 10, 20, 30 and 60 cm depth in each experiment plot. 15 min averaged data from soil temperature sensors were stored in a datalogger (Em 50, Decagon, Washington, USA) and 30 min averaged data from volumetric soil water content sensors were stored in a second datalogger (CR1000, Campbell Scientific, Logan, UT, USA).

2.3 Crop growth and development

2.3.1 LAI and biomass measurements

Above ground biomass of plants adjacent to vegetation plots were harvested. Leaf area (*LA*) was determined with a Leaf Area Meter (LI-3000A, LI-COR, USA) and leaf area index (*LAI*) was calculated as leaf area per ground area. Total aboveground biomass was collected, dried (60 °C, 48 hours) and weighed. Plant height of representative plants was manually measured every month. Crop yield of paddy and rainfed rice was estimated based on 1000-grain-weight of oven dried (moisture percent of dried grain = ~14%) harvested samples (n=6). 1000-grain-weight is regarded as a standard and stable parameter for the yield estimation of crop and is the total grain weight of the oven-dried 1000 grains (Yoshida, 1981). To limit the errors and variations of yield estimation, 1000-grain-weight is used as a standard parameter for the crops with smaller grain sizes such as cereals and 100-grain-weight is used as a standard parameter for larger grain sizes such as beans and peas.

2.3.2 High resolution remote sensing for NDVI of rice fields

An Unmanned Aerial Vehicle (UAV) equipped with Miniature Multiple Camera Array (Mini MCA) (Tetracam, Inc., USA) with 450, 550, 650, 800, 830, and 880 nm bands and 10 cm ground resolution at 300 m altitude was used. For radiometric calibration of MCA images, calibration targets (black, white and gray) and evaluation points (baresoil, cement, asphalt, crop) were set up next to the paddy field. A cropscan instrument (Cropscan Inc., USA.) was used to calibrate and evaluate the reflectance data obtained by the UAV system, based on the pre-installed reflectance points and calibration plates (*Figure II-3*).

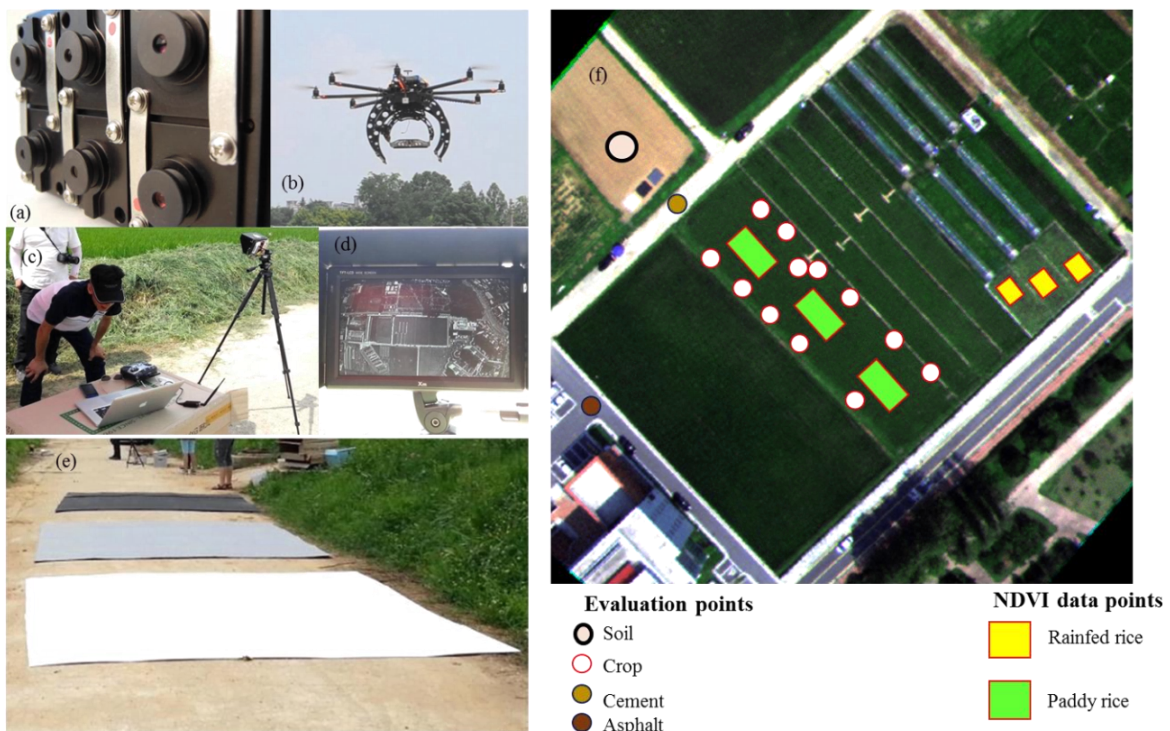


Figure II-3 Remote sensing with Unmanned Aerial Vehicle. (a) Miniature Multiple Camera Array (Mini MCA) with 450, 550, 650, 800, 830, and 880 nm bands and 10 cm ground resolution at 300 m altitude; (b) mini MCA mounted on the UAV; (c and d) real time quality control of the remote sensing pictures; (e) Calibration plates (black, gray and white); (f) NDVI data sampling points (yellow for rainfed rice and green squares for paddy rice) and remote sensing data evaluation points (soil (light orange circle), crop (white circle), cement (gold circle) and asphalt (dark orange circle)).

Remote sensing campaigns were carried out at noon of DOY 172, 192, 206, 220 and 233. Remote sensing images were analyzed by ENVI software (Exelis Visual Information Solutions, Inc., USA.). Three sampling points for each treatment plots of both rainfed and paddy rice were used to calculate the normalized difference vegetation index (*NDVI*) as:

$$NDVI = \frac{NIR - Red}{NIR + Red} \quad (2.1)$$

where *NDVI* is normalized different vegetation index, *NIR* is near infrared and *Red* is red wavelengths.

2.3.4 Estimation of daily *NDVI*, *LAI* and crop yield

Daily *NDVI* was estimated by combining measured *NDVI* data and simulated daily crop growth and development of rice by the GRAMI crop growth model (for details see Ko et al., 2015, 2006; Maas, 1993a; Maas, 1993b). Using the environmental data inputs, GRAMI crop growth model simulates daily crop growth by calculating growing degree-days, absorption of incident radiation energy by leaf, daily increase in above ground biomass, *LAI* partitioning from produced biomass and crop yield estimation. The model was calibrated and validated against measured values of the same rice varieties cultivated in 2010 and 2011. Finally, based on the relationship between measured *LAI* and *NDVI*, daily *NDVI* was estimated from the simulated *LAI*.

2.4 Canopy gas exchange measurements

Canopy fluxes were measured on canopy vegetation plots (three replications per treatment) where soil collars were permanently installed soon after seeding of rainfed and planting of paddy rice. CO₂ and H₂O fluxes of rainfed rice were measured by a custom built open chamber constructed according to Pape et al. (2009) and successfully tested by Dubbert et al. (2013). H₂O flux was measured by a Cavity Ring-Down Spectrometer (CRDS, Picarro, Santa Clara, USA) and CO₂ fluxes were measured by a portable Infra-Red Gas Analyzer (LI-820, LI-COR,

USA). Both carbon and water fluxes were calculated as differential CO₂ or H₂O concentration (i.e., the CO₂ or H₂O concentration difference between the air samples taken from the chamber inlet and outlet). Air inlet to the chamber was stabilized by a buffer bottle (200 L). Outlet air from the chamber was pumped to the analyzers via tubes heated up to 38°C to avoid condensation.

Because the heavy weight of the open chamber was hard to handle in paddy soil condition, CO₂ fluxes of paddy rice was measured by custom built closed chambers described by Li et al. (2008) and Otieno et al. (2012). CO₂ fluxes from both chambers did not differ. H₂O fluxes were only measured in rainfed rice since open and flow-through chamber type was more suited to measure H₂O fluxes (Dubbart et al., 2014b, 2013; Pape et al., 2009). Ecosystem respiration (R_{eco}) was measured by insulated opaque PVC dark chambers on crop canopy. Soil respiration (R_{soil}) was measured from bare soil plots next to the vegetation plots. Data were collected from 6:00 hr. to 18:00 hr. in one and a half hour interval. Fluxes were recorded within 10 minutes of placing the chambers on soil collar. Diurnal courses of canopy fluxes were recorded during four important crop growth stages, namely; seedling (DOY 140 to 170), tillering (DOY 170 to 180), heading (DOY 200 to 210) and maturity (DOY 210 to 220).

Gross Primary Production was calculated as:

$$GPP = (-NEE) + R_{eco} \quad (2.2)$$

where GPP is gross primary production, NEE is net ecosystem CO₂ exchange and R_{eco} is ecosystem respiration. Total daytime fluxes were calculated by integrating hourly carbon and water fluxes from 6:00 to 20:00 hr.

2.5 Estimation of evapotranspiration of rice field

Evapotranspiration of rainfed and paddy rice field was estimated with a Penman-Monteith type ET model modified by the Food and Agriculture Organization of the UN ($56PM$ model) (Allen

et al., 1998). In this study, the *56PM* model was modified specifically for rice before the estimation of daily *ET* and was reported detail in Chapter 4: Model development for evapotranspiration.

2.6 Estimation of daily carbon exchange of rice field

To study seasonal ecosystem water use efficiency of rainfed and paddy rice, daily ecosystem carbon fluxes were estimated. Gross primary production was estimated based on the chamber measured canopy light use efficiency, daily *NDVI* and *PAR* and estimation is based on the Monteith (1972):

$$GPP = LUE \times fPAR \times PAR \quad (2.3)$$

where *GPP* is the gross primary production, *LUE* is the canopy light use efficiency, *PAR* is the incident photosynthetic active radiation (Glenn et al., 2008; Running et al., 2004) and *fPAR* is the fraction of incident to absorbed *PAR*. *fPAR* was calculated by *NDVI-fPAR* model, following Choudhury (1987) and Goward and Huemmrich (1992):

$$fPAR = \frac{(NDVI - NDVI_{min})(fPAR_{max} - fPAR_{min})}{(NDVI_{max} - NDVI_{min})} + fPAR_{min} \quad (2.4)$$

where, *fPAR* is the fraction of incident to absorbed *PAR*, *NDVI* is the normalized vegetation index of rice field, *NDVI_{min}* and *NDVI_{max}* are minimum and maximum *NDVI*, *fPAR_{max}* is 0.95 while *fPAR_{min}* is 0.001.

Light use efficiency (*LUE*) is the ratio of gross primary production to absorbed *PAR* (Gitelson et al., 2014; Glenn et al., 2008; Monteith, 1972; Running et al., 2004) and thus *LUE* was calculated based on chamber measured *GPP* and absorbed *PAR*. Absorbed *PAR* (*aPAR*) was calculated as the product of *NDVI* derived *fPAR* (see equation (2.4)) and incident *PAR*.

Daily ecosystem respiration of rainfed and paddy rice was calculated following (Reichstein et al., 2002) as:

$$R_{eco} = R_{ecoref} \times f(T_{soil}) \times g(SWC) \quad (2.5)$$

where $g(SWC)$ is the saturation function (Bunnell et al., 1977a; 1977b; Reichstein et al., 2002); R_{ecoref} is reference ecosystem respiration, $f(T_{soil})$ is the function developed by Lloyd and Taylor, (1994) as:

$$f(T_{soil}) = e^{E_0 \left(\frac{1}{T_{ref}-T_0} - \frac{1}{T_{soil}-T_0} \right)} \quad (2.6)$$

where T_{ref} and T_0 are fixed to 15 and -46 °C, respectively, T_{soil} is the soil temperature at 5 cm depth; E_0 is the activation energy and was considered as a free parameter. Simulated CO₂ fluxes were verified by measured CO₂ fluxes.

2.7 Partitioning evapotranspiration

2.7.1 Partitioning diurnal ET fluxes by $\delta^{18}O$ isotopes

Sampling and measurement of source water $\delta^{18}O$: $\delta^{18}O_{rain}$ and $\delta^{18}O_{soil}$

Rainwater samples for $\delta^{18}O$ analysis were collected for every rain events throughout the crop growing season and samples were kept frozen in glass vials at -20 ° C until analysis. Soil samples (n=3 per each soil profile) for soil water extraction and $\delta^{18}O$ analysis were collected from 5, 10, 30, and 60 cm soil depth on DOY 172, 182, 192, 202, 205 and 218. Soil samples were stored in glass vials, immediately sealed with parafilm and kept frozen at -20 °C until soil

water extraction. Frozen rain and soil water samples were packed in an insulated shipping box with ice packs and were transported from S.Korea to Germany within 24 hours. Soil water samples were extracted by cryogenic distillation according to (Dubbart et al., 2013). Soil water samples were kept frozen until $\delta^{18}O$ analysis.

$\delta^{18}O$ analysis of rain and soil water samples was performed by CO₂ headspace equilibration on a Micromass Isoprime IRMS (Isoprime Elementar, Hanau, Germany) with micro gas autoamplifier (Micromass, UK). Water samples were equilibrated by He (5.0) with 5% CO₂ (5.0) for 24 hours at room temperature. For $\delta^{18}O$ calculation versus VSMOW, three different laboratory standards (light = -19.47 ‰, mean = -9.50 ‰ and heavy = 0.79 ‰) were analyzed 5 times prior to every batch of 10 water samples. Laboratory standards were regularly calibrated against VSMOW, SLAP and GISP water standard (IAEA, Vienna). Analytical precision was ± 0.1 ‰.

$\delta^{18}O_{ET}$, $\delta^{18}O_E$ and water fluxes measurement

A Cavity Ring-Down Spectrometer (CRDS, Picarro, Santa Clara, USA) was used to measure water fluxes and $\delta^{18}O$ isotopic composition of evaporated vapors from bare soil plots and canopy vegetation plots (three replications). All the water flux and $\delta^{18}O$ measurements were carried out in the mentioned plots where soil collars were permanently installed soon after seeding of rainfed rice, before the first sampling. The CRDS calibration was done three times a day using a standards delivery module and vaporizer (SDM, Picarro, Santa Clara, USA) with two laboratory standards that were regularly calibrated against VSMOW and SLAP. Measurement precision was <0.2 ‰. Ambient and sampling air (i.e., outlet air from the chamber) were measured alternately until stable values were reached, which was <10 min. Finally, 5 min interval values were averaged for the calculation of evaporation (E) and evapotranspiration (ET) with the gas exchange equations of (von Caemmerer and Farquhar, 1981). To control the condensation bias over $\delta^{18}O_{ET}$ fluxes measured during the morning, $\delta^{18}O_{ET}$ data collected at 12:00, 14:00 and 18:00 hours were used to partition evapotranspiration of rice.

Isotope signatures of evaporation and evapotranspiration were calculated by mass balance:

$$\delta^{18}O = \frac{w_{out}\delta_{out} - w_{in}\delta_{in}}{w_{out} - w_{in}} \quad (2.7)$$

where w_{out} and w_{in} are the H₂O concentration at outlet of the chamber and ambient air at the inlet of the chamber and δ_{out} and δ_{in} are their isotope ratios.

Calculation of $\delta^{18}O_E$, $\delta^{18}O_T$ and T/ET

Vegetation influences on evaporative water isotope signatures of a vegetation system and $\delta^{18}O$ signatures of bare-soil evaporation is reported to be significantly different to that of the soil underneath of vegetation (Dubbert et al., 2013; Wang et al., 2014; D. Yakir and Sternberg, 2000; Zimmermann et al., 1967). Therefore, $\delta^{18}O$ signatures measured on bare-soil plot cannot represent as the $\delta^{18}O$ signatures of the soil evaporation of a vegetation system ($\delta^{18}O_E$). Thus, oxygen isotope signatures of soil evaporation of canopy plot needs ($\delta^{18}O_E$) to be calculated although $\delta^{18}O_E$ was measured on bare-soil plot. $\delta^{18}O_E$ bare-soil plot was only used for the validation of calculated $\delta^{18}O_E$ of canopy plot. $\delta^{18}O_E$ of canopy plot was calculated following Craig and Gordon (1965):

$$R_E = \frac{1}{\alpha_k \alpha^+ (1-h)} (R_e - \alpha^+ h R_a) \quad (2.7.1)$$

where, R_E is the ratio of heavy to light water isotope ($^{18}O/^{16}O$) of evaporated water vapor and R_e is the isotope ratio of soil water at the evaporating site, which is the isotope ratio of extracted soil water. R_a is the isotope ratio of ambient water vapor. α_k is the kinetic fractionation factor and α^+ is the equilibrium fractionation factor (α_k and $\alpha^+ > 1$; Majoube, 1971; Merlivat, 1978).

$\delta^{18}O_T$ was calculated based on stable water isotope signature of leaf water at the evaporating sites ($\delta^{18}O_e$). Following Dongmann et al. (1974) (see also Cuntz et al., 2007; Dubbert et al., 2014), $\delta^{18}O_T$ was calculated as an iterative solution of the ordinary differential equation for leaf water at the evaporating sites in non-steady state (equation 2.7.2).

$$R_e(t + dt) = R_c + (R_e(t) - R_c)e^{-\frac{g_t w_i}{\alpha^k \alpha^+ V_m} dt} \quad (2.7.2)$$

where, $R_e(t + dt)$ is the isotope ratio of leaf water at the evaporating sites at time $t + dt$, $R_e(t)$ is the isotope ratio of leaf water at the evaporating sites at time t . g_t is total conductance ($\text{mol m}^{-2} \text{s}^{-1}$) calculated based on canopy temperature, w_i is the humidity in the stomatal cavity, i.e., vapor saturation at leaf temperature ($\text{mol H}_2\text{O mol air}^{-1}$), V_m the mesophyll water volume (mol m^{-2}), where gravimetric estimates of lamina water volume were used, α^k and α^+ are the kinetic and equilibrium fractionation factors, respectively. R_c is the Craig and Gordon steady-state isotope ratio at the evaporating sites, i.e., Eq. (2.7.1) rearranged for R_e with the isotope ratio of xylem. R_x was estimated by the source water isotopic ratio, i.e., soil water isotopic ratio assuming there was no fractionation during soil water uptake. Finally, the isotopic signature of plant transpiration was calculated by using the Craig and Gordon formulation (see Eq. (2.7.1)) after assuming R_e as the isotopic signature of leaf water at the evaporating sites in the non-steady-state.

After the calculation of $\delta^{18}O_E$ and $\delta^{18}O_T$ of rice canopy, contribution of transpiration to evapotranspiration ($T/ET = ft$) was calculated as:

$$ft = \frac{\delta^{18}O_{ET} - \delta^{18}O_E}{\delta^{18}O_T - \delta^{18}O_E} \quad (2.7.3)$$

2.7.2 Daily *ET* partitioning

Daily *ET* calculation is explained detail in Chapter 4. To partitioning daily *ET* to canopy transpiration and evaporation, canopy transpiration (T) was calculated by Penman Monteith (1965) equation but used the net radiation at the height of the crop canopy (R_{nsC}) instead of net solar radiation (R_n).

$$\lambda T = \frac{\Delta(R_{nsC} - G) + (\rho C_p (e_s - e_a)) / r_a}{\Delta + \gamma (1 + \frac{r_c}{r_a})} \quad (2.7.4)$$

where T is the canopy transpiration, λ is the latent heat of vaporization of water vapor, Δ is the slope of the saturation vapor pressure temperature relationship, R_n is the net radiation, G is the soil heat flux, $e_s - e_a$ is the vapor pressure deficit of the air, ρ is the mean air density at constant pressure, C_p is the specific heat of the air, r_a is aerodynamic resistance, r_c is the canopy resistance which was calculated based on measured leaf resistance and γ is the psychrometric constant. To estimate R_{nsc} , incoming net radiation (R_n) was partitioned into R_{nsc} (net radiation intercepted by crop canopy) and R_{nss} (residual net radiation reaching the soil surface). R_{nss} was calculated according to Beer's law (Zhou et al., 2006):

$$R_{nss} = R_n * \exp(-C_r LAI) \quad (2.7.5)$$

where C_r is the extinction coefficient of the vegetation for net radiation and is in the range of 0.5 to 0.7; 0.6 was applied in our case (Kelliher et al., 1995; Mo et al., 2004).

2.8 Crop water use efficiency of rice

In the search of profitable water saving rice production practices, the ratio of leaf's photosynthetic carbon assimilation rate to water loss (leaf water use efficiency) is regarded as a physiological yardstick to define the water use efficiency of a certain crop. On the other hand, for the water use efficiency of the crop under the real field situation, the ratio of biomass production per water use (agronomic water use efficiency) is another yardstick to define the water use efficiency (Alberto et al., 2013; Luo, 2010; Tuong and Bhuiyan, 1999). Moreover, the importance of rice production on global carbon and water cycling process is increasing (Kim et al., 2013; Lindner et al., 2015), demonstrating both the agronomical and ecological importance of rice worldwide. Therefore, considering water use efficiency from an ecological viewpoint (ecosystem water use efficiency (WUE_{eco})) is equally important specifically under global climate change scenarios (Tallec et al., 2013; Zeri et al., 2013). To fulfil the aim of this study, water use efficiency of rainfed and paddy rice were calculated at leaf, canopy, agronomic and ecosystem scales and at short-temporal and long-temporal scales.

2.8.1 Leaf water use efficiency

Leaf gas exchange measurement

To calculate leaf water use efficiency, maximum photosynthetic CO₂ assimilation (A_{max}) and transpiration (T) of an uppermost fully expanded leaf (at controlled leaf cuvette microenvironment at CO₂ concentration of 400 $\mu\text{mol mol}^{-1}$ and PAR of 1500 $\mu\text{mol m}^{-2} \text{s}^{-1}$) was measured at different growth stages by portable gas exchange analyzer (GFS-3000, Heinz Walz GmbH, Effeltrich, Germany). Based on measured A_{max} and T , instantaneous water use efficiency ($inWUE$), which is governed by environmental conditions, was calculated as the ratio of A_{max} to T . Moreover, intrinsic water use efficiency (WUE_i) which is a genetically defined water use efficiency of a plant and which is widely applied in the selection of higher water use efficient crops, was calculated as the ratio of measured maximum assimilation rate (A_{max}) to stomatal conductance (g_s). Measurements dates are provided in Table (II-2).

$\delta^{13}C$ analysis and integrated leaf WUE estimation

Development stage integrated leaf WUE was estimated based on $\delta^{13}C$ analysis of the leaf drymass of the whole canopy, i.e., leaves including the leaf sheaths, which was harvested at different crop growth stages. $\delta^{13}C$ discrimination ($\Delta^{13}C$) of leaf drymass is determined by the ratio of sub-stomatal CO₂ concentration (C_i) and atmospheric CO₂ concentration (C_a), which is linked to the photosynthetic CO₂ assimilation (A) and stomatal conductance (g_s) of leaf (Farquhar and Richards, 1984; Farquhar et al., 1989). Thus, at the end of every leaf and canopy flux measurement campaigns, leaves over the whole canopy were harvested (n=3 to 8) and frozen under -20 °C until they were freeze-dried by the vacuum freeze drier (SFDSF24, Samwon freezing co., Seoul, Korea). Freeze-dried leaf samples of the whole canopy were milled and samples were kept in exetainer until bulk leaf $\delta^{13}C$ was determined by IRMS (Isoprime Elementar, Hanau, Germany) with elemental analyzer. $\delta^{13}C$ Kauri wood (IAEA No. 298) as laboratory standard and Acetanilide (Carlo Erba Instruments Cod. 338 367 00) as C/N concentration laboratory standard were analyzed three times every ~10 samples. Measurements of $\delta^{13}C$ are referenced to Pee Dee Belemnite (PDB).

Growth stage integrated intrinsic WUE ($WUE_{i-\Delta^{13}C}$) of rainfed and paddy rice were determined based on stable isotopic discrimination of rice leaves (including the leaf sheaths) ($\Delta^{13}C$). $\Delta^{13}C$ was calculated from bulk leaf $\delta^{13}C$ analyzed from the freeze-dried leaf samples of the whole canopy harvested at different crop growth stages throughout the season.

2.8.2 Ecosystem and canopy water use efficiency

WUE_{eco} is defined as the ratio of gross primary production (GPP) to evapotranspiration (ET) (equation 2.8.2).

$$WUE_{GPP} = \frac{GPP}{ET} \quad (2.8.2)$$

Ecosystem WUE can also defined as the ratio of net ecosystem carbon exchange (NEE) to ET (equation 2.8.3).

$$WUE_{NEE} = \frac{NEE}{ET} \quad (2.8.3)$$

Although it is reported to include vapor pressure deficit effects on WUE (Beer et al., 2009; Dubbert et al., 2014b), there was any VPD effects on WUE during our monsoon 2013 field study in S. Korea. WUE_{eco} calculated after including VPD effects and excluding the VPD effects were no different (Data not shown). Thus, the VPD effects were excluded in equation (2.8.2 and 2.8.3).

2.8.3 Agronomic water use efficiency

Agronomic WUE (WUE_{agro}) is defined as the ratio of biomass production (grain yield) per amount of evapotranspiration (ET) (equation 2.8.4).

$$WUE_{agro} = \frac{\text{grain yield}}{ET} \quad (2.8.4)$$

All different *WUE* calculations were summarized in the *table II-3*.

2.9 Statistical Analysis

Two statistical tests were used to evaluate the model performance of *daily NDVI, LAI, ET, GPP and Reco* simulation: i) root mean square error (*RMSE*, equation 2.8.5) and ii) model efficiency (*ME*, equation 2.8.6) (Nash and Sutcliffe, 1970).

$$RMSE = \left[\frac{1}{N} \sum_{i=1}^n (S_i - M_i)^2 \right]^{1/2} \quad (2.8.5)$$

where, *RMSE* = root mean square difference, S_i = the i^{th} simulated value, M_i = the i^{th} measured value, and n = the number of data.

$$ME = 1 - \frac{\sum_{i=1}^n (S_i - M_i)^2}{\sum_{i=1}^n (M_i - M_{avg})^2} \quad (2.8.6)$$

where, *ME* = Nseff model efficiency, S_i = the i^{th} simulated value, M_i = the i^{th} measured value, M_{avg} = the averaged measured value, and n = the number of data.

To test for a relationships between daily average environmental variables (*Radiation, T_{air}, T_{soil}, VPD, SWC*) and measured canopy fluxes (sum of day time *NEE, GPP, Reco, ET*), a Spearman rank order correlation was performed. To compare the water use efficiencies of the rainfed rice and paddy rice, the normality of all of *WUEs* and *WUE* component data were tested by Shapiro-Wilk test. When the data is normally distributed, t-test was performed and otherwise, Wilcoxon-Mann-Whitney Rank Sum test (a non-parametric ANOVA) was performed. All statistical analysis were performed using R statistical software version 3.1.2 (R Core Team, 2014).

Table II-2 Field measurements campaigns carried out in 2013.

DOY	Rainfed canopy fluxes	Paddy canopy fluxes	NDVI – UAV	LAI, Biomass, $\Delta^{13}C$	Rainfed leaf fluxes	Paddy leaf fluxes
157					*	
168						*
167		*				
172	*		*	*		
175		*				
177						*
181					*	
182	*					
192	*		*	*		
196						*
197		*				
200		*				
202					*	
203	*					
206	*		*	*	*	
213						*
218	*					
219		*				
220			*	*		
224					*	
233			*	*		

Table II-3 Different water use efficiency calculation methods applied in this study

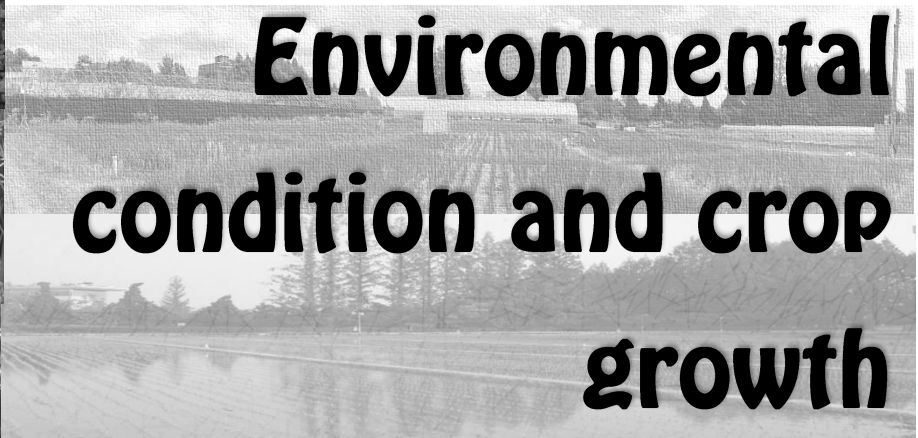
Water use efficiencies	Temporal scale	Spatial scale	Equations	Methods
WUE_i	Seconds to Day	Leaf	$WUE_i = A_{max}/g_s$ where A_{max} is maximum CO ₂ assimilation and g_s is stomatal conductance to H ₂ O	<ul style="list-style-type: none"> A_{max} and g_s of an uppermost fully expanded leaf was measured at different growth stages by a gas exchange analyzer with a leaf cuvette where microenvironment CO₂ 400 μmolmol^{-1} and PAR 1500 $\mu\text{molm}^{-2}\text{s}^{-1}$)
$inWUE$	Seconds to Day	Leaf	$inWUE = A/T$ where A is CO ₂ assimilation and T is transpiration	<ul style="list-style-type: none"> A_{max} and T of an uppermost fully expanded leaf was measured at different growth stages by a gas exchange analyzer with a leaf cuvette where microenvironment CO₂ 400 μmolmol^{-1} and PAR 1500 $\mu\text{molm}^{-2}\text{s}^{-1}$)
$WUE_{i\Delta^{13}C}$	Growth stage (Integrated days)	Bulk leaf	$WUE_{i\Delta^{13}C} = \frac{p_a \left(1 - \frac{\Delta^{13}C - a}{b - a} \right)}{1.6}$ where p_a is atmospheric CO ₂ partial pressure, a is the friction during binary diffusion of air which is 4.4‰, b is the friction duration carboxylation in C ₃ plants (29.5‰), factor 1.6 is the ratio of diffusivities of water vapor and CO ₂ in the air.	<ul style="list-style-type: none"> Leaf samples of the whole canopy of rainfed and paddy rice were collected at different growth stages (n=6). Harvested leaf samples were freeze-dried and stored under the moisture free condition, until the $\delta^{13}C$ analysis.
$inWUE_{\Delta^{13}C}$	Growth stage (Integrated days)	Bulk leaf	$WUE_{i\Delta^{13}C} / VPD$ (Farquhar et al., 1989)	<ul style="list-style-type: none"> Bulk leaf $\delta^{13}C$ was divided by the average VPD of the specific growth stage which biomass was harvested.

Table II-4 Different water use efficiency calculation methods applied in this study (Continued)

Water use efficiencies	Temporal scale	Spatial scale	Equations	Methods
$WUE_{c-Abg/Tc}$	Growth stage (Integrated days)	Canopy	$WUE_{c-Abg/Tc} = Abg/Tc$ <p>Where <i>Abg</i> is above ground biomass harvested at a specific crop growth stage and <i>Tc</i> is the integrated canopy transpiration of days within the specific growth stage</p>	<ul style="list-style-type: none"> Growth stage integrated canopy <i>WUE</i> was calculated as the ratio of dried above ground biomass harvested at a specific growth stage to the integrated daily canopy transpiration of the days within the specific growth stage.
WUE_{eco}	Day to Season	Ecosystem	<p>WUE_{eco} can be calculated as the ratio of gross CO₂ fluxes to evapotranspiration : $WUE_{eco} = GPP/ET$</p> <p>WUE_{eco} can also be calculated as the ratio of net CO₂ fluxes to evapotranspiration: $WUE_{eco} = NEE/ET$</p> <p>Where <i>GPP</i> is gross primary production, <i>NEE</i> is net primary production and <i>ET</i> is evapotranspiration .</p>	<ul style="list-style-type: none"> Daily WUE_{eco} was calculated based on measured ecosystem carbon and water fluxes, measured at different growth stages. Growing season WUE_{eco} was calculated based on the integrated carbon and water fluxes of the whole growing season (i.e., 120 days).
WUE_{agro}	Season	Field	$WUE_{agro} = Grain\ yield / ET$	<ul style="list-style-type: none"> Number of panicles and spikelets of three replicated sample plots (1m² size) of rainfed and paddy rice were counted. All the panicles from the sample plots were harvested and oven-dried. Randomly selected 1000 rice grains were weight and % of filled grains were counted. Finally, grain yield (Kgha⁻¹) is calculated and WUE_{agro} was calculated as the ratio of grain yield to crop seasonal total <i>ET</i> (m³ha⁻¹).
TE (Transpiration efficiency)	Season	Field	$TE = Grain\ yield / T$	<ul style="list-style-type: none"> Crop season <i>TE</i> is calculated as the ratio of <i>grain yield</i> (Kgha⁻¹) to crop season total transpiration (m³ha⁻¹).

3

Environmental condition and crop growth



III. Environmental condition and crop growth

3.1 Meteorological conditions of the study site

3.1.1 General meteorological conditions

The weather condition of the study area generally followed the typical East Asian temperate monsoon climate system. Annual total rainfall of 1332 mm in 2013 was less compared to 30 years annual average of 1391 mm (1981-2010) (Choi et al., 2013). There was a dry period with almost no rainfall between DOY 190 and 235, which resulted in very low ($0.18 \text{ m}^3\text{m}^{-3}$) volumetric soil, water content. However, because of high intensity of some rain events, the total precipitation, 972.6 mm of rice growing season (i.e., May to September) was above the mean of 30 years total precipitation, 799.2 mm. Daily solar radiation reached its annual maximum, $26.9 \text{ MJm}^{-2}\text{d}^{-1}$, in May but onward from the end of June, daily solar radiation declined, as low as $2.0 \text{ MJm}^{-2}\text{d}^{-1}$ in July with $5 (\pm 1.8)$ sunshine hours per day. Mean, minimum and maximum air temperature (T_{air}) during rice growing season were $23.4 \text{ }^\circ\text{C}$, $13.9 \text{ }^\circ\text{C}$ (May) and $28.8 \text{ }^\circ\text{C}$ (August), respectively. The highest daytime relative humidity (RH) was 98.31 %, occurring in August and the lowest daytime RH , 51.73 % in May. Minimum and maximum wind speed was 0.3 (May) to 2.37 ms^{-1} (July) (Figure III- 1a, 1b, 1c).

Under paddy rice condition, water availability was not limited as irrigation was supplied while rainfed rice had two significant dry periods due to the lack of precipitation. The first dry period was reported in between DOY 190 and 205, during the last stage of panicle initiation (Booting) and the second dry period was reported in between 215 and 235, during the flowering stage. Both dry periods happened during the critical crop growth stages, which are reported as the most susceptible growth stages to water stress. Despite of those two dry period, rainfed rice also had enough water supply due to high intensity rain events in monsoon 2013.

An increase in air temperature (T_{air}) was reported during the dry period (between DOY 190 and 235, Figure III-1). T_{air} during that period was the highest of monsoon rice growing season 2013.

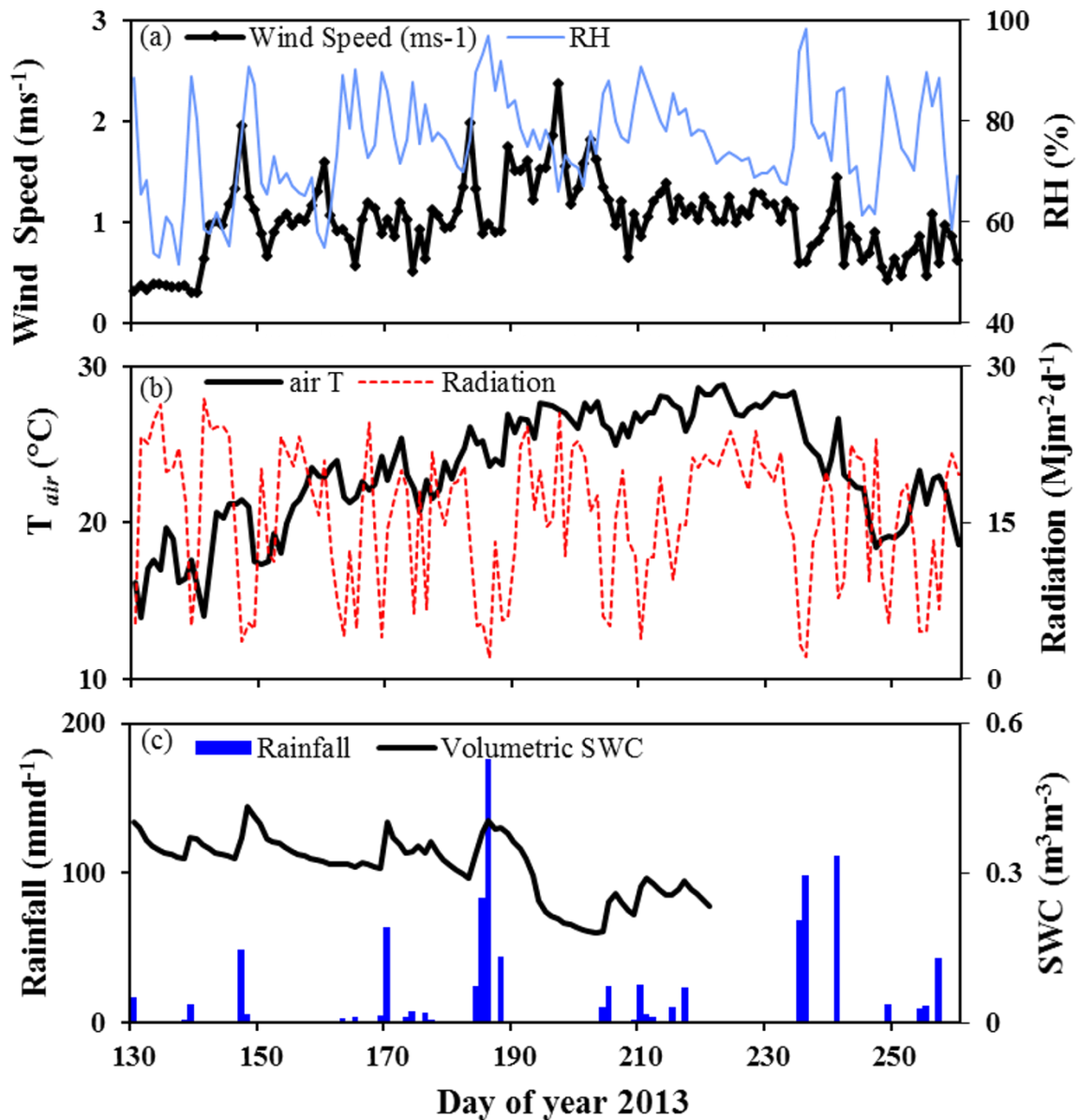


Figure III-1 Meteorological conditions during monsoon 2013. (a) daily averages of wind speed (ms^{-1}) and relative humidity (%); (b) daily averages of air temperature ($^{\circ}\text{C}$) and radiation ($\text{Mjm}^{-2}\text{d}^{-1}$); (c) daily total rainfall (mmd^{-1}) and daily average volumetric soil water content at 5cm depth (m^3m^{-3}). *Note:* Volumetric soil water content data is not available starting from the day of year 221 as the volumetric soil water sensors were uninstalled from the site of study, to ship back to Bayreuth.

3.2 Crop growth and development of rainfed and paddy rice

3.2.1 LAI, plant height and biomass development

Both rainfed and paddy rice had similar trends of *LAI* although rainfed rice showed slightly lower *LAI* from the end of June onwards (*Figure III-2*, black and white circles). The peak growth for both rainfed and paddy rice was in the end of July with a maximum plant height of 0.80 ± 0.97 m and 0.89 ± 0.66 , and *LAI* of 2.97 ± 1.21 m²m⁻² and 3.29 ± 0.65 m²m⁻², respectively (*Table 3.1*). Seasonal trend of *LAI* was simulated for the field scale and seasonal *LAI* was the mean *LAI* of the whole rice field. Thus, variation between mean *LAI* of the field and calculated based on the biomass harvest was noted. Seasonal *LAI* and plant height of both paddy and rainfed rice differed significantly (*LAI*: $W=101$, $p < 0.001$; plant height: $W= 93$, $p < 0.001$; $n=6$). Field measured *LAI* fitted well to the simulated daily values by GRAMI crop growth model ($R^2 = 0.76$ and $Nseff$ $ME=0.65$).

Table III-1 Measured mean leaf area index and plant height of rainfed and paddy rice ($n=6 \pm$ SD)

DOY	Rainfed		Paddy	
	LAI (m ² m ⁻²)	Height (m)	LAI (m ² m ⁻²)	Height (m)
172	0.74 ± 0.28	0.12 ± 0.10	1.14 ± 0.33	0.18 ± 0.05
192	2.12 ± 0.40	0.60 ± 0.22	2.99 ± 0.42	0.64 ± 0.12
206	2.49 ± 0.40	0.78 ± 0.32	3.78 ± 0.51	0.88 ± 0.36
220	2.69 ± 0.01	0.80 ± 0.97	3.38 ± 0.40	0.89 ± 0.66
233	2.28 ± 0.19	0.80 ± 0.22	2.89 ± 0.33	0.86 ± 0.28

Crop growth and development of rice is classified in three stages (International Rice Research Institute classification): vegetative, reproductive and maturity stage or four stages (Food and Agriculture Organization classification): initial, crop development, mid-season and late season stage. Seasonal crop development of rainfed and paddy rice was shown in *figure III-2*. Both rainfed and paddy rice were seeded on the same date but rainfed rice was directly seeded in the

field while paddy rice was seeded in the nursery under controlled environment. Germination of rainfed rice took almost 20 days while paddy rice took less than 10 days. As the transition of initial crop growth stage to crop development stage is classified by the initiation of panicle primordium, initial growth stage of paddy rice was 10 days shorter than that of rainfed rice. As shown in *figure III-2*, the biomass development (leaf area and stem elongation) changed rapidly during crop development and mid-season stages (in June and July) which resulted a significant *LAI* and biomass weight differences between the start and end of the crop growth stage. Paddy rice developed faster than rainfed rice showing earlier panicle initiation, heading and flowering. Paddy rice started grain filling at around DOY 210 while rainfed rice grain filled at around DOY 215, five days later than paddy rice. Rainfed rice had shorter crop-development and Mid-Season stage compared to paddy rice (5 days shorter) However, both rainfed and paddy rice reached maturity almost at the same time.

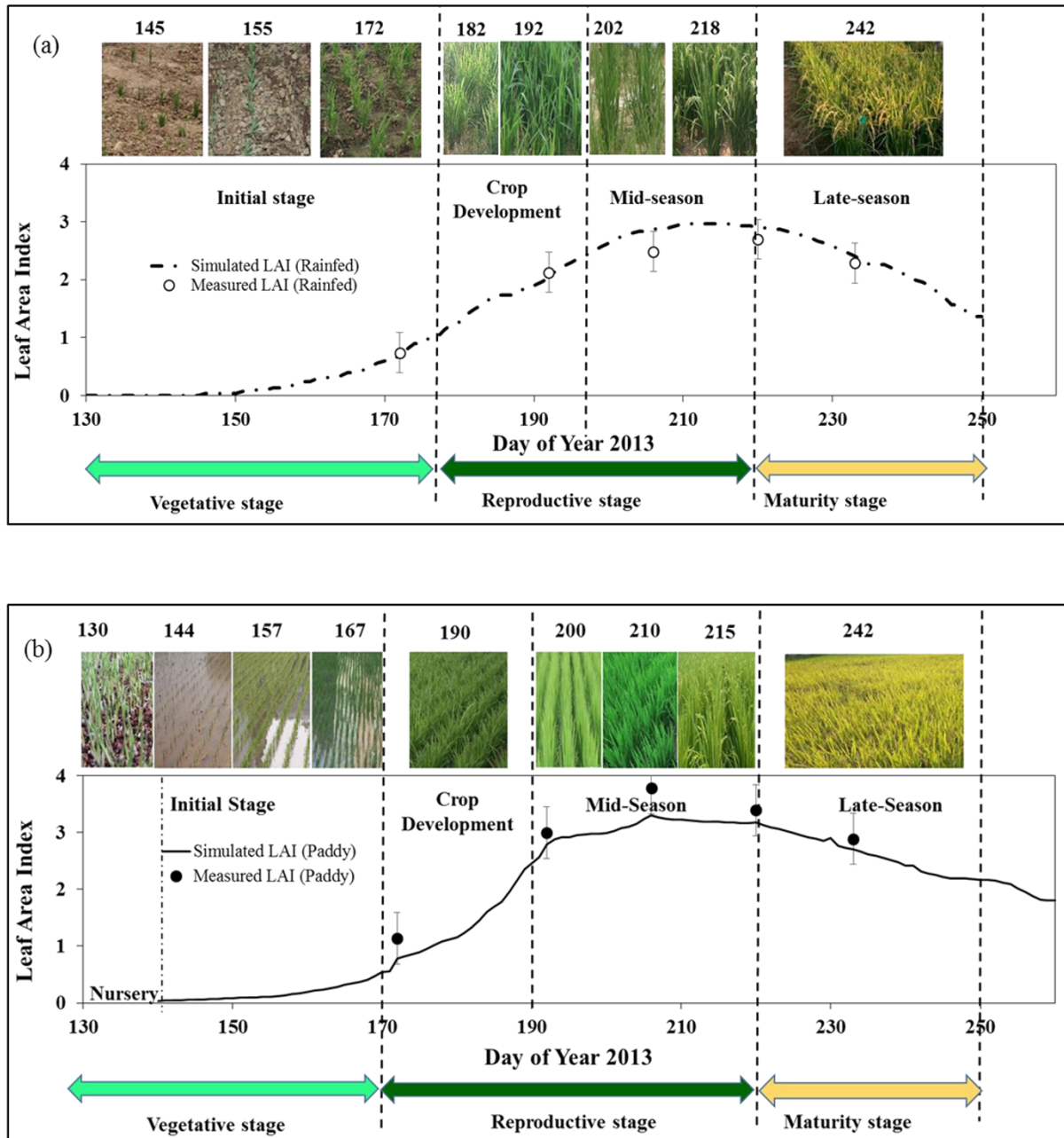


Figure III-2 Seasonal leaf area index, crop growth and development of (a) rainfed and (b) paddy rice. Crop growth stages were classified according to International Rice Research Institute (IRRI) and Food and Agricultural Organization (FAO). IRRI classified rice crop growth as vegetative, reproductive and maturity stages while FAO classified Initial stage (IS), Crop development (CD), Mid-Season (MS) and Late-Season (LS) stages. Numbers above the pictures were day of year of photo-shoot.

During the late-season stage, on DOY 240, total biomass of rainfed and paddy rice was harvested, dried and compared (*Figure III.3*). Similar to *LAI*, plant height and crop development of rainfed and paddy rice, total dry weight (rainfed rice = $16.62 \pm 1.56 \text{ tha}^{-1}$; paddy rice = $18.13 \pm 1.17 \text{ tha}^{-1}$) was also significantly different ($W = 138, p < 0.05$). Higher total dry weight in paddy rice was mainly due to its significantly higher stem weight ($W=94, p < 0.05$) and slightly higher grain weight ($W=26, p = 0.24$). Higher root shoot ratio was also observed in the rainfed rice (0.28) compared to paddy rice (0.19).

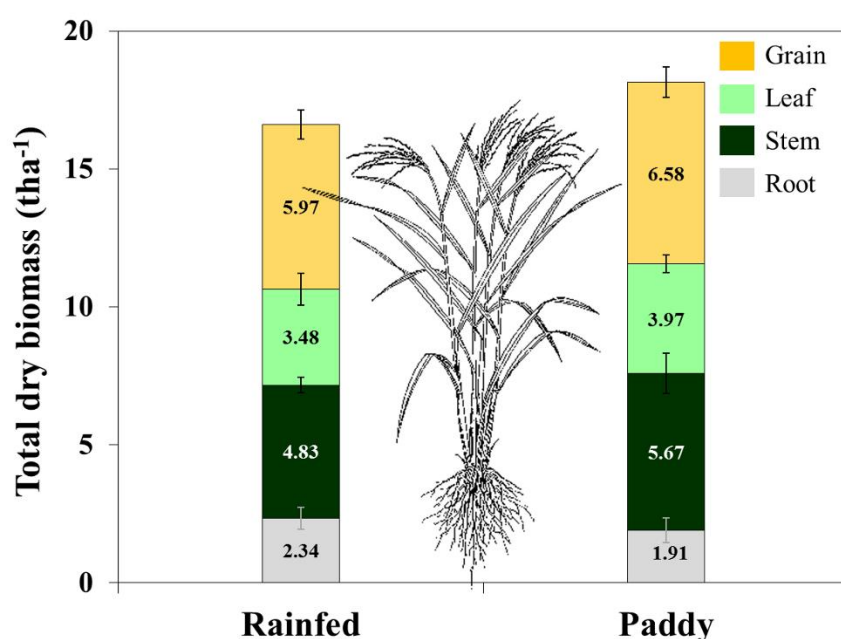


Figure III-3 Biomass distribution of rainfed and paddy rice. Biomass sampling was done during the late season stage. (n=3 - 8, \pm SD).

3.2.2 Crop yield and Yield components

Grain yield of rice is defined by genetically fixed physiologic factors, environmental conditions and resource use limitation. Crop yield of rice depends on the so-called yield components (number of panicles, number of spikelets and percentage of filled-grain and 1000 grain weight) which are genetically fixed parameters for a certain rice variety and which govern rice grain yield. Yield components of a certain rice variety should not vary significantly except the slight variations due to other factors such as microclimatic, resource availability, pest and diseases.

All of the yield components and grain yield of rainfed rice were not significantly different (Table III-2) as the same rice variety (*Unkwang*) was planted under rainfed and paddy conditions. However, rainfed had slightly higher number of panicle per square meter and 1000-grain-weight with lower number of spikelet per square meter and filled grain percent. Grain yield was also not significantly different but paddy rice was slightly higher than that of rainfed rice (only 9.53 % higher).

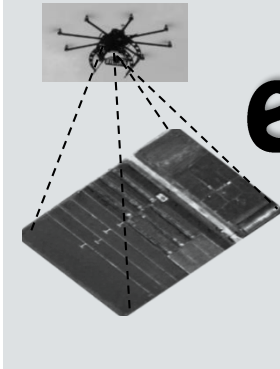
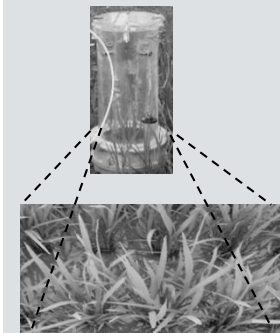
Table III-2 Statistics for yield components and grain yield of rainfed and paddy rice (n=3 to 8, \pm SD). Wilcoxon-Mann-Whitney Rank Sum test was performed to test the differences between rainfed and paddy rice. W and p are test statistics of Wilcoxon-Mann-Whitney Rank Sum test.

Crop	Yield components				Yield (tonha ⁻¹)
	No. Panicle m ⁻²	No. Spikelets m ⁻²	% filled-grain	1000-grain-weight	
Rainfed	225.17 \pm 25.56	105.00 \pm 5.26	0.86 \pm 0.02	29.38 \pm 0.75	5.98 \pm 0.55
Paddy	221.83 \pm 9.63	108.66 \pm 4.89	0.94 \pm 0.01	29.14 \pm 0.62	6.61 \pm 0.63
W	15.50	11.00	11.00	21.00	26.00
p	> 0.05	> 0.05	> 0.05	> 0.05	> 0.05

3.3 Summary

Although rainfed rice had longer initial growth stage due to the lower soil temperature (15.31 to 20.22 °C) during the germination period, it flowered and matured within the same period with paddy rice. Crop growth and development of rice was rapid in both rainfed and paddy condition and *LAI* of the starting point of a growth stage significantly different to that of end of that stage. *LAI*, plant height and total biomass dry weight of paddy rice was higher than that of rainfed rice. Yield components and grain yield of paddy and rainfed rice were not significantly different although rainfed rice had 9.53 % lower grain yield compared to paddy rice.

4



**Model
development for
evapotranspiration**



IV. Model development for evapotranspiration

4.1. Estimation of evapotranspiration

Evapotranspiration can be estimated by monitoring the exchange of energy/water above the vegetated surface (for example, eddy covariance systems, canopy chamber measurements), or by means of hydrological balance (Lysimeters, soil water budget) (Kool et al., 2014). Knowing the ET of a certain crop, in other words, crop actual water use, can improve irrigation water management and reduce unnecessary water loss. Therefore, models estimating ET have been developed since the early 1950s.

Penman (1948) developed the first evaporation model for open water, bare soil and grass. Following Penman's work, Monteith (1965) modified the model by combining crop physiological aspects to Penman's purely physical model (Ziemer, 1979). Since then, Penman Monteith (1965)'s so called "one layer PM model" is widely applied to estimate evapotranspiration. Following the Penman Monteith (1965), the Food and Agriculture Organization developed a simplified Penman Monteith model. The *FAO* modified Penman Monteith model is described detail in the *FAO's* irrigation and drainage paper (No. 56) and thus the model is called as *FAO 56 PM* or *56PM* and widely applied by agronomists (Allen et al., 1998) (Equation 4.1). The *56PM* estimates ET based on the reference crop evapotranspiration (ET_0) multiplied to the sum of the transpiration coefficient (K_{cb}) and a evaporation coefficient (K_e) of the crop of interest (Alberto et al., 2011, 2014; Allen et al., 1998; Payero and Irmak, 2013).

$$ET = (K_{cb} + K_e) \times ET_0 \quad (4.1)$$

where ET is the crop evapotranspiration, K_{cb} is the transpiration coefficient equivalent to the ratio of transpiration to potential evapotranspiration, K_e is the evaporation coefficient equivalent to the ratio of soil evaporation to potential evapotranspiration, ET_0 is the reference evapotranspiration. The *FAO 56 PM ET* model (equation 4.1.) firstly calculate evapotranspiration for a well-watered and healthy reference grass or alfalfa crop by applying fixed physiological parameters for grass and alfalfa. Thus, evapotranspiration of reference

grass or alfalfa is termed as reference crop ET (ET_0). Later, ET for the crop of interest is estimated multiplying ET_0 and the crop coefficient of the crop of interest and its respective growth stage. The *FAO 56 PM* model has two approaches of crop ET estimation: single crop coefficient (K_c) approach, in other words, an evapotranspiration coefficient approach and a dual crop coefficient (K_{cb}) approach, where ET coefficient is accounted separately into a transpiration coefficient (K_{cb}) and a soil evaporation coefficient (K_e) (Allen et al., 1998).

4.1.1 Reference crop ET (ET_0)

As pointed out above, the reference crop ET (ET_0) is the evapotranspiration of a reference crop, which is a well-managed and watered grass or alfalfa. ET_0 estimation can be done by parameterization of the classical Penman - Monteith (1965) model. Models such as Priestley and Taylor (1972) (PT) and Makkink (1957) (Mk) simply multiply the microclimatic factors with dimensionless empirically derived correlation coefficients. The Mk and PT are ET_0 estimations based on energy budget concept while the *56PM* is based on combination of the plant physiological and energy budget concepts. The *56PM* (Allen et al., 1998) parameterizes all crop factors such as canopy resistance or aerodynamic resistance by applying measured standard values of the reference crop (grass in this study) following all the calculation steps of the classical Penman-Monteith (1965).

As ET of a certain crop is estimated based on the reference crop ET (ET_0), the precision of ET estimation depends on how well reference crop ET (ET_0) is estimated. Thus, different reference crop ET (ET_0) models were tested in this study, namely: 1) the *56PM* model which is a highest data demanding method among the simplified *PM* type ET models; 2) the Priestley –Taylor model (PT) which only needs radiation, temperature and relative humidity, and 3) the Makkink's model (Mk) which also needs the same data as the PT .

Estimation of ET_0 by the 56PM model (1998)

Reference crop evapotranspiration of a grass cropped surface was calculated by the *56PM* model (*56PM*), which is a modified version of the Penman-Monteith (1965) ET model (Allen et al., 1998):

$$\lambda ET_0 = \frac{\Delta(R_n - G) + (\rho C_p (e_s - e_a)) / r_a}{\Delta + \gamma \left(1 + \left(\frac{r_c}{r_a}\right)\right)} \quad (4.1.1)$$

where ET_0 is reference crop evapotranspiration, λ is the latent heat of vaporization of water vapor, Δ is the slope of the saturation vapor pressure temperature relationship, R_n is the net radiation, G is the soil heat flux, $e_s - e_a$ is the vapor pressure deficit of the air, ρ is the mean air density at constant pressure, C_p is the specific heat of the air, r_a is the aerodynamic resistance, r_c is the canopy resistance and γ is the psychrometric constant.

The parameterization of the *56PM* is done by assuming a reference grass crop of 0.12 m height with a canopy resistance of 70 sm^{-1} and albedo of 0.23. Based on that assumption, aerodynamic resistance (r_a) to vapor, heat and momentum transfer from the crop canopy at the standardized height of 2 m above the crop canopy which is 0.12 m height is calculated.

$$r_a = \frac{\ln\left(\frac{z_m - d}{z_{om}}\right) \left(\ln\left(\frac{z_h - d}{z_{oh}}\right)\right)}{k^2 u_2} = \frac{208}{u_2} \quad (4.1.2)$$

where r_a is aerodynamic resistance (sm^{-1}) at 2 m height, z_m is height of wind speed measurement (m), z_h is height of humidity measurements, z_{om} is roughness length governing the momentum transfer (m) which is $0.123h$ according to Allen (1998), z_{oh} is roughness length governing the heat and vapor transfer (m) which is $0.1z_{om}$ according to (Allen et al., 1998), k is von Karman's constant (0.41) and u_2 is wind speed at 2 m height.

Canopy resistance of grass reference crop is calculated by equation (4.1.3) by assuming a crop height of 0.12 m, stomatal resistance of a single leaf of 100 sm^{-1} .

$$r_c = \frac{r_l}{LAI_{active}} \approx 70 \text{ sm}^{-1} \quad (4.1.3)$$

Where r_c is canopy resistance (sm^{-1}), r_l is resistance of a grass leaf (sm^{-1}) and LAI_{active} is sunlit leaf area index.

Finally, the parameterized *56PM* model to calculate ET_0 of grass reference surface (equation 4.2) can be described as:

$$ET_0 = \frac{0.408\Delta(R_n - G) + \gamma \frac{900}{T+273} u_2 (e_s - e_a)}{\Delta + \gamma(1 + 0.34u_2)} \quad (4.1.4)$$

where ET_0 is reference crop evapotranspiration, Δ is the slope of the saturation vapor pressure temperature relationship, R_n is the net radiation, G is the soil heat flux which is zero at daily ET calculation (Allen 1998), $e_s - e_a$ is the vapor pressure deficit of the air, r_a is aerodynamic resistance, r_c is the canopy resistance and γ is the psychrometric constant.

Estimation of ET_0 by the Priestley and Taylor's model (1972)

Limitations of the *56PM* ET_0 model are the need of multiple climatic data and canopy resistance parameterization and better estimation of ET depends on quality and availability of climatic data (Allen 2006). Thus, in case of limited climatic data availability, other ET_0 models which could perform as well as *56PM* needs to be tested. The Priestley and Taylor (1972) (*PT*) proposed a reference evapotranspiration model (ET_0) which main input parameters are net radiation, temperature and relative humidity.

$$ET_0 = \alpha * \frac{\Delta}{\Delta + \gamma} * (R_n - G) \quad (4.1.5)$$

where $\alpha = 1.26$, which is empirically determined dimensionless correlation, Δ is the slope of the saturation vapor pressure temperature relationship, R_n is the net radiation, G is the soil heat flux and γ is the psychrometric constant. The *PT* model is widely applied in the case of unavailability of meteorological variables needed for the *56PM* model, such as wind speed

Estimation of ET_0 by the Makkink's model (1957)

Reference crop evapotranspiration of a grass cropped surface (ET_0) was calculated by the Makkink model (Makkink, 1957):

$$ET_0 = 0.61 * \frac{\Delta}{\Delta + \gamma} * \frac{R_s}{2.45} - 0.12 \quad (4.1.6)$$

where Δ is the slope of the saturation vapor pressure temperature relationship, R_s is the solar radiation and γ is the psychrometric constant.

The 56PM modifications

The tendency of underestimation of the 56PM model has been reported and the fixed r_c value of 70 sm^{-1} is considered as a possible reason (Rana et al., 1994; Steduto and Hsiao, 1998; Steduto et al., 2003, 1997; Todorovic, 1999; Ventura et al., 1999; Zhao, 2014). Allen et al. (2006) argued to keep using $r_c = 70 \text{ sm}^{-1}$ for daily ET_0 calculations. However, studies on irrigated grassland in different locations across the world observed an r_c range from 10 to 130 sm^{-1} (Katerji and Rana, 2006), highlighting the need of localized and case specific parameterization of canopy resistance (r_c) as recommended by Monteith, 1965. Thus, the 56PM model (equation 4.5) was modified by replacing the recommended r_c value (70 sm^{-1}) with 80, 100 and 120 sm^{-1} . 56PM model modified with new r_c values were named as: $m56PM_{80}$, for the 56PM model with fixed $r_c = 80 \text{ sm}^{-1}$; $m56PM_{100}$ for the 56PM model with fixed $r_c = 100$ and $m56PM_{120}$ for the 56PM model with fixed $r_c = 120$.

Estimation of the ET_0 specifically for rice: $m56PM_{mrc}$

As rice is one of the most economically important crop and a major agroecosystem of global land cover, a better ET_0 estimation specifically for the rice is needed. In other words, better ET_0

estimation of well-watered rice is necessary for the better estimation of actual evapotranspiration of rice or at least for the better estimate of potential evapotranspiration of rice. Thus, instead of the hypothetical parameters for a grass canopy provided by the *56PM*, measured crop physiological parameters (leaf resistance to water vapor transfer, plant height and *LAI*) for well-irrigated and healthy rice were applied to estimate reference crop evapotranspiration of rice.

4.1.2 Performance of different ET_0 models

The accurate estimate the reference crop ET (ET_0) is the key for the best estimation of actual evapotranspiration (ET). Hence, different ET_0 estimation methods were compared, evaluated to select the best-performed ET_0 estimation method. Reference crop ET was estimated by the Makkink (1957) (*Mk*), the Priestley-Taylor (1972) (*PT*), the *FAO 56PM* (1998) (*56PM*), the modified *56PM* models (*m56PM₈₀*, *m56PM₁₀₀*, *m56PM₁₂₀*) and evaluated the best estimate by comparing with the *m56PM_{mrc}* model which estimated reference crop ET of rice while the rest estimate that of reference grass. All models (*Mk*, *PT*, *56PM*, *m56PM₈₀*, *m56PM₁₀₀*, *m56PM₁₂₀*) underestimated ET_0 compared to *m56PM_{mrc}* which used healthy and well-maintained rice as reference crop. The *Mk* performed better than other models ($R^2=0.63$, $SE=0.39$, $p<0.05$). Out of six different test models, the *PT* overestimated ET_0 compared the *56PM* model with measured r_c (*m56PM_{mrc}*) ($R^2=0.53$, $SE=0.46$, $p<0.05$). For the classical *FAO 56* reference ET estimation for paddy rice, applying fixed r_s value at 120 sm^{-1} (*m56PM₁₂₀*) improved the reference ET estimation rather than using the recommended value, 70 sm^{-1} .

Table IV-1 Correlation coefficient between conventional reference crop evapotranspiration (ET_0 , grass as reference crop) models and ET_0 model modified specifically for rice (healthy, well-irrigated rice as reference crop). R^2 is determination of coefficients, SE is standard error, SD is standard deviation, p (t-test) is level of significant of the test, ET_0 ratio is the ratio of rice crop ET_0 and grass reference crop ET_0 , and Ranking is model performance ranked according to the ratio of $m56PM_{mrc}$ ET_0 to other ET_0 .

Model name	R^2	SE (SD)	p (t-test)	ET_0 ratio	Ranking
	n=120				
<i>Mk</i>	0.65	0.39 (0.99)	<0.05	1.22	2
<i>PT</i>	0.53	0.46 (0.94)	<0.05	1.59	6
<i>56PM</i>	0.60	0.42 (0.64)	<0.05	1.10	5
<i>m56PM₈₀</i>	0.61	0.42 (1.08)	<0.05	1.08	5
<i>m56PM₁₀₀</i>	0.62	0.41 (1.05)	<0.05	1.05	4
<i>m56PM₁₂₀</i>	0.63	0.40 (1.02)	<0.05	1.02	3
<i>m56PM_{mrc}</i>	-	-	-		1

4.2 Crop coefficients

4.2.1 Basal crop coefficient (K_{cb}): The *FAO* recommended K_{cb}

In the *FAO 56* dual crop coefficient approach of Allen et al. (1998), the basal crop coefficient or transpiration coefficient (K_{cb}) is calculated based on seasonal change in vegetation ground cover. Estimates of K_{cb} for several crops including rice is provided as a K_{cb} curve with four growth stages (initial, development, mid-season, and late season) and it is recommended to use the estimated K_{cb} values after specific climatic adjustment:

$$K_{cb} = K_{cb (Recommended)} + [0.04(u_2 - 2) - 0.004(RH_{min} - 45)] \left(\frac{h}{3}\right)^{0.3} \quad (4.2.1)$$

where, K_{cb} (*Recommended*) is the recommended K_{cb} values for rice provided in the *FAO* irrigation and drainage paper 56, u_2 is the growing season mean daily wind speed at 2 m height, RH_{min} is the growing season minimum value of RH and h is the growing season mean plant height.

Although the *FAO 56* does not recommend adjusting K_{cb} for the initial growth stage, initial K_{cb} adjustment was also done in this study because of the use of younger seedlings. Transplanting younger seedlings (10 days after the germination), suspected to have lower initial K_{cb} than recommended values which are derived from paddy fields transplanted with seeding at older age (between 20 and 30 days after germination).

Table IV-2 The *FAO56* recommended basal crop coefficients (K_{cb}) and adjusted K_{cb} by climatic conditions at the site of study by equation 4.2.1.

	Initial	Mid-season	Late-season
<i>FAO 56</i> K_{cb}	1	1.15	0.45
<i>Adjusted</i> K_{cb}	0.93	1.09	0.39

The *FAO 56* recommended developing a K_{cb} value for the whole period of each growth stage as its K_{cb} value is mean value for the whole growth stage, i.e., K_{cb} initial is the mean K_{cb} value of the whole initial growth stage. Therefore, the *FAO* recommended K_{cb} curve (Basal crop coefficient curve) can be developed by a simple integration of the initial, mid-season and late-season K_{cb} values in *table IV.2*. However, as mentioned in section (3.2), *LAI* development of rice within a growth stage was very fast. For example, *LAI* of paddy rice on DOY 172 and 192, which were the start and end of crop development stage, were significantly different. Therefore, K_{cb} of the start and end of crop development stage might significantly different and applying mean K_{cb} value for a certain crop growth stage, especially after the crop development stage when canopy development change very first, may not be the best way to estimate the daily crop *ET*. Thus, instead of the recommended K_{cb} values, a better temporal resolution of basal crop coefficient curve needs to be developed.

4.2.2 Basal crop coefficient (K_{cb}): *NDVI* derived K_{cb}

A daily basal crop coefficient (K_{cb}) curve representing the actual crop growth and development was developed after following Choudhury (1994). Daily K_{cb} of the whole rice field was calculated based on daily and high resolution *NDVI* of the whole field:

$$K_{cb} = 1 - \left[\frac{NDVI_{max} - NDVI}{NDVI_{max} - NDVI_{min}} \right]^{k'/k''} \quad (4.2.2)$$

where $NDVI_{max}$, $NDVI_{min}$ and $NDVI$ are vegetation indices for dense canopy, bare soil and normal vegetation respectively, k' is a damping coefficient derived from the correlation of *LAI* and the ratio of canopy transpiration to potential evapotranspiration, k'' is a damping coefficient derived from correlation of *LAI* and *NDVI*. The relationships between the ratio of unstressed transpiration (T) to reference crop evapotranspiration (ET_0) and leaf area index (*LAI*), relationships between *LAI* and vegetation indexes has been shown (Choudhury, 1994; Duchemin et al., 2006; Sellers, 1985). Damping coefficient k' is the coefficient derived by exponential correlation of the ratio of calculated daily T to reference ET_0 and *LAI* while damping coefficient k'' is the coefficient derived by exponential correlation of *LAI* and *NDVI*.

4.2.3 Evaporation coefficient: K_e

The evaporation coefficient (K_e) was calculated according to Allen et al. (1998). K_e is maximal when the topsoil is wet or flooded and K_e is minimal to zero when the topsoil is dry. The upper limit of K_c (K_{cmax}), an upper limit of evaporation and transpiration from cropped surfaces, need to be defined before calculating K_e since the evaporation rate never equaled evapotranspiration and K_e needs to be limited by K_{cmax} .

$$K_{cmax} = \max \left(\left\{ 1.2 + [0.04(u_2 - 2) - 0.004(RH_{min} - 45)] \left[\frac{h}{3} \right]^{0.3} \right\}, (K_{cb} + 0.05) \right) \quad (4.2.3)$$

where K_{emax} is the upper limit of evaporation and transpiration from a cropped surface, u_2 is the wind speed (ms^{-1}), RH_{min} is the minimum relative humidity and K_{cb} is the transpiration coefficient derived by equation (4.2.2).

The soil evaporation process is assumed to be controlled by stages: Stage 1: an energy limiting stage and Stage 2: a falling-rate stage (Allen et al., 1998; Monteith, 1981; Ritchie, 1972). The soil evaporation reduction coefficient (K_r) is 1 when the soil surface is wet; K_r decreases when the water content in the topsoil is limiting, and K_r becomes zero when the total evaporable water (TEW = maximum amount of water that can be evaporated) in the topsoil is depleted. TEW for a complete drying cycle was estimated as:

$$TEW = 1000(\theta_{FC} - 0.5\theta_{WP}) * Z_e \quad (4.2.4)$$

where TEW is the maximum depth of water that can evaporated from the soil when topsoil is completely wet (mm), θ_{FC} is the soil water content at field capacity (m^3m^{-3}), θ_{WP} is the soil water content at wilting point (m^3m^{-3}) and Z_e is the depth of surface soil layer (0.1 m). K_r for paddy rice is fixed at 1 since soil surface is flooded most of the time and soil surface is wet even during the drainage period. K_r of rainfed rice was calculated as:

$$K_r = (TEW - D_{e,i-1}) / (TEW - REW) \quad (4.2.5)$$

where K_r is the soil evaporation reduction coefficient dependent on soil water depletion, $D_{e,i-1}$ is the cumulative depth of evaporation depletion from topsoil at the end of the day ($i-1$), TEW is the total evaporable water (mm) calculated by equation (4.2.4) and REW is the readily evaporable water which is cumulative depth of depletion of evaporable water from the soil surface layer at the end of stage one. During stage one drying, K_r is 1 and during stage two drying, K_r is 1 when $D_{e,i-1} \leq REW$.

Finally, the evaporation coefficient (K_e) is calculated as:

$$K_e = K_r(K_{cmax} - K_{cb}) \leq FEW * K_{cmax} \quad (4.2.6)$$

where K_e is the soil evaporation coefficient, K_r is the evaporation reduction coefficient, K_{cmax} is the maximum value of K_c and FEW is the fraction of soil surface exposed and wetted.

4.2.4 Crop coefficients of rainfed and paddy rice

Crop evapotranspiration can be estimated by multiplying the reference crop ET (ET_0) to the sum of crop transpiration (K_{cb}) and soil evaporation (K_e) coefficients of the crop of interest. Since crop transpiration and soil evaporation strongly link to the status of crop development and fraction on ground cover, transpiration and evaporation coefficients of paddy and rainfed rice was estimated based on seasonal and spatial $NDVI$ analysis. The basal crop coefficient of paddy rice and rainfed rice (*Figure IV-1*) were not significantly different except during the initial crop growth stage (IS) when paddy rice had significantly higher K_{cb} than rainfed rice ($W=20.2$, $p \leq 0.05$). Based on 0.5 x 0.5 square meter scale spatial K_{cb} map, significant spatial variation of K_{cb} was found throughout the crop growing season in rainfed rice ($W=21.5$, $p \leq 0.05$). However, in paddy rice, there was no significant spatial variation of K_{cb} starting from Mid-season stage (MS). A significant increase in K_{cb} was found along with the crop growth and development of rice. Leaf area development in both rainfed and paddy rice was fast starting from the crop development stage and increase in LAI were significant even within 15 days. Thus, $NDVI$ and K_{cb} of both paddy and rainfed rice differ significantly within ~15 growing days highlighting the needs of K_{cb} curve for rice with better temporal resolution than the *FAO* recommended 3 growing stage average K_{cb} curve (*Table IV-2*). Moreover, the *FAO* recommended K_{cb} for initial stage of rice was significantly higher than $NDVI$ derived K_{cb} while the *FAO* recommended K_{cb} for Late-season stage was significantly lower than that of $NDVI$ ($W=20.01$, $p < 0.05$). However, the *FAO* recommended K_{cb} and $NDVI$ derived K_{cb} for the mid-season were not significantly different.

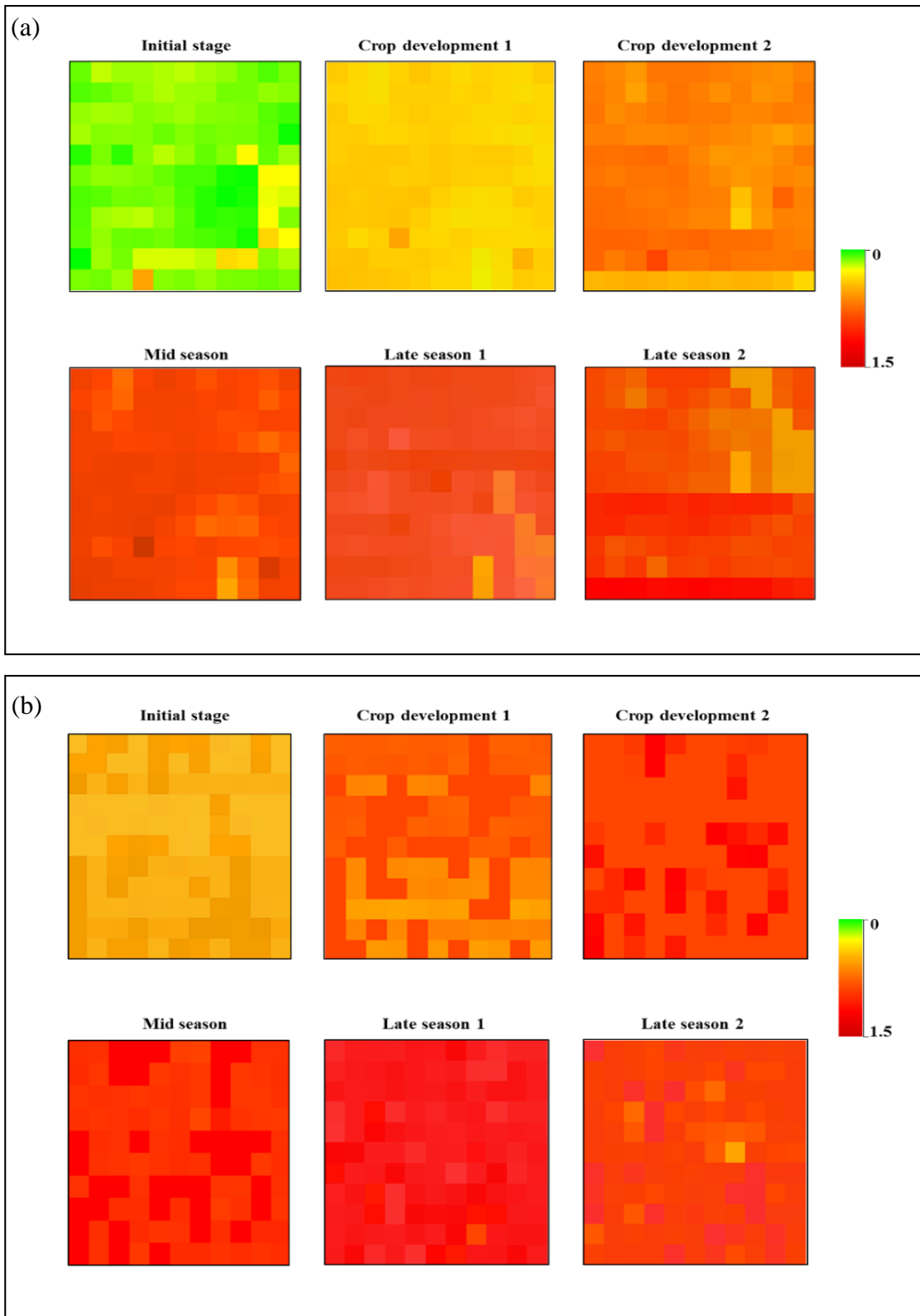


Figure IV-1 NDVI derived basal crop coefficient (K_{cb}) of paddy and rainfed rice at different crop growth stages: (a) rainfed rice; (b) paddy rice; $0.5 \times 0.5 \text{ m}^2$ ground resolution.

The daily evaporation coefficients (K_e) of paddy and rainfed rice are presented in *figure (IV-2)*. K_e of paddy rice was higher during the early growth stages where the field was flooded and crop cover (LAI , K_{cb}) was minimal. K_e of paddy rice gradually decrease along with increased in crop cover (LAI , K_{cb}) and reached to the lowest K_e starting from late season stage where flooded water was drained. However, K_e of paddy was always higher than that of rainfed rice. K_e of rainfed rice was mainly governed by available soil moisture. Sharp increases in K_e of rainfed rice followed each rain events and a significant increase in K_e after rain events showed even under the flooded condition.

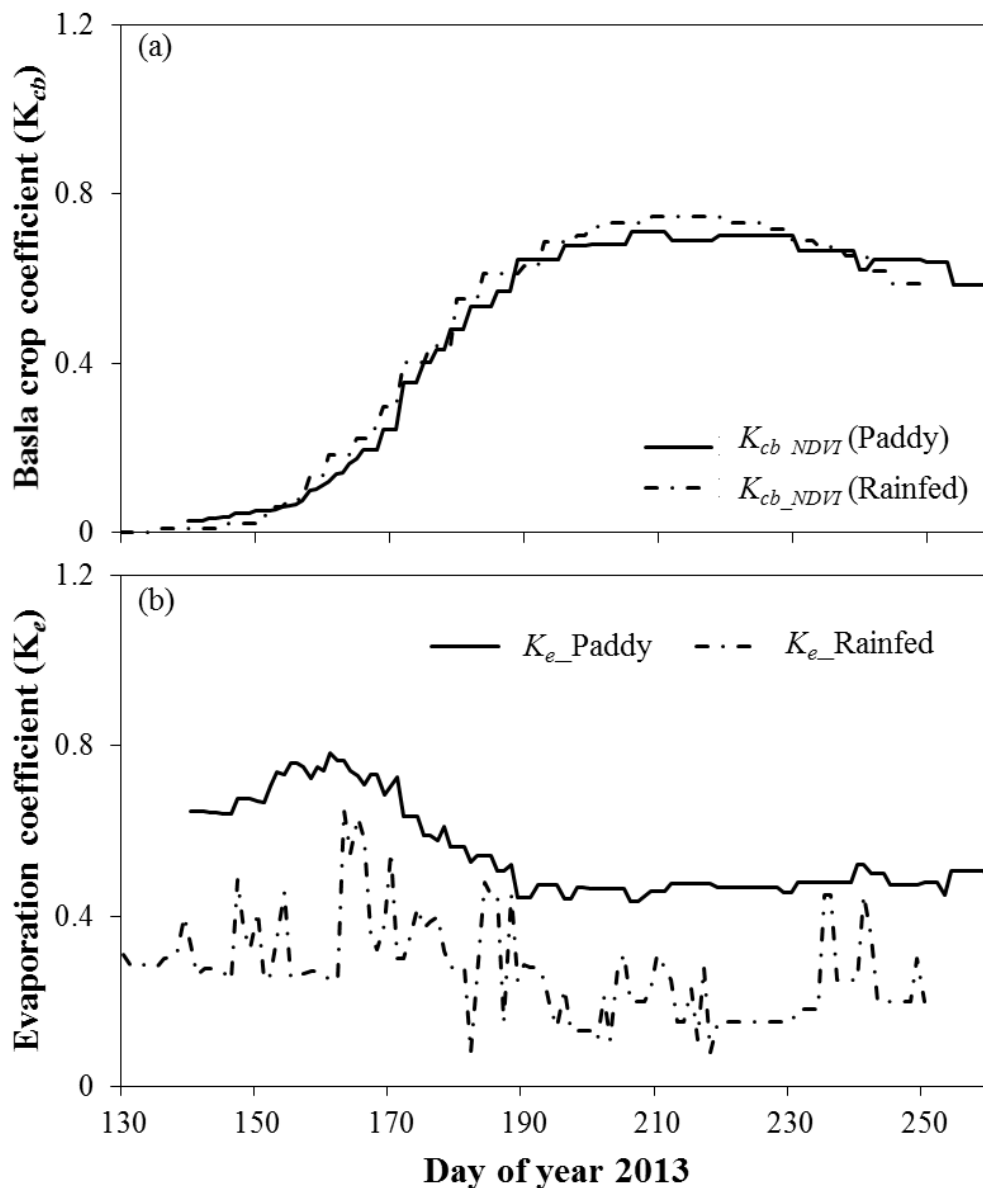


Figure IV-2 Daily crop coefficients of paddy and rainfed rice: (a) Transpiration coefficient or basal crop coefficient, K_{cb} ; (b) Evaporation coefficient, K_e .

4.3 Evapotranspiration estimation by three different models

Daily crop *ET* of rainfed and paddy rice was estimated by radiation driven methods (the *Mk* and the *PT* models) and combination methods (the *56PM* model and modifications). Estimated crop *ET* by different models was compared with chamber measured crop *ET* (Table IV-2, Figure IV-3). The *56PM* model which used the measured growth stage average leaf resistance of rice in combination with *NDVI* derived basal crop coefficient ($m56PM_{mrc} + K_{cb_NDVI}$) performed the best ($R^2=0.95$, $p < 0.05$, $RMSE = 0.10$, $NSeff\ ME = 0.76$, $CV (RMSE) = 0.08$). The original *56PM* (*56PM* with canopy conductance of 70 sm^{-1}) model in combination with both *FAO* recommended K_{cb} values and *NDVI* derived K_{cb} values performed better than *PT* and *Mk* (Table 4.3). However, applying fixed canopy conductance 80, 100 and 120 sm^{-1} ($m56PM_{80}$, $m56PM_{100}$, $m56PM_{120}$) instead of the *FAO 56* recommended 70 sm^{-1} showed better model performance with higher modelling efficiency. Among the compared different *ET* models; two radiation based models and one Penman type combination model, the *PM* type models performed better than radiation based models of the Makkink 1957 and the Priestley-Taylor 1972. However, in the case of limited meteorological data availability to perform *56PM ET₀* model, radiation based Makkink, 1957 (*Mk*) in combination with the *FAO 56* recommended K_{cb} values would be an option to estimate crop evapotranspiration as it performed better ($R^2 = 0.70$, $p < 0.05$, $RMSE = 0.21$, $ME (Nseff) = -1.76$, $CV (RMSE) = 0.17$) than another radiation based model, Priestley-Taylor (the *PT*, 1972).

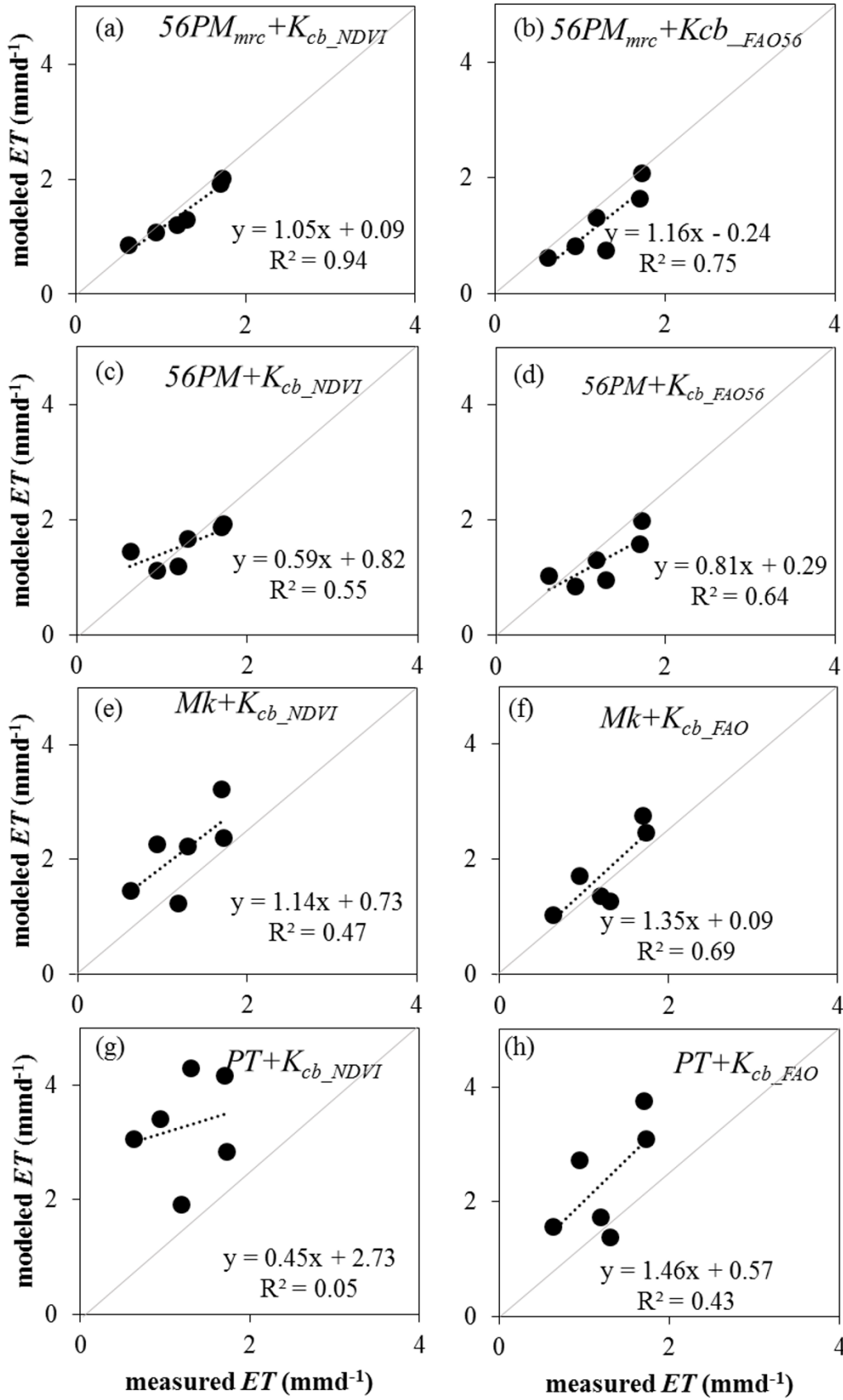


Figure IV-3 Comparison of measured ET versus estimated ET by different estimation methods. (n=6). The models used for panel a-h are provided in table 4.3, together with statistics.

Table IV-3 Comparison of different crop *ET* estimation methods. *Mk*, *PT*, *56PM*, *m56PM₈₀*, *m56PM₁₀₀*, *m56PM₁₂₀* are conventional reference crop *ET* (*ET₀*, grass as reference crop) estimation methods while *m56PM_{mrc}* is reference crop *ET* of rice (*ET₀*, healthy and well-watered rice as reference crop). *K_{cb_FAO}* is the FAO recommended hypothetical basal crop coefficients (Provided in section (4.2.1), Table (4.2) while *K_{cb_NDVI}* is *NDVI* derived basal crop coefficient. *R²* is determination of coefficients, *RMSE* is root mean square error, *p* (t-test) is level of significant of the test, *CV (RMSE)* is coefficient of variation determined by *RMSE*, *ME (Nseff)* is model efficiency and *Score* is the score of model performance ranked based on *ME* and *R²*.

Crop <i>ET</i> estimates	<i>R²</i>	<i>p</i> (t-test)	<i>RMSE</i>	<i>CV (RMSE)</i>	<i>ME (Nseff)</i>	<i>Score</i>
	n=6					
<i>Mk</i> + <i>K_{cb_FAO}</i>	0.70	<0.05	0.21	0.17	-1.76	5
<i>Mk</i> + <i>K_{cb_NDVI}</i>	0.47	0.13	0.28	0.23	-5.74	6
<i>PT</i> + <i>K_{cb_FAO}</i>	0.43	0.16	0.30	0.24	-10.53	7
<i>PT</i> + <i>K_{cb_NDVI}</i>	0.05	0.68	0.38	0.31	-30.80	8
<i>56PM</i> + <i>K_{cb_FAO}</i>	0.64	0.06	0.24	0.19	0.32	3
<i>56PM</i> + <i>K_{cb_NDVI}</i>	0.55	<0.05	0.26	0.21	-0.05	3
<i>m56PM₈₀</i> + <i>K_{cb_FAO}</i>	0.45	0.14	0.29	0.23	0.28	3
<i>m56PM₈₀</i> + <i>K_{cb_NDVI}</i>	0.41	0.06	0.25	0.20	0.35	3
<i>m56PM₁₀₀</i> + <i>K_{cb_FAO}</i>	0.46	0.14	0.23	0.20	0.51	2
<i>m56PM₁₀₀</i> + <i>K_{cb_NDVI}</i>	0.41	0.07	0.25	0.18	0.49	2
<i>m56PM₁₂₀</i> + <i>K_{cb_FAO}</i>	0.45	0.08	0.29	0.23	0.52	2
<i>m56PM₁₂₀</i> + <i>K_{cb_NDVI}</i>	0.45	<0.05	0.25	0.20	0.57	2
<i>m56PM_{mrc}</i> + <i>K_{cb_FAO}</i>	0.75	<0.05	0.20	0.16	0.50	2
<i>m56PM_{mrc}</i> + <i>K_{cb_NDVI}</i>	0.94	<0.05	0.10	0.08	0.76	1

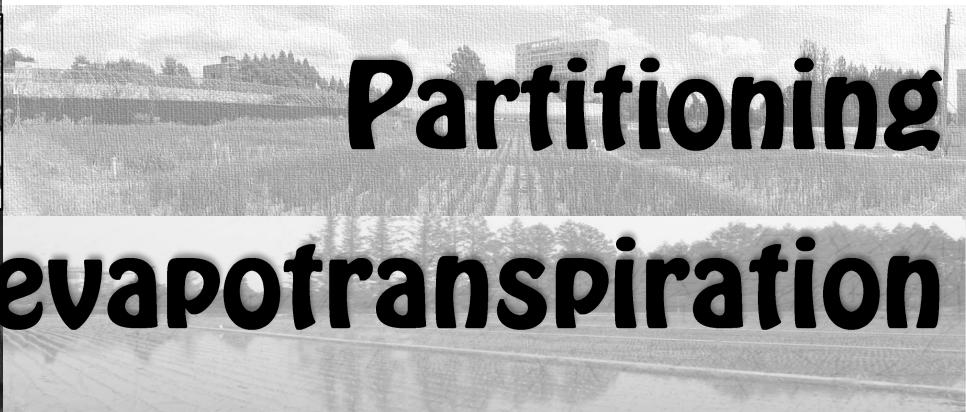
4.4 Summary

According to this study, reference crop ET (ET_0) estimation for a specific crop rather than grass performed better for the crop ET estimation. Grass reference crop (ET_0) estimated by fixing the canopy resistance at 100 and 120 sm^{-1} could be applied in the estimation of crop ET of rice when crop specific parameters to calculate the canopy conductance of rice is not available. Especially for rice and other agricultural crops, when environmental data to calculate ET_0 by the *56PM* method are not available, the *Mk* method is recommended as it performed better than the *PT*. The *FAO* recommended basal crop coefficient for rice did not represent well to the paddy rice cultivated in this study. Recommended K_{cb} value for initial stage was higher than *NDVI* derived daily K_{cb} while recommended K_{cb} value for late season stage was lower than *NDVI* derived K_{cb} highlighting the need to develop crop and regional specific K_{cb} curves with better temporal resolutions. For the better ET estimation, *NDVI* derived basal crop coefficient (K_{cb}) should be used in combination with crop specific modifications of the reference crop ET (ET_0) estimations. Otherwise, the use of K_{cb} derived from *NDVI* showed almost no different to the use of the *FAO* recommended K_{cb} values.

5



Partitioning evapotranspiration



V. Partitioning evapotranspiration

5.1 Partitioning seasonal *ET* by modeling approach

To compare the seasonal crop water use of rainfed and paddy rice, it is necessary to partition soil evaporation and plant transpiration in both rainfed and paddy rice. Therefore, evapotranspiration of rainfed and paddy rice was partitioned by estimating daily crop evapotranspiration (Chapter 4) and canopy transpiration.

5.1.1 Estimation of daily canopy transpiration

Daily canopy transpiration (T_c) of paddy and rainfed rice was estimated by the *FAO 56* dual crop coefficient approach ($K_{cb} \times ET_0$, details in the chapter 4) and *PM* approach (see details in the chapter 2, section 2.7.2). The *FAO 56* dual crop approach showed a similar trend to the *PM* based estimation (*Figure V-1*). Therefore, from this point onwards, T_c estimated by the *FAO 56* dual crop coefficient approach was used to partition the simulated daily *ET* fluxes.

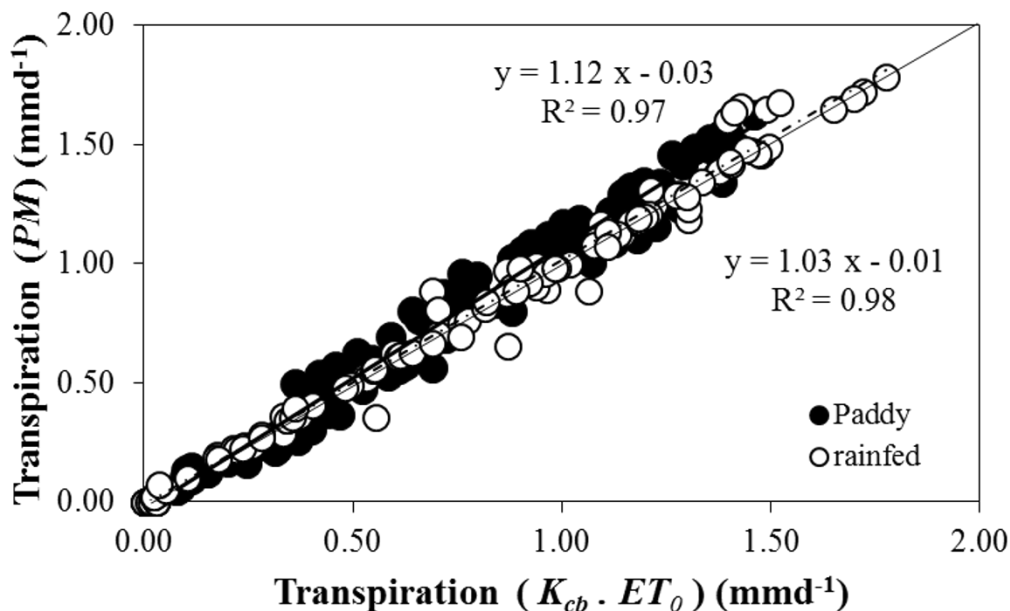


Figure V-1 Canopy transpiration of rainfed and paddy rice modelled by the original *PM* (Monteith 1956) (net radiation intercepted by canopy as radiation input) and the *FAO 56* dual crop coefficient ($K_{cb} \times ET_0$) (Allen, 1998).

5.1.2 Partitioning daily evapotranspiration

Seasonal variation of daily crop ET of paddy and rainfed rice is shown in *Figure (V-2)*. Daily crop ET was simulated by the $56PM_{mrc}$ and $NDVI$ derived K_{cb} model (details in chapter 4) while daily transpiration (T) was also derived by the *FAO 56* dual crop coefficient approach. In the monsoon season 2013, daily crop ET of rainfed rice ranged from 0.34 mmd^{-1} to 2.18 mmd^{-1} . Crop ET of both rainfed and paddy rice reached its peak on DOY 220 (Mid-season stage) and declined onward. Daily average and growing season total ETs of rainfed rice were $1.21 \pm 0.47 \text{ mmd}^{-1}$ and $138.75 \text{ mmseason}^{-1}$. Compare to rainfed rice, paddy rice had significantly higher crop ET since from the initial crop growth stage throughout the entire growing season ($W=15$, $p \leq 0.05$). In paddy rice, peak ET was found during the initial stage when there was lowest crop canopy development. Maximum and minimum crop ETs of paddy rice were 4.20 mmd^{-1} and 0.62 mmd^{-1} respectively. Average and crop season total ETs of paddy rice were $1.96 \pm 0.76 \text{ mmd}^{-1}$ and $239.88 \text{ mmseason}^{-1}$ (*Figure V.2*). Evapotranspiration (ET) of paddy rice was 42.16 % higher than that of rainfed rice. However, there was no difference between crop season total canopy transpiration (T) although T of paddy rice was 11.02 % higher than that of rainfed rice. Transpiration of both rainfed and paddy followed a similar seasonal trend. Along with the increased ground cover area as the result of seasonal crop canopy development (LAI), canopy transpiration (T) was lower than evaporation (E) during the initial crop growth stage when the plants were small until the mid of crop development stage (around DOY 180). Later on, E declined and T increased to its maximum of 1.79 mmd^{-1} for rainfed rice and 1.63 for paddy rice on DOY 223, which was a dry and clear sky day. Although paddy rice had lower maximum T compared to rainfed rice, total T of paddy was 11.02 % higher than that of rainfed rice. Lower T of paddy on a certain day, especially on the days under high air temperature and clear sky condition, was probably due to the higher E as E can reduce T by regulating micro-climate as reported by the studies of Agam et al. (2012), Leuning et al. (1994) and Tolk et al. (1995).

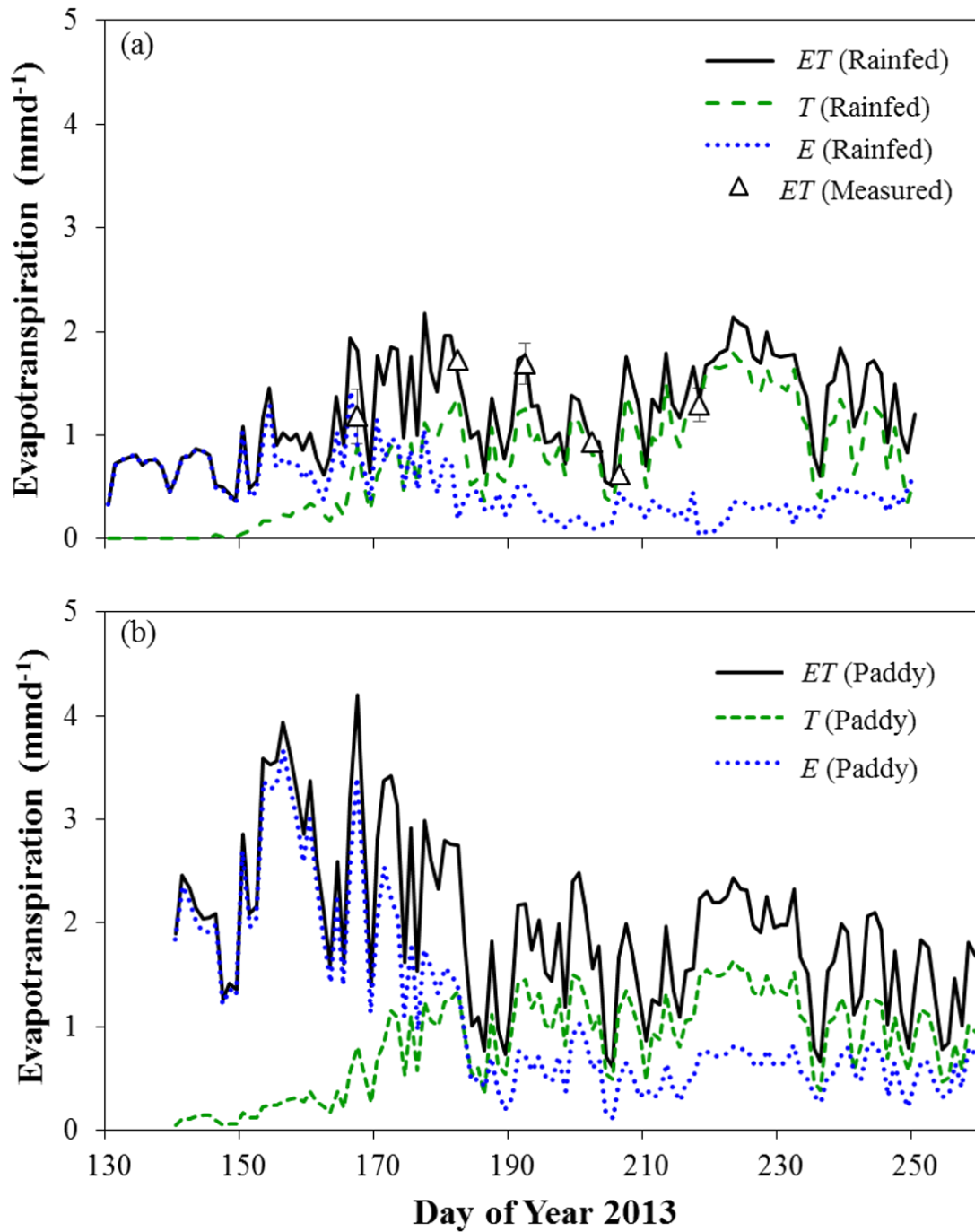


Figure V-2 Daily evapotranspiration (black line), canopy transpiration (green dashed line) and evaporation (blue dotted line) of rainfed rice (a) and paddy rice (b). ($n=3, \pm\text{SD}$)

Minimum crop ET of both paddy and rainfed rice occurred on rainy days with low radiation, low atmospheric VPD and low T_{air} and T_{soil} . On the other hand, crop ET peaks of rainfed and paddy rice were reported on different day of years. Crop ET peak of rainfed rice was reported on DOY 223 when T_{air} and T_{soil} were the highest. However, crop ET peak of paddy rice was reported on DOY 145, a day with highest atmospheric VPD (1.55 kPa) and high radiation (23.42 $Mjm^{-2}d^{-1}$). Based on the analysis of relationship between chamber measured crop ET and environmental variables, evapotranspiration of rainfed rice was mainly driven by the T_{air} , T_{soil} and VPD (Spearman's $\rho = 0.65, 0.57, 0.47$, respectively, $p \leq 0.01$) while that of paddy rice was driven by the radiation and VPD (Spearman's $\rho = 0.87, 0.67$, respectively, $p \leq 0.01$).

Daily contribution of transpiration to evapotranspiration (T/ET) of rainfed and paddy rice was calculated based on the simulated daily T and ET . T/ET of both rainfed and paddy rice steadily increased with the increasing canopy density (LAI). T/ET of rainfed rice had a negative relationship to soil water content (SWC) ($R^2=0.49$) while that of paddy had no significant relationship to SWC . When SWC decreased below $0.30 m^3m^{-3}$ in rainfed and $0.4 m^3m^{-3}$ in paddy rice, SWC was no longer the main determining factor driving T/ET . Instead, VPD and radiation were the factors driving T/ET (Spearman's $\rho = 0.72$, respectively, $p \leq 0.01$). The water fluxes from rainfed rice was mainly dominated by transpiration ($T/ET = 0.65$) while that of paddy rice was mainly driven by evaporation ($T/ET = 0.42$). When soil water content (SWC) declined below field capacity, T contributed 80 to 90% of H_2O flux in rainfed rice.

Table V-1 Environmental variables controlling crop evapotranspiration of rainfed rice. Spearman rank order correlation was performed by using chamber measured ET and environmental variables.

	<i>ET</i>	<i>T</i>	<i>Radiation</i>	<i>T_{air}</i>	<i>T_{soil}</i>	<i>VPD</i>	<i>SWC</i>	<i>Windspeed</i>
<i>ET</i>								
Spearman's (ρ)			0.43	0.65	0.57	0.47	-0.36	0.43
P			0.00	0.00	0.00	0.00	0.00	0.00
<i>T</i>								
Spearman's (ρ)	0.89		0.23	0.76	0.59	0.48	-0.56	0.39
P	0.00		0.01	0.00	0.00	0.00	0.00	0.00
<i>Radiation</i>								
Spearman's (ρ)	0.43	0.23		-0.02	0.10	0.81	-0.04	0.12
P	0.00	0.01		0.86	0.27	0.00	0.65	0.21
<i>T_{air}</i>								
Spearman's (ρ)	0.65	0.76	-0.02		0.82	0.19	-0.58	0.62
P	0.00	0.00	0.86		0.00	0.03	0.00	0.00
<i>T_{soil}</i>								
Spearman's (ρ)	0.57	0.59	0.10	0.82		0.22	-0.38	0.72
P	0.00	0.00	0.27	0.00		0.01	0.00	0.00
<i>VPD</i>								
Spearman's (ρ)	0.47	0.48	0.81	0.19	0.22		-0.25	0.24
P	0.00	0.00	0.00	0.03	0.01		0.01	0.01
<i>SWC</i>								
Spearman's (ρ)	-0.36	-0.56	-0.04	-0.58	-0.38	-0.25		-0.26
P	0.00	0.00	0.65	0.00	0.00	0.01		0.00
<i>Windspeed</i>								
Spearman's (ρ)	0.43	0.39	0.12	0.62	0.72	0.24	-0.26	
P	0.00	0.00	0.21	0.00	0.00	0.01	0.00	

Table V-2 Factors controlling crop evapotranspiration of paddy rice. Spearman rank order correlation was performed by using chamber measured ET and environmental variables.

	<i>ET</i>	<i>T</i>	<i>Radiation</i>	<i>T_{air}</i>	<i>T_{soil}</i>	<i>VPD</i>	<i>SWC</i>	<i>Windspeed</i>
<i>ET</i>								
Spearman's (ρ)		0.36	0.87	0.00	0.26	0.67	0.07	0.20
P		0.00	0.00	0.96	0.00	0.00	0.45	0.03
<i>T</i>								
Spearman's (ρ)	0.36		0.48	0.63	0.70	0.44	-0.62	0.25
P	0.00		0.00	0.00	0.00	0.00	0.00	0.01
Radiation								
Spearman's (ρ)	0.87	0.48		0.06	0.30	0.78	-0.18	0.24
P	0.00	0.00		0.51	0.00	0.00	0.05	0.01
<i>T_{air}</i>								
Spearman's (ρ)	0.00	0.63	0.06		0.86	0.29	-0.70	0.55
P	0.96	0.00	0.51		0.00	0.00	0.00	0.00
<i>T_{soil}</i>								
Spearman's (ρ)	0.26	0.70	0.30	0.86		0.38	-0.67	0.48
P	0.00	0.00	0.00	0.00		0.00	0.00	0.00
<i>VPD</i>								
Spearman's (ρ)	0.67	0.44	0.78	0.29	0.38		-0.34	0.39
P	0.00	0.00	0.00	0.00	0.00		0.00	0.00
<i>SWC</i>								
Spearman's (ρ)	0.07	-0.62	-0.18	-0.70	-0.67	-0.34		-0.17
P	0.45	0.00	0.05	0.00	0.00	0.00		0.06
<i>Windspeed</i>								
Spearman's (ρ)	0.20	0.25	0.24	0.55	0.48	0.39	-0.17	
P	0.03	0.01	0.01	0.00	0.00	0.00	0.06	

5.2 Partitioning daytime ET by $\delta^{18}O_{ET}$ approach

After partitioning the daily ET of rainfed and paddy rice by model simulation (Section 5.1 of this chapter), the measured daytime ET fluxes were also partitioned to analyze the short-term changes of the ET . The stable water isotope ($\delta^{18}O$) approach was applied for the daytime ET fluxes partitioning.

5.2.1 $\delta^{18}O$ of precipitation

Average $\delta^{18}O$ precipitation ($\delta^{18}O_{RF}$) varied from -4.27 ‰ to -10.68 ‰. The highest and lowest stable oxygen isotope values ($\delta^{18}O$) of precipitation were measured in May (the beginning of Monsoon season) and August, respectively, following the regional patterns (Kim and Nakai, 1988; Lee et al., 2013, 2003, 2007; Lee and Kim, 2007). $\delta^{18}O$ composition of precipitation decreased (more negative) from DOY 169 onward (*Figure V-3a*, blue circles). $\delta^{18}O$ soil water followed the patterns of precipitation (*Figure V-3a*) pointing that precipitation was the only source of soil water.

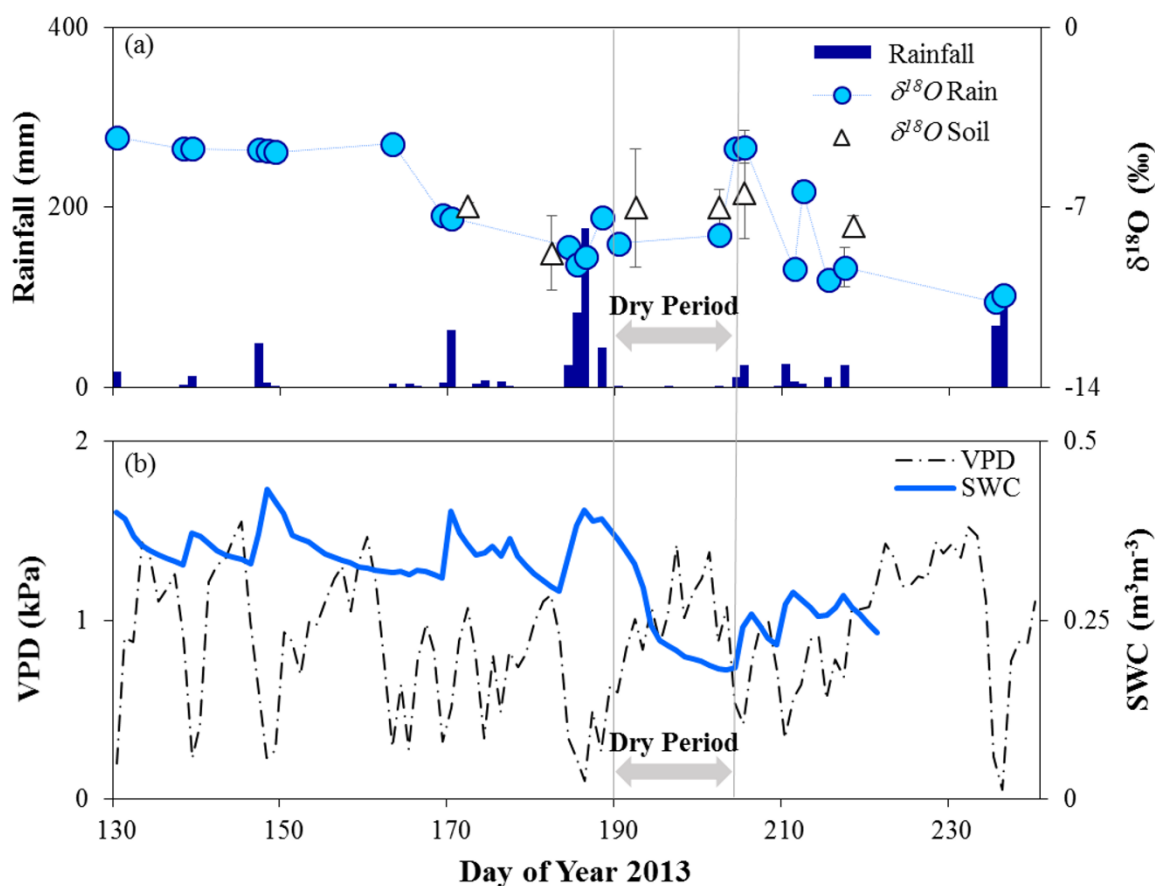


Figure V-3 Daily precipitation (dark blue bars), $\delta^{18}O$ of rainwater (light blue cycle) and extracted soil water (white triangle), ($n=3 - 8$, mean values \pm SD) (b) Daytime VPD (dotted line) and soil water content (thick blue line).

5.2.2 Volumetric soil water content, soil temperature and $\delta^{18}O$ of soil water

Due to the influence of precipitation, which was the only water source, and fluctuation of evaporative demand, the oxygen isotopic composition in the soil differed with the soil profile depth as well as the sampling date. $\delta^{18}O$ composition between 10 and 30 cm depths generally reflected the isotopic composition of precipitation (~ -7 to -8 ‰) (Figure V-3a). At 5 cm depth, $\delta^{18}O$ of soil water ($\delta^{18}O_s$) was enriched compared to lower soil profile and the most enriched $\delta^{18}O_s$ (-6.03 ± 1.28) was found on DOY 192 (Figure V-4).

At the beginning of the growing season, volumetric soil water content (SWC) of different soil profile depths were similar (Figure V-4). However, following the rain events, SWC was increased (up to $0.31 m^3m^{-3}$ at 5 cm depth and $0.45 m^3m^{-3}$ at lower soil profile depths)

significantly. Soil temperature (T_{soil}) was always highest in the upper soil layer (27.57 to 28.82 °C at 5 cm depth) although DOY 205 had a rather low T_{soil} (25.67 °C) (*Figure V-4*).

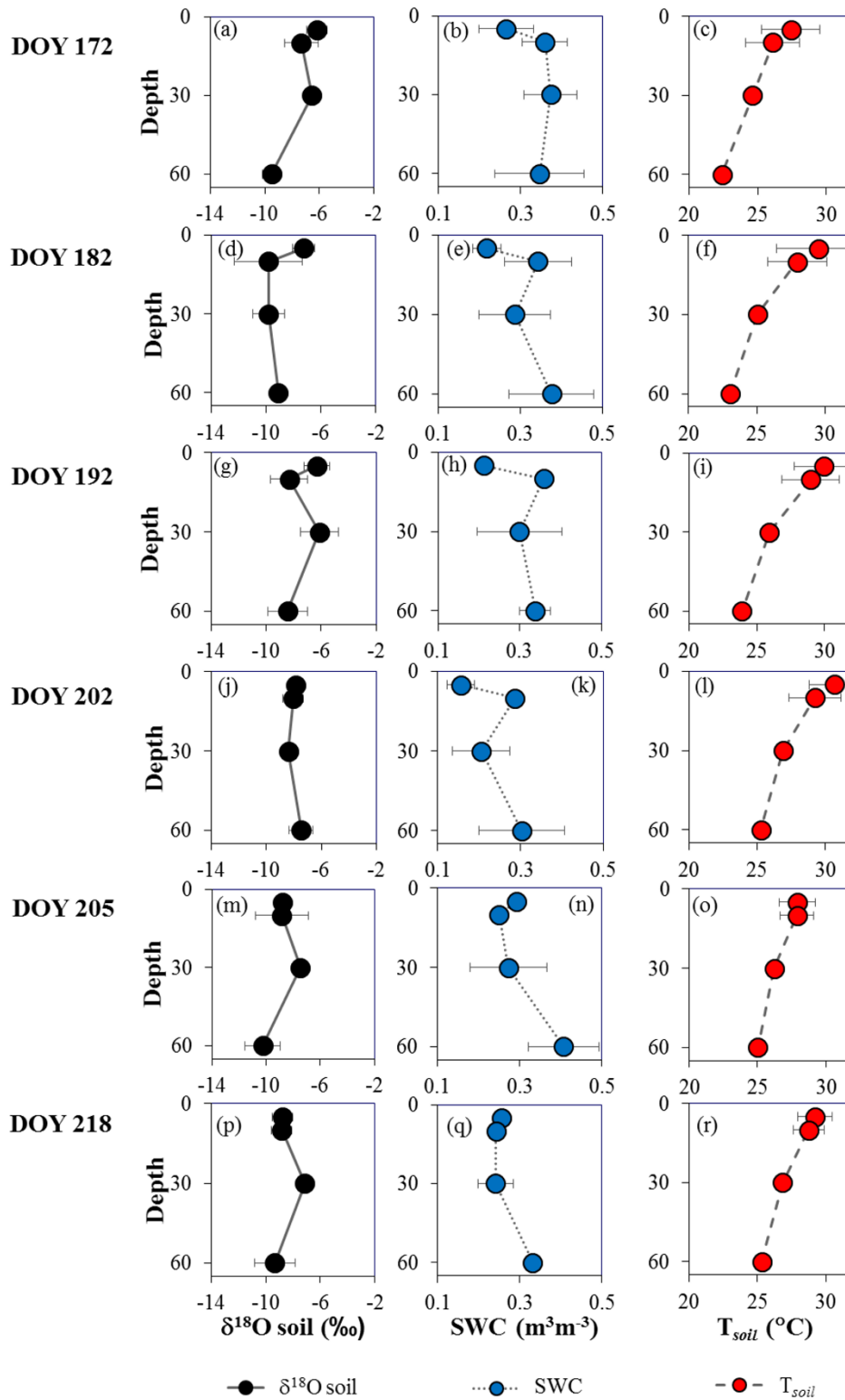


Figure V-4 Profile of volumetric soil water content at different depths, 5, 10, 30, 60 cm (SWC, dotted line with blue circle, $n=3$, mean values \pm SD), soil temperature (T_{soil} , dashed line with red circle, $n=3$, mean values \pm SD) and soil $\delta^{18}O$ ($\delta^{18}O_s$, black line with black circle, $n=3$, mean values \pm SD) of rainfed rice field on DOY 172, 182, 192, 202, 205 and 218.

5.2.3 Measured $\delta^{18}O_{ET}$, modelling $\delta^{18}O_E$, $\delta^{18}O_T$ and partitioning ET

Throughout the crop season, measured ET of crop canopy was highest during midday and the peak midday ET of $2.89 \pm 0.11 \text{ mmolm}^{-2}\text{s}^{-1}$ was occurred on DOY 192. During the dry period, the peak midday ET was significantly lower than the values of other measured days (1.26 ± 0.05 at 12:00 hour of DOY 202). After the dry period followed by a heavy rain event, peak ET increased up to $2.86 \pm 0.36 \text{ mmolm}^{-2}\text{s}^{-1}$ again on DOY 218 and it was found during the midday as before the dry period. Measured $\delta^{18}O_{ET}$ of rainfed rice crop canopy ranged from $-21.85 \pm 6.79 \text{ ‰}$ to $-10.07 \pm 0.25 \text{ ‰}$, throughout the monsoon 2013 (Figure V-6 a, e, i, m, q and u).

The isotope signatures of soil evaporation ($\delta^{18}O_E$) and plant transpiration ($\delta^{18}O_T$) influenced the isotope signatures of evapotranspiration ($\delta^{18}O_{ET}$). Based on $\delta^{18}O_E$ of crop plot and $\delta^{18}O_T$ of plant, contributions of plant transpirations to evaporations (ft) can be predicted. Therefore, $\delta^{18}O_E$ of canopy was modelled based on Craig and Gordon model (Figure V-6 b, f, j, n, r, v, black straight line). The model was validated with CRDS measured bare soil $\delta^{18}O_E$. Measured $\delta^{18}O$ signatures of bare soil evaporation ($\delta^{18}O_E$) were between -9.56 ‰ to -20.40 ‰ and thus $\delta^{18}O_E$ was highly depleted compared to soil $\delta^{18}O$ ($\delta^{18}O_s$) and rain $\delta^{18}O$. Modelled bare soil $\delta^{18}O_E$ fitted well to measured bare soil $\delta^{18}O_E$ ($R^2 = 0.74$, Figure V-5). Calculated $\delta^{18}O_E$ of crop plot was between -23.88 ‰ and -33.31 ‰ , which is more depleted compare to bare soil $\delta^{18}O_E$.

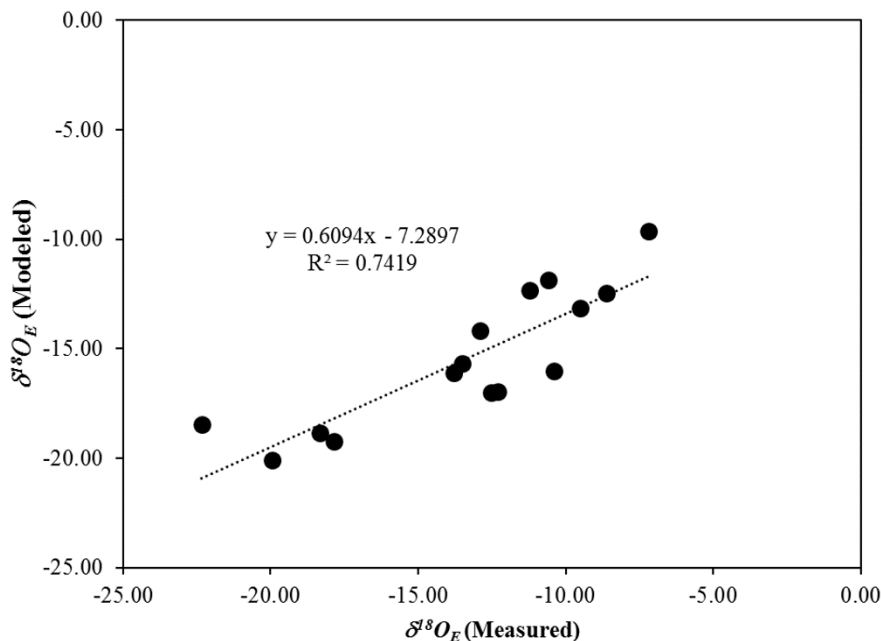


Figure V-5 CRDS based measured $\delta^{18}O$ of the soil evaporation of bare soil plot evaporation, $\delta^{18}O_E$ against modelled $\delta^{18}O_E$. $\delta^{18}O_E$ measurements were carried out on DOY 177, 193, 199, 207, and 220, at 12:00, 14:00 and 18:00 hours. Modeled $\delta^{18}O_E$ was calculated based on measured $\delta^{18}O$ of soil water at 5 cm ($\delta^{18}O_s$), measured $\delta^{18}O$ of ambient air ($\delta^{18}O_a$), soil temperature at 5 cm, air temperature, relative humidity and soil water content data of the day and time of interest.

$\delta^{18}O_T$ was also calculated by the non-steady state model (*Figure V-6 b, f, j, n, r, v*, dashed line) (See Chapter 1, section 1.3 for the explanation of the stable isotopic steady and non-steady state). $\delta^{18}O_T$ calculated at non-steady state ranged from -7.20 ‰ to -9.38 ‰ throughout the crop season. Water resident time was calculated by equation 2.3.2 as bulk leaf water (V_m) divided by the one-way water flux out of the leaf ($g_{tw}w_i$) which gave the water resident time less than 30 minutes). $\delta^{18}O_T$ was mostly the same as that of source water at root zone ($\delta^{18}O_s$ of the soil depth between 10 cm and 30 cm).

Contribution of transpiration to evapotranspiration (ft) was calculated based on calculated $\delta^{18}O_E$ and $\delta^{18}O_T$ of crop plot (*Figure V-6 c, g, k, o, s, w*). ft of rainfed rice canopy showed a clear diurnal pattern, ranging the values from 0.28 to 0.88. ft was always higher than 0.50 throughout the crop season except on DOY 205, which was a cloudy and humid day. The highest ft was found on DOY 182 at 12:00 hour and DOY 202 at 18:00 hour, which were extremely dry days with higher T_{air} under clear sky. On DOY 182, ft was higher throughout the whole day, which highlight the higher transpiration compare to soil evaporation loss (*Figure V-6 h*).

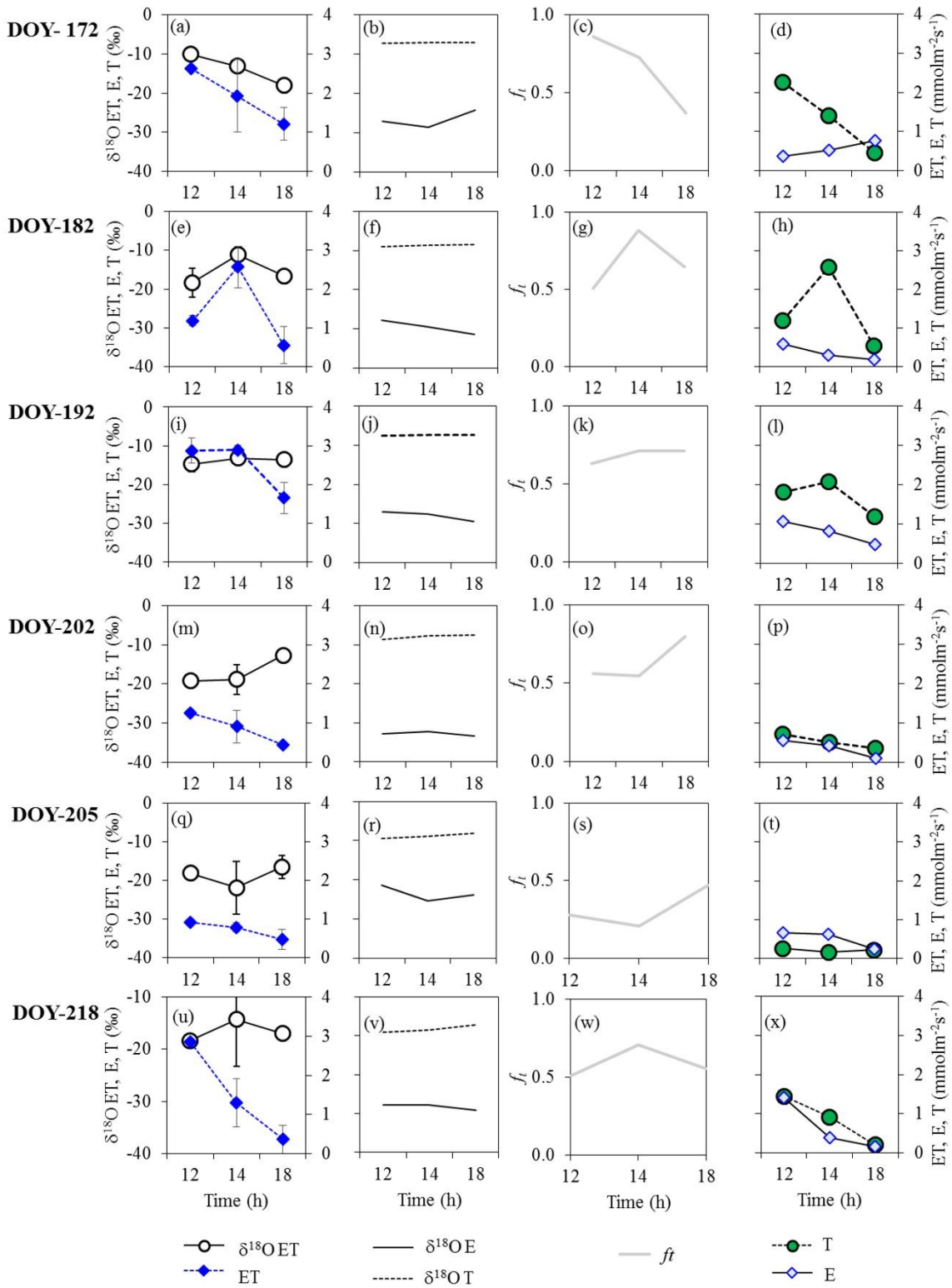


Figure V-6 CRDS based measured ET , $\delta^{18}O_{ET}$ (a,e,i,m,q,u, white cycle = $\delta^{18}O_{ET}$, blue diamond = ET , $n=3$, mean values \pm SD), modeled $\delta^{18}O_E$ and $\delta^{18}O_T$ (b,f,j,n,r,v, black line = $\delta^{18}O_E$, dashed line = $\delta^{18}O_T$), diurnal contribution of T to ET (f_t) (c,g,k,o,s,w). Each panel represents to day of year 172, 182, 192, 202, 205 and 218 respectively.

5.3 Comparing $\delta^{18}O$ and PM derived fraction of T to ET (T/ET)

Fractions of T to ET of rainfed rice were calculated based on 56PM model based daily ET and T fluxes and compared with the daytime average ft derived from $\delta^{18}O$ ET partitioning (See section 2.7.1 for detail calculation procedure). T/ET calculated by the 56PM approach showed a similar trend to that of $\delta^{18}O$ approach (Figure V-7) ($R^2 = 0.53$; Nseff $ME = 0.52$). However, the absolute value of T/ET calculated based on $d18O$ approach and 56PM modeling cannot be expected to be identical or similar because the $\delta^{18}O$ T/ET was the mean value of the only three measuring points of a day while 56PM modeled T/ET was the daily values. For example, on DOY 205 and 218, T/ET ($\delta^{18}O$) was significantly lower than that of 56PM, given the fact that T/ET ($\delta^{18}O$) was the mean of the three measurement points of the day, while T/ET (56PM) was the daily value. Nevertheless, although the T/ET ($\delta^{18}O$) on DOY 205 was lower than 0.5 (i.e., crop transpiration contributed less than 50% of evapotranspiration), T/ET derived by both approaches showed that crop transpiration shared more than 50% of evapotranspiration of rainfed rice fields in terms of crop season total, as well as, during the vegetative growth stages and reproductive stages (DOY 170 onward).

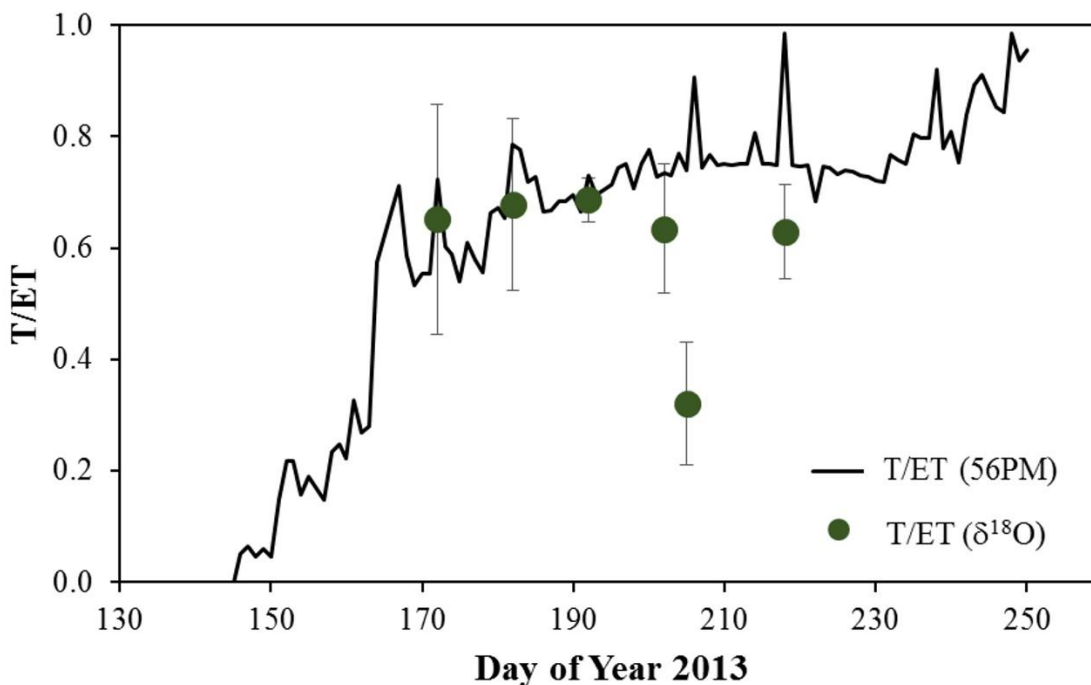


Figure V-7 T/ET of rainfed rice derived by stable water isotope approach (dark green circles) and 56PM approach (line). T/ET ($d18O$) was the average ft calculated for 12:00, 14:00 and

18:00 hour of the respective day ($n=3 \pm \text{SD}$, be noted that the value is the mean of 3 different measurement times of the day) while T/ET (56PM) was the daily T/ET .

5.4 Summary

Stable water isotope based ET partitioning was applied to rainfed rice and compared with the 56PM based partitioning approach applied to the same rainfed rice. The 56PM based partitioning performed well ($R^2= 0.53$; Nseff $ME = 0.52$) to see the seasonal crop water use and water losses.

Evapotranspiration (ET) of paddy rice was 42.16 % higher than that of rainfed rice ($F=29.7$, $p \leq 0.01$). However, there was no significant difference between total seasonal canopy transpiration (T) although T of paddy rice was 11.02 % higher than that of rainfed rice ($F = 0.23$, $p = 0.55$). Evapotranspiration of rainfed rice was mainly driven by T_{air} , T_{soil} and VPD (Spearman's $\rho = 0.65, 0.57, 0.47$, respectively, $p \leq 0.01$) while that of paddy rice was driven by radiation and VPD (Spearman's $\rho = 0.87, 0.67$, respectively, $p \leq 0.01$). H_2O fluxes from rainfed rice was mainly dominated by transpiration ($T/ET = 0.65$) while that of paddy rice was mainly driven by evaporation ($T/ET = 0.42$). Under the water limited condition, when soil water content was lower than field capacity ($< 0.30 \text{ m}^3\text{m}^{-3}$), T contributed 80 to 90% of H_2O flux in rainfed rice.

6



VI. Water use efficiency of rainfed and paddy rice

Water use efficiency (*WUE*) of several rice production practices, rice varieties have been studied and many *WUE* improvement approaches were introduced (Bouman and Tuong, 2001; Bouman et al., 1994; Tuong et al., 2005). However, some studies mainly focused on the *WUE* improvement from the genetic and crop physiological point of view by studying and comparing genetic and physiological controls over leaf and plant *WUE* (Blum, 2009; Condon et al., 2004; Rebetzke et al., 2008a). Some studies directly focused on the grain yield improvement per irrigation or field water use (Bouman and Tuong, 2001; International Rice Research Institute [IRRI], 2002). On the other hand, attempting to improve the water use of rice production system, which is an important agroecosystem and which shared significant areas of global vegetation cover, may affect regional ecosystem water cycling process. Since plants link global water and carbon cycle through the photosynthesis and transpiration process, changes in regional water cycle could also affect carbon cycle (Kuglitsch et al., 2008), understanding changes in *WUEs* at different temporal and spatial scales is essential to improve *WUE* of rice ecosystems in a balance and sustainable way. Therefore, comparison of the leaf, canopy and ecosystem water use efficiency of rainfed and paddy are reported detail in this section.

6.1. Water use efficiency from the physiological point of view

6.1.1 Short term Leaf water use efficiency (*WUE_i*)

Intrinsic *WUE* ($WUE_i = A_{max}/g_s$) of the fully expanded flag leaves (the uppermost) of both rainfed and paddy rice measured under fixed environmental conditions (microenvironment CO_2 400 $\mu\text{mol mol}^{-1}$ and PAR 1500 $\mu\text{mol m}^{-2} \text{s}^{-1}$) were not significantly different ($n=12$ to 16, $W = 94$, $p = 0.22$, Table VI-2) but slightly higher in rainfed rice.

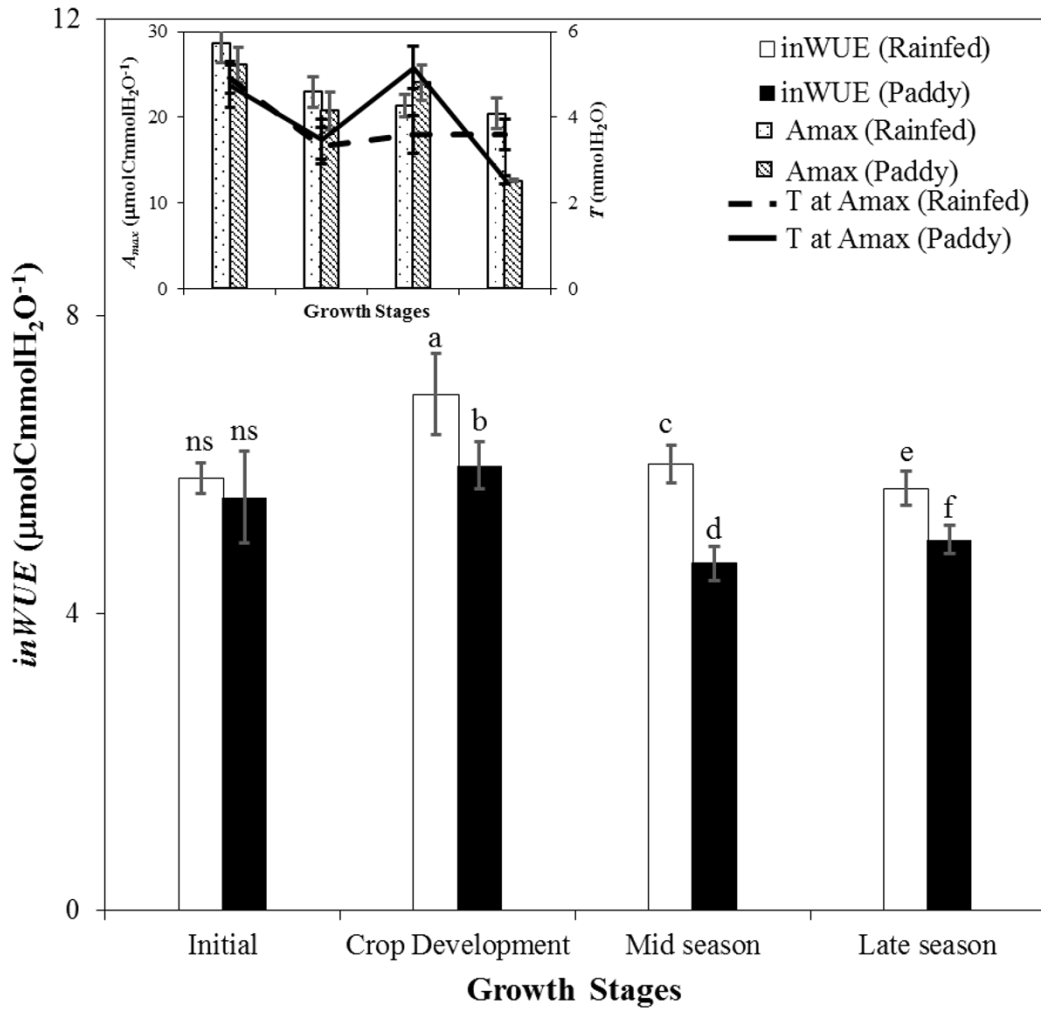


Figure VI-1 Instantaneous water use efficiency (*inWUE*) of rainfed and paddy rice ($n=3$ to $6 \pm \text{SD}$ for each growth stages). The instantaneous water use efficiency was calculated as the ratio of maximum assimilation to transpiration (A_{max}/T). A_{max} was the maximum assimilation and T was the transpiration of the uppermost rice leaf. Both A_{max} and T were measured under $1500 \mu\text{molm}^{-2}\text{s}^{-1}$ PAR and $400 \mu\text{molmol}^{-1}$ CO_2 and A_{max} (black for paddy and white for rainfed rice) and T (straight line for paddy and dashed line for rainfed rice) were provided in the small panel.

Leaf *WUE* is coupled by two physiological factors, CO_2 assimilation rate and stomatal conductance to water (g_s) in the case of intrinsic *WUE* (WUE_i). In the case of instantaneous *WUE* (*inWUE*), leaf *WUE* is controlled by not only the physiological factors (A and g_s) but also the environmental factors (especially *VPD*). Significantly higher *inWUE* was observed in the rainfed rice ($W=110$, $p < 0.05$, *Figure VI.1*) except the initial growth stage. Overall crop

growth season mean A_{max} measured at the uppermost leaves of rainfed rice was not significantly different to that of paddy rice ($W=94$, $p=0.22$, $n=12 \pm SD$, *Figure VI-1*, *Table VI-2*). In addition, crop growth season mean T of both rainfed and paddy rice measured at the uppermost leaves were not significantly different ($W=125$, $p=0.20$, $n=12 \pm SD$, *Figure VI-1*, *Table VI-1*). However, A_{max} of the rainfed rice at the late season stage was significantly higher than that of paddy rice ($W=32$, $p < 0.05$, $n=4 \pm SD$, *Figure VI-1*) while during the rest of crop growth stages, it was slightly but not significantly higher than paddy rice ($W=65$, $p=0.32$, $n=4$ to 12 , *Figure VI.1*). According to the multivariate correlation analysis, *inWUE* of the rainfed and paddy rice was strongly correlated to T (negative correlation, Spearman $\rho = -0.52$, $p < 0.01$, data not shown) and V_{cmax}/g_s , which is the ratio of maximum carboxylation capacity to stomatal conductance (positive correlation, Spearman $\rho = 0.62$, $p < 0.01$, *Figure VI-2 c*). Moreover, comparing either the overall growth season mean stomatal conductance (g_s) or measured at a specific crop growth stage showed a significantly higher leaf scale g_s of the paddy rice ($W=76$, $p < 0.05$, $n=4$ to $12 \pm SD$, *Table VI-1*). Thus, the higher leaf scale instantaneous *WUE* (*inWUE*) of rainfed rice was due to its efficient stomatal regulation to maximize the carbon assimilation per water use (V_{cmax}/g_s).

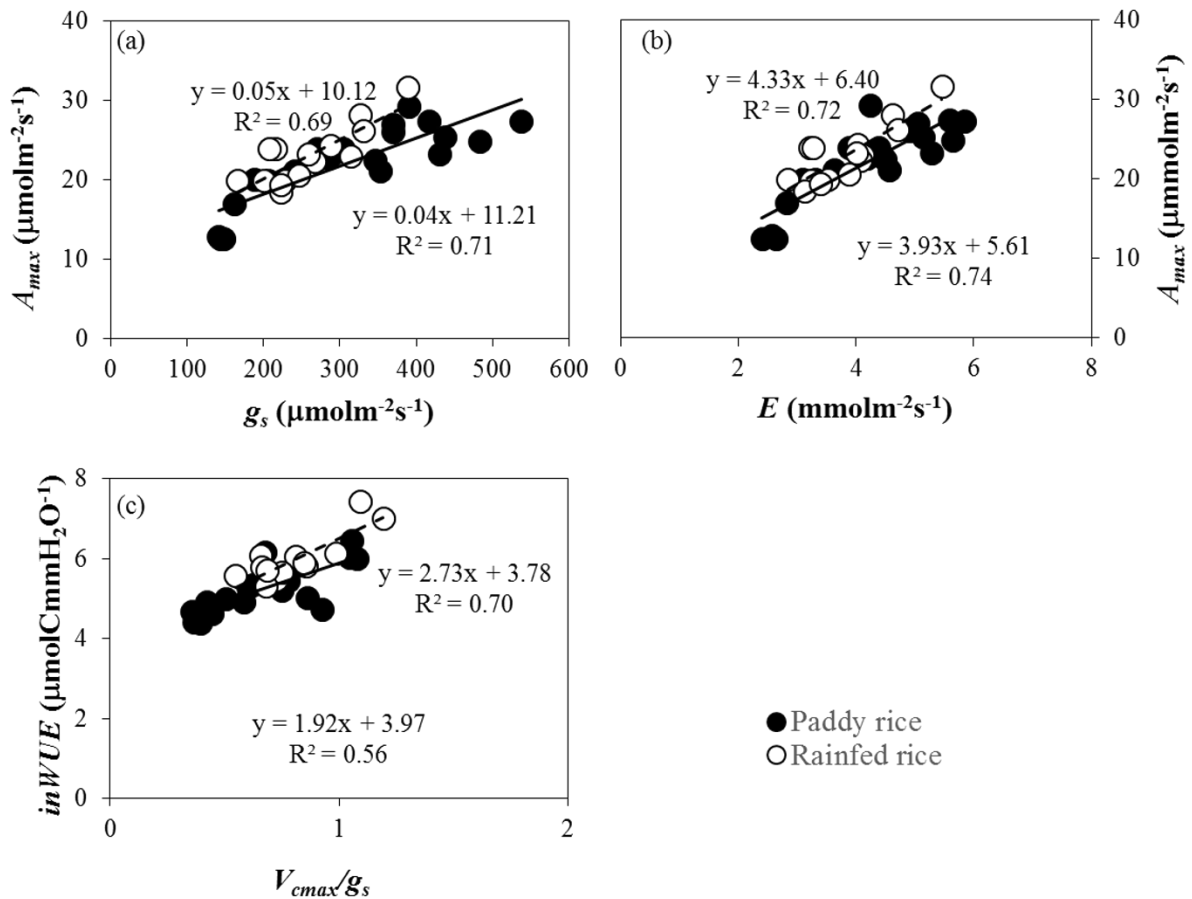


Figure VI-2 Correlations between (a) Maximum assimilation (A_{max}) and stomatal conductance to H_2O (g_s) of rainfed (black circles) and paddy rice (white circles) measured at the uppermost flag leaves under the controlled environment $1500 \mu\text{molm}^{-2}\text{s}^{-1}$ PAR, 400 PPM CO_2 ; (b) Maximum assimilation (A_{max}) and Transpiration (T) of rainfed (black circles) and paddy rice (white circles) leaves; (c) Instantaneous WUE ($inWUE$) and V_{cmax}/g_s . All the measurements were done during Initial, Crop development, Mid-season and Late season stages.

6.1.2 Integrated leaf water use efficiency

To determine the integrated water use efficiency differences of rainfed and paddy rice over the time of leaf development, growth stage integrated intrinsic water use efficiency (WUE_i) and instantaneous water use efficiency ($inWUE$) were calculated based on the $\delta^{13}\text{C}$ stable isotope discrimination ($\Delta^{13}\text{C}$) of the aboveground biomass samples collected from the entire canopy

(See the chapter 2, *table II-3* for the detail WUE_i calculation from $\Delta^{13}C$). $\delta^{13}C$ isotope discrimination ($\Delta^{13}C$) showed a clear and similar seasonal trend (*Figure VI-3b*) which also followed along with the precipitation water input (*Figure VI-3a*). Although the same rice variety was cultivated as rainfed and paddy rice, flooded paddy rice discriminated more against the $\delta^{13}C$ compared to the water limited rainfed rice ($t = -7.23$, $p < 0.01$, $n = 3$ to 12, *Figure VI-3 b*). The higher $\delta^{13}C$ discrimination of the paddy rice was in accordance with the higher stomatal conductance (g_s) of the paddy rice measured at the uppermost leaf and under the controlled chamber conditions (*Figure VI-1*).

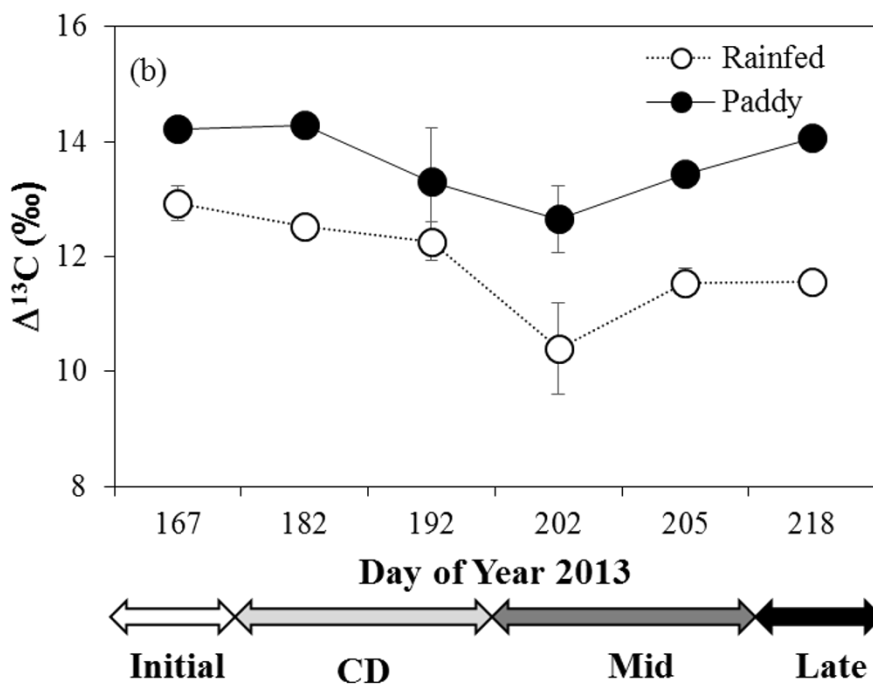
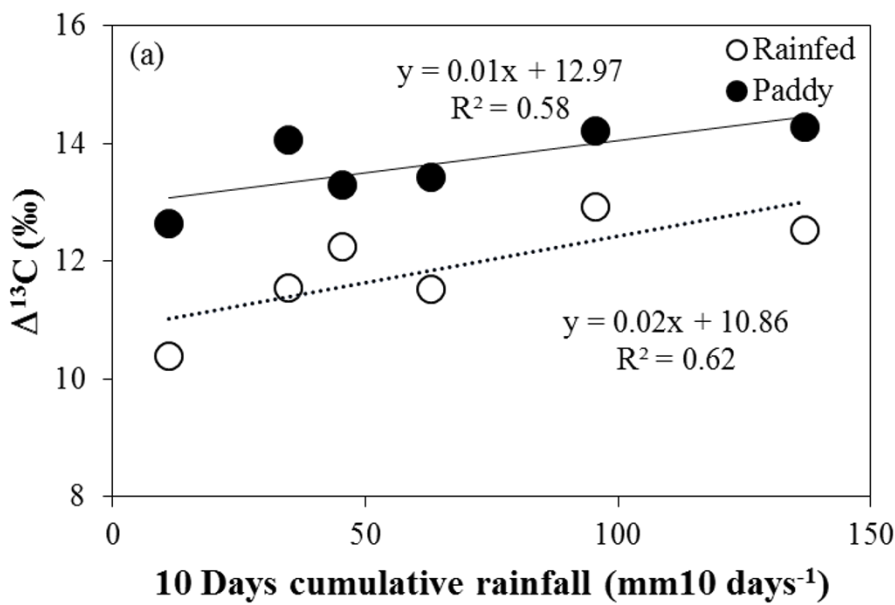


Figure VI-3 $\delta^{13}C$ carbon isotope discrimination ($\Delta^{13}C$) of rainfed and paddy rice above ground biomass harvested at different growth stages: (a) $\Delta^{13}C$ discrimination of rainfed rice (white circle) and paddy rice (black circle) correlated to the sum of the precipitation recorded within 10 days before the leaf biomass harvest (b) $\Delta^{13}C$ of rainfed rice (white circle) and paddy rice (black circle) followed the same seasonal trend although rainfed rice had lower carbon isotope discrimination (n=3 - 12, \pm SD).

Growth stage integrated intrinsic WUE ($WUE_{i-\delta^{13}C}$) and instantaneous WUE ($inWUE_{-\delta^{13}C}$) of rainfed and paddy rice were calculated based on $\delta^{13}C$ isotope discrimination ($\Delta^{13}C$) calculated based on measured $\delta^{13}C$ of bulk leaf biomass of the whole plant canopy of the rainfed and paddy rice harvested at each specific growth stages.

Integrated leaf water use efficiencies (integrated over the time of leaf development and the whole canopy); $WUE_{i-\delta^{13}C}$ and $inWUE_{\delta^{13}C}$ of rainfed and paddy rice were significantly different ($WUE_{i-\delta^{13}C}$: n=3 - 12, t=8.42, p < 0.05; $inWUE_{\delta^{13}C}$: n=3 to 12, t=9.14, p < 0.05). Temporal and canopy integrated intrinsic water use efficiency of ($WUE_{i-\delta^{13}C}$) of the rainfed rice was significantly higher than that of paddy rice (*Figure VI-4*; olive color bars for rainfed rice and dark green color bars for paddy rice). For the instantaneous water use efficiency ($inWUE$), temporal and canopy integrated $inWUE$ ($inWUE_{\delta^{13}C}$; *Figure VI-4*; white bars for rainfed and black bars for paddy rice) showed a similar result to that of short term $inWUE$ (Section 6.1.1). $inWUE_{\delta^{13}C}$ of the rainfed rice was higher than that of paddy rice (*Figure VI-4*) which is in line with *Figure VI-1*, rainfed rice with higher carbon assimilation per water use.

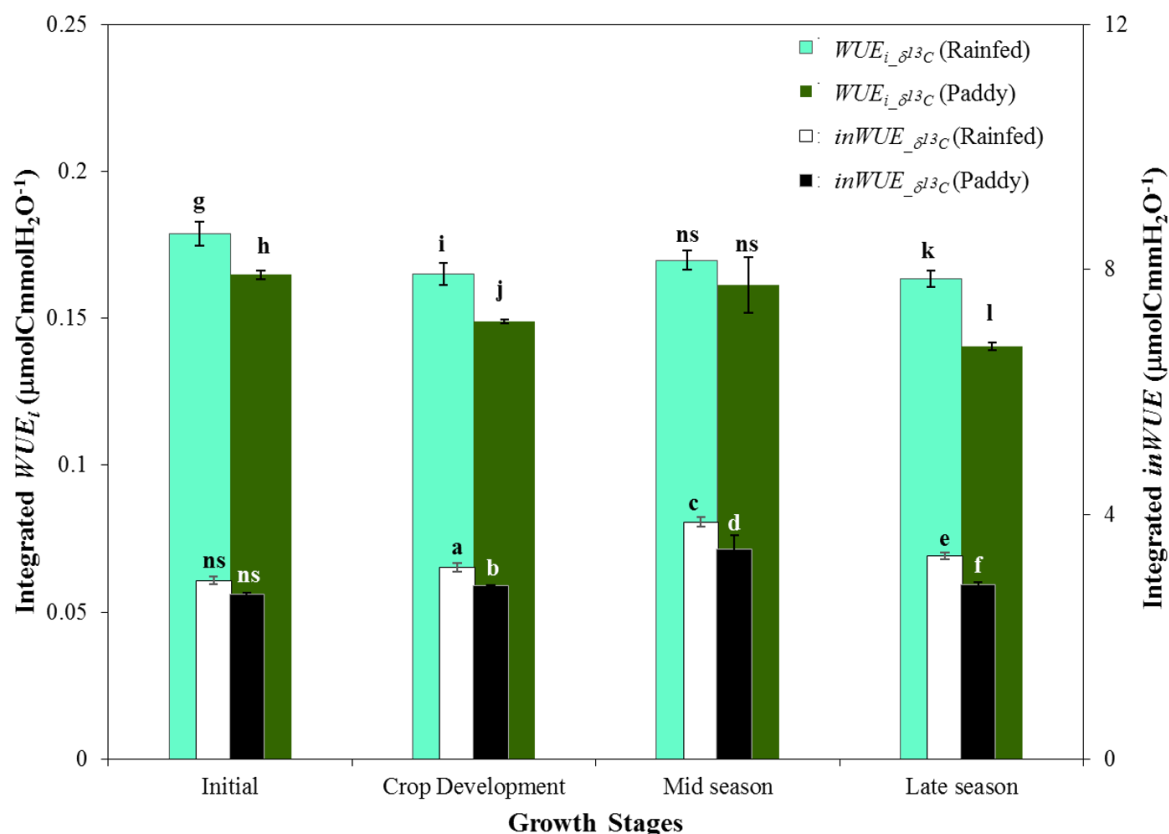


Figure VI-4 Growth stage integrated intrinsic water use efficiency ($WUE_{i-\delta^{13}C}$, light green for rainfed and dark green for paddy rice) and instantaneous water use efficiency ($inWUE_{\delta^{13}C}$, white for rainfed and black for paddy rice). Growth stage integrated WUE_i was calculated based on measured $\Delta^{13}C$ isotope values of bulk leaves harvested at different growth stages. Growth stage integrated $inWUE$ was calculated by multiplying the $\Delta^{13}C$ derived integrated WUE_i with growth stage average atmospheric VPD ($n=3$ to $12 \pm SD$)

6.1.3 Integrated canopy water use efficiency (WUE_{c-intg})

To consider the aspects of productivity, canopy WUE was calculated based on above ground biomass production per water use ($WUE_{c-Abg/Tc}$), as the ratio of the ratio of dry weight of the above ground biomass harvested at a specific growth stage to the integrated daily canopy transpiration of the same growth stage. WUE_{c-intg} of paddy rice was significantly higher than that of rainfed rice ($n=12$, $W=44.00$, $p < 0.05$). Thus, canopy WUE of paddy rice calculated

based on the above ground biomass production per water use (transpiration) was higher than that of rainfed rice.

As explained in the chapter (3), paddy rice performed better in terms of crop growth and development with higher *LAI*, higher stem biomass and slightly higher grain yield. On the other hand, rainfed rice reached higher leaf water use efficiency (*inWUE*) based on gas exchange analysis (*Figure VI-1*) and integrated leaf *WUE* ($WUE_{i-\delta^{13}C}$ and $inWUE_{\delta^{13}C}$) calculated based on $\delta^{13}C$ discrimination (*Figure VI-6*) clearly indicating that the causes at the expense of lower g_s and productivity.

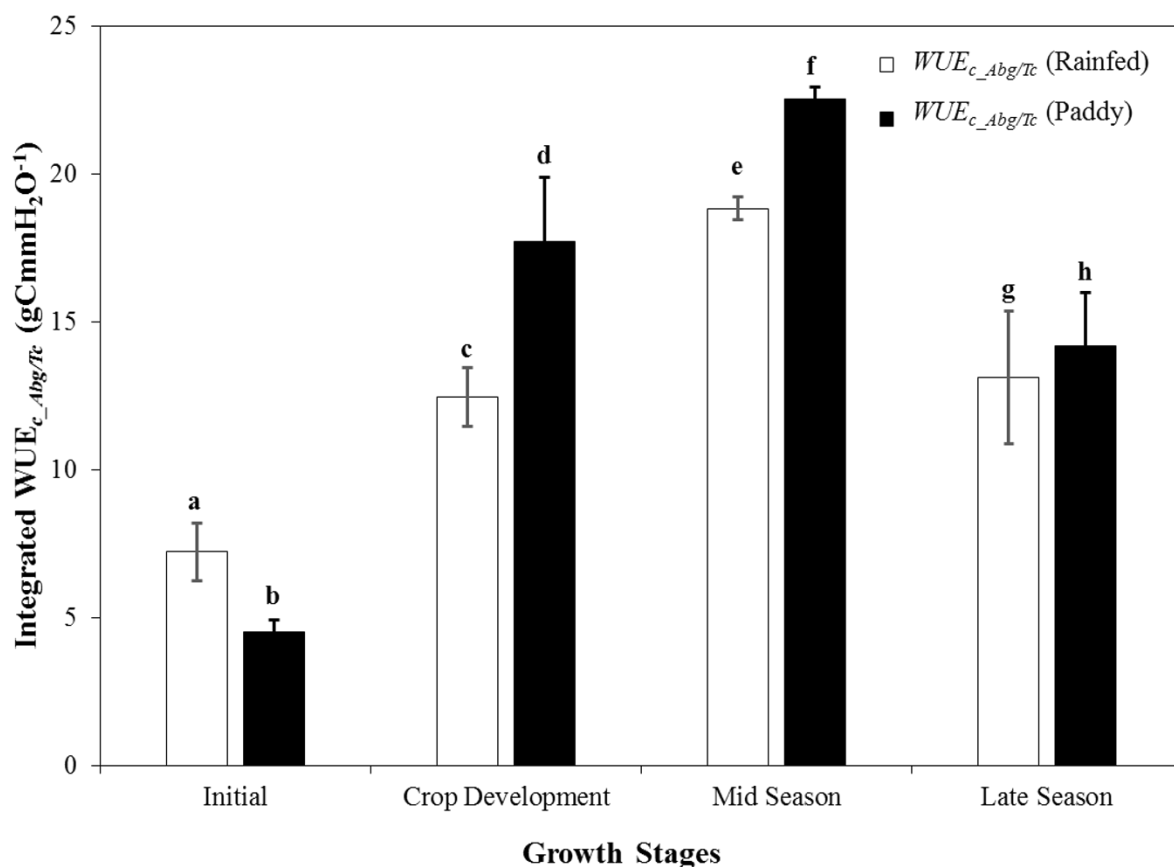


Figure VI-5 Growth stage integrated canopy water use efficiency ($WUE_{c-Abg/Tc}$) of rainfed rice (white) and paddy rice (black); $n=3 - 6 \pm SD$. $WUE_{c-Abg/Tc}$ was calculated as the ratio of dry weight of above ground biomass harvested at a specific growth stage to the integrated daily canopy transpiration of the same growth stage.

6.2 Agronomic water use efficiency

As pointed out in section 6.1.3, paddy rice could produce more above ground biomass per transpiration water use compare to that of rainfed rice. Hence, paddy rice was more productive than rainfed rice in terms of biomass production per transpiration. However, since the final targeted product of rice production is the grain yield and not the carbon gain nor total biomass gain, water use efficiency of both rice production systems were also calculated as the ratio of grain yield to evapotranspiration, i.e., agronomic water use efficiency (WUE_{agro}). Moreover, field scale transpiration use efficiency (TE) of two systems were also compared to evaluate the impacts of evaporative water loss over WUE_{agro} .

WUE_{agro} of rainfed rice was significantly higher than that of paddy rice ($n=12$, $W=36$, $p < 0.05$, *Figure VI-6*) due to its significantly lower season total crop evapotranspiration (42.16 %) with only 9.53 % lower grain yield. However, after excluding the evaporative loss, transpiration use efficiency (TE) of paddy was a bit higher but not statistically different to that of rainfed rice ($n=12$, $W=23$, $p = 0.48$, *Figure VI-6*). This indicates that higher WUE_{agro} of rainfed rice was only due to its lower evaporative water losses. Paddy rice with higher $WUE_{c_Abg/Tc}$, TE and slightly higher grain yield was more productive in terms of carbon assimilation per transpiration use but had higher evaporative water losses.

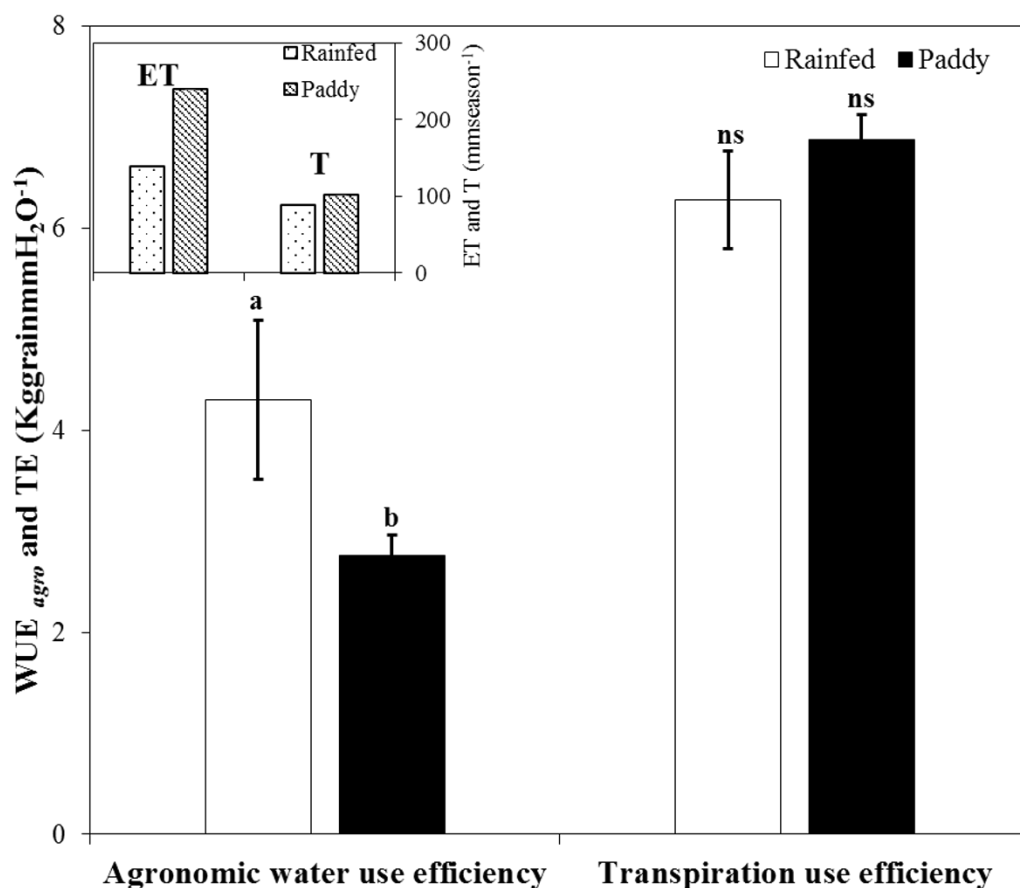


Figure VI-6 Agronomic water use efficiency ($WUE_{agro} = \text{Grain yield}/ET$) and transpiration use efficiency ($TE = \text{Grain yield}/T$) of rainfed and paddy rice. Both T and ET were calculated as the sum of daily T , and ET of the whole crop season (i.e., 120 days) ($n = 12$, \pm SD)

6.3 Ecosystem water use efficiency

After studying the carbon and water exchange in the rainfed and paddy rice ecosystems, the ecosystem water use efficiency (WUE_{eco}) of rainfed and paddy rice were also compared.

6.3.1 Carbon and water exchange in rainfed and paddy rice

To investigate the role of carbon and water exchange on WUE_{eco} we measured canopy gas exchange (NEE , GPP , R_{eco} and ET) at different growth stages. For the seasonal trend, daily NEE , GPP , R_{eco} and ET were simulated and validated against the chamber measured fluxes, showing a good agreement between measured and modelled data (NEE : $ME=0.86$, $RMSE=$

0.58, $R^2 = 0.86$; GPP : $ME=0.95$, $RMSE=0.63$, $R^2=0.99$; R_{eco} : $ME= 0.72$, $RMSE= 0.51$, $R^2= 0.75$; ET : $ME=0.82$, $RMSE=0.13$, $R^2=0.97$). Rainfed and paddy rice systems showed significantly different water and carbon fluxes ($n=12$, $W=54.00$, $p \leq 0.05$; *Figure VI.9*). Evapotranspiration (ET) of paddy rice was 42.16 % higher than that of rainfed rice (See detail in the chapter 4). However, there was no significant difference between canopy transpiration (T) although T of paddy rice was 11.02 % higher than that of rainfed rice

Growing season total gross primary production ($GPP = \text{sum of simulated daily } GPP \text{ during monsoon rice growing season 2013}$) of paddy and rainfed rice were not significantly different. However, paddy rice had significantly lower ecosystem respiration (R_{eco}) in both, chamber measured and simulated daily R_{eco} , hence net ecosystem exchange (NEE) was higher in paddy rice (*Figure VI.7*). Growing season total ecosystem respiratory carbon loss in rainfed rice was 48.65 % of the gross carbon fluxes while paddy rice ecosystem respiratory carbon loss was only 33.77 % of the gross fluxes. Both measured and simulated R_{eco} of rainfed and paddy rice was strongly correlated to T_{air} and T_{soil} (Spearman's $\rho = 0.74$, 0.80 , respectively for paddy; Spearman's $\rho = 0.74$, 0.80 , respectively for rainfed, $p \leq 0.01$). According to dark chamber measured soil and plant respiration, R_{eco} of paddy rice was dominated by plant respiration (R_{pt}) while R_{eco} of rainfed rice was mainly dominated by soil respiration (R_{soil}). Therefore, higher respiratory carbon loss of rainfed rice system was clearly due to its higher soil respiration.

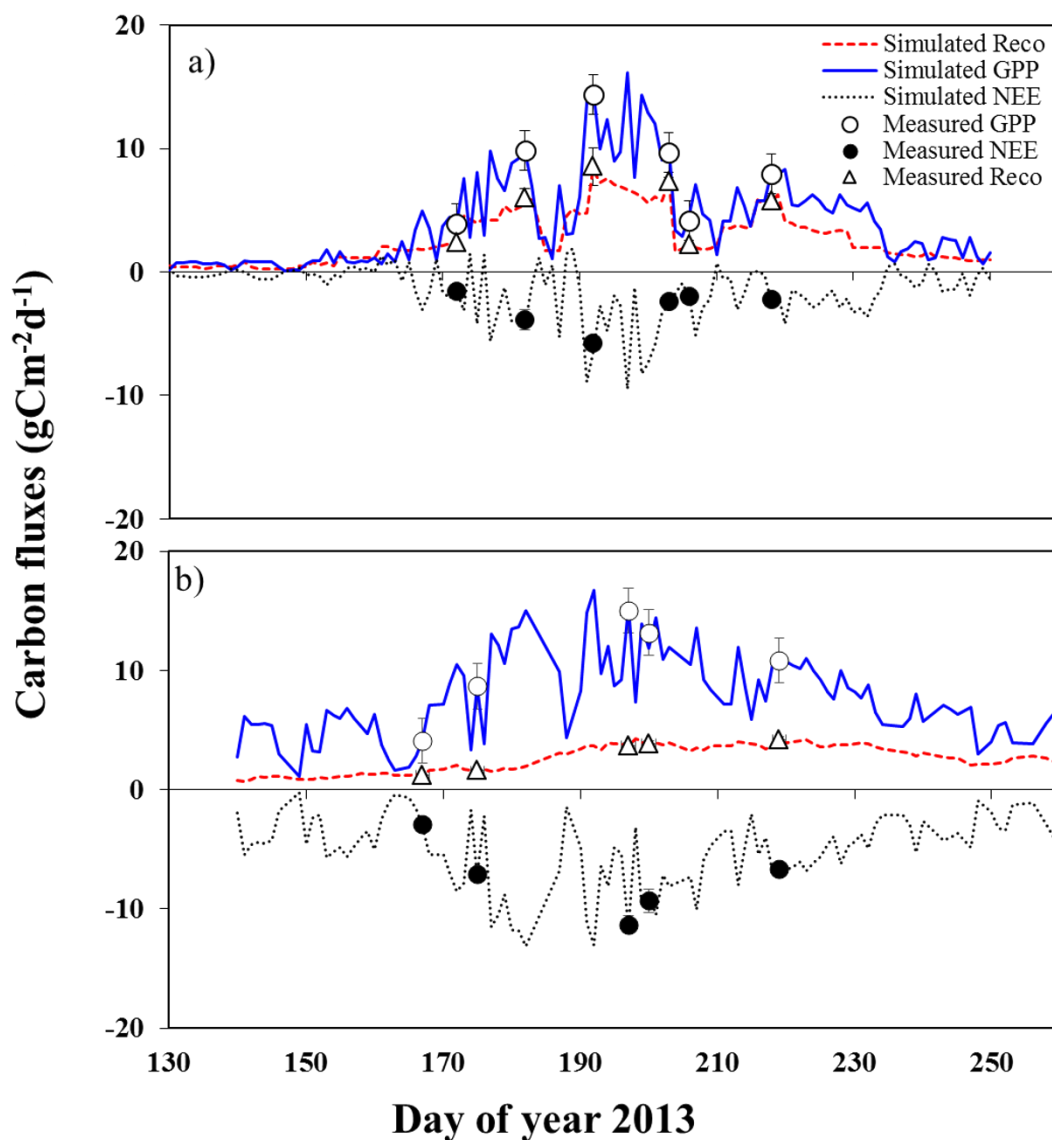


Figure VI-7 Daily carbon fluxes of paddy and rainfed rice: (a) rainfed rice; (b) paddy rice (simulated gross primary production, blue line; measured gross primary production, white circle; simulated ecosystem respiration, red dashed-line; measured ecosystem respiration, white triangle; simulated net ecosystem exchange, black dotted line; chamber measured net ecosystem exchange, black circle); $n=3 \pm \text{SD}$.

6.3.2 Ecosystem water use efficiency of rainfed and paddy rice

Rainfed rice had higher ecosystem water use efficiency ($WUE_{eco} = GPP/ET$) than paddy rice (Figure VI.8). Interestingly, after excluding the differences in evaporative water loss (i.e.,

GPP/T), there was no significant difference between paddy and rainfed rice ($n=12$, $W=44.00$, $p = 0.39$, data not shown). Thus, lower GPP/ET of paddy rice was mainly due to its higher evaporative losses and not because of its ecosystem productivity.

Moreover, if the differences in ecosystem respiratory carbon losses of paddy and rainfed rice (i.e., ecosystem water use efficiency as the balance of net ecosystem carbon and water fluxes (NEE/ET), NEE/ET of both paddy and rainfed were not different to each other ($n=12$, $W=62.50$, $p = 0.58$). No different in NEE/ET of rainfed and paddy rice systems revealed the dominant role of higher respiratory carbon losses in rainfed rice ecosystem carbon exchange and ecosystem water use efficiency. Similarly, the effect of evaporation was excluded from net ecosystem water fluxes (i.e., NEE/T), paddy significantly had higher water use ($n=12$, $W = 13.00$, $p \leq 0.05$), pointing the dominant impacts of evaporative losses over NEE/ET . These results clearly show that ecosystem water use efficiency was not simply a ratio of GPP to ET but the effects of respiratory carbon loss and evaporative water loss over WUE_{eco} should also be considered in the calculation of WUE_{eco} .

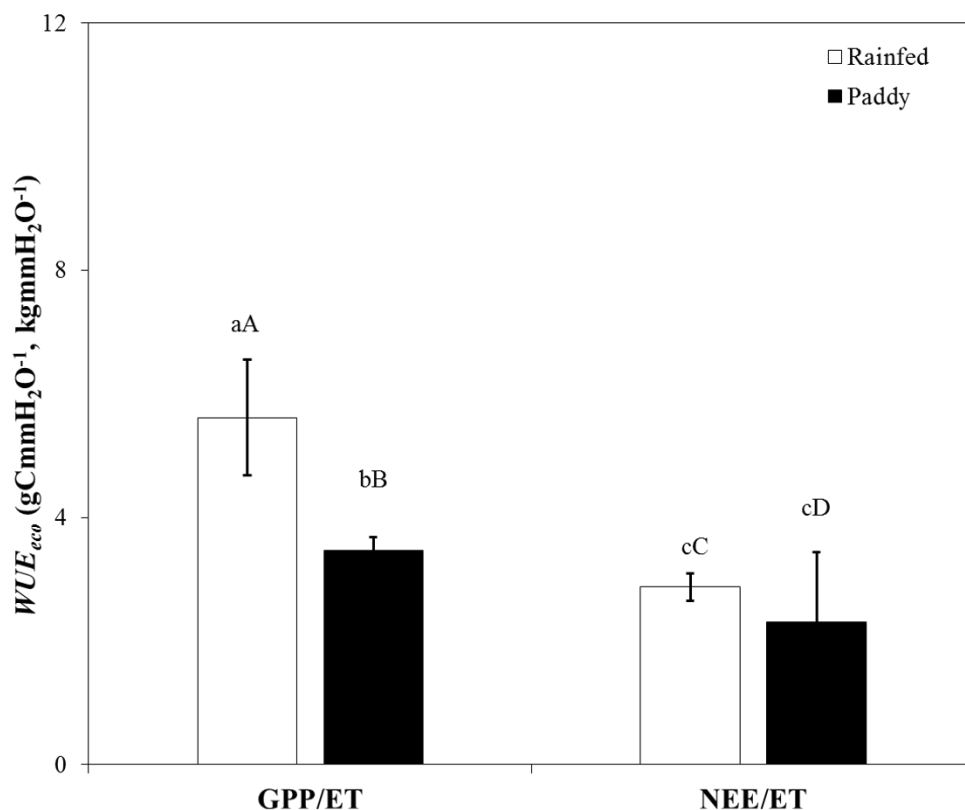


Figure VI-8 Comparing ecosystem water use efficiency of rainfed and paddy rice to highlight the importance of evaporation and ecosystem respiration in the definition of WUE_{eco} ; $n=12 \pm SD$

Table VI-1 Summary statistics of the components of different spatiotemporal water use efficiencies of rainfed and paddy rice. Wilcoxon-Mann-Whitney Rank Sum test was performed to compare different *WUE* components of rainfed and paddy rice. All of the values except the values labeled as “Field scale” and “Growing Season” are the overall crop growth season means. Values labeled as “Field scale” and “Growing Season” are the integrated values over the growing season.

Spatial Scale	Temporal Scale	Variables	Rainfed		Paddy		<i>W</i>	p-value (95%)
			Mean	SD	Mean	SD		
<i>n</i> = 12								
Leaf	Seconds (Both A_{max} and g_s were measured under controlled environment condition.)	A_{max} ($\mu\text{mol m}^{-2}\text{s}^{-1}$)	23.36	3.79	20.88	5.54	94.00	0.20
		$g_{sat, Amax}$ ($\text{mmol m}^{-2}\text{s}^{-1}$)	253.18	60.34	289.24	112	76.00	< 0.05
		T ($\text{mmol m}^{-2}\text{s}^{-1}$)	3.88	0.78	3.79	1.13	77.00	0.80
	Time integrated*	$\Delta^{13}\text{C}$ (‰)	11.73	1.06	13.75	0.63	31.00	< 0.05
Field (Agronomy)	Time integrated*	Abg (g)	710.26	673.52	925.48	762	56.00	0.38
		ET (mm)	89.85	40.31	151.84	na	27.00	< 0.05
		T (mm)	45.07	30.52	48.53	na	72.00	0.24
	Growing Season	$Yield$ (t ha^{-1})	5.98	0.57	6.61	0.68	26.00	0.24
		ET (m^3ha^{-1})	1388	68	2399	na	No statistical analysis is available.**	
		T (m^3ha^{-1})	898	57	1009	na		
Ecosystem	Days	NEE ($\text{gCm}^{-2}\text{d}^{-1}$)	3.36	1.78	6.49	2.46	19.00	< 0.05
		GPP ($\text{gCm}^{-2}\text{d}^{-1}$)	9.03	4.12	9.21	3.55	66.00	0.76
		R_{eco} ($\text{gCm}^{-2}\text{d}^{-1}$)	5.62	2.48	2.72	1.40	126.00	< 0.05
		ET (mm d^{-1})	1.48	0.32	2.89	na	15.00	< 0.05
		T (mm d^{-1})	1.15	0.31	1.27	na	54.00	0.29
	Growing Season	NEE (tCha^{-1})	3.99	1.47	5.52	2.21	No statistical analysis is available.**	
		GPP (tCha^{-1})	7.79	2.65	8.32	1.89		
		R_{eco} (tCha^{-1})	3.79	2.42	2.81	1.61		
		ET (m^3ha^{-1})	1388	68	2399	na		
		T (m^3ha^{-1})	898	57	1009	na		

Note: * $\Delta^{13}\text{C}$ was calculated based on the biomass harvested at different crop growth stages.

** Above ground biomass (Abg) was harvested at different crop growth stages. ET and T were daily-integrated values for the same crop growth stages of the harvested biomass

*** Statistical test was not done for the growing season totals, which were simulated.

Table VI-2 Comparison of different spatiotemporal water use efficiencies of rainfed and paddy rice. Wilcoxon-Mann-Whitney Rank Sum test was performed to compare different *WUEs* of rainfed and paddy rice.

Spatial Scale	Temporal Scale	Variables	Rainfed		Paddy		<i>W</i>	p-value (95%)
			Mean	SD	Mean	SD		
			<i>n</i> = 12					
Leaf	Seconds	WUE_i (A/g_z)	0.09	0.02	0.08	0.02	94.00	0.22
		$inWUE$ (A/T)	6.12	0.73	5.38	0.83	110.00	< 0.05
		$WUE_{i-\delta^{13}C}$ $\Delta^{13}C$	0.16	0.03	0.16	0.11	72.00	0.38
	Time integrated*	$inWUE_{\delta^{13}C}$ $\Delta^{13}C$	3.22	1.29	3.05	1.16	90.00	0.30
		$WUE_{c-Abg/Tc}$ Abg/T_c	12.15	6.62	15.72	7.60	44.00	< 0.05
	Canopy	Time integrated**						
Field (Agronomy)	Growing Season	TE	6.70	0.70	6.41	0.72	23.00	0.48
		$Yield/T$						
		WUE_{agro}	4.27	0.42	2.75	0.28	36.00	< 0.05
		$Yield/ET$						
Ecosystem	Days	NEE/ET	2.20	0.89	2.39	1.06	62.50	0.58
		NEE/T	2.83	1.13	4.96	1.14	13.00	< 0.05
		GPP/ET	5.97	2.03	3.51	1.91	119.00	< 0.05
		GPP/T	7.62	2.38	7.01	1.50	44.00	0.39
	Growing Season	NEE/ET	2.88	0.22	2.30	0.41	No statistical analysis is available.***	
		NEE/T	4.44	0.63	5.47	0.17		
		GPP/ET	5.61	0.94	3.47	0.19		
		GPP/T	8.68	1.87	8.25	0.48		

Note: * $\Delta^{13}C$ was calculated based on the biomass harvested at different crop growth stages.

** Above ground biomass (*Abg*) was harvested at different crop growth stages. *ET* and *T* were daily-integrated values for the same crop growth stages of the harvested biomass.

*** Statistical test was not done for the growing season totals, which were simulated.

6.4 Summary

Comparing the water use efficiency of rainfed and paddy rice at different temporal and spatial scales indicates that both intrinsic (A/g_s) and instantaneous (A/T) water use efficiency of the uppermost leaves of both rainfed and paddy rice cannot represent the biomass related water use efficiencies (i.e., $WUE_{c_Abg/Tc}$ and WUE_{agro}).

Rainfed rice was water use efficient compared to paddy rice, in terms of WUE_{agro} (*Grain yield/ET*) and WUE_{eco} (*GPP/ET*). However, if the higher evaporative losses of paddy rice and the higher respiratory losses of rainfed rice systems were taken into account, ecosystem and agronomic water use efficiency of both systems were almost the same.

7



VII. Discussion and outlook

7.1 Evapotranspiration estimation methods

Among the several models to estimate ET developed since the 1950s, the *FAO* modified Penman-Monteith crop ET model (*56PM*) performed the best after combing with field measured basic leaf physiological parameters and remotely sensed *NDVI* data.

The quality of estimated ET by the *56PM* depends largely on the quality of reference crop ET (ET_0) estimates (Cruz-Blanco et al., 2014; López-Urrea et al., 2006): the estimation ET_0 for a specific crop of interest rather than the grass reference crop performed better ET estimation of that crop (Chapter 4 of this study). Application of field measured leaf resistance of the crop of interest in the calculation of canopy resistance of the ET_0 model enhanced the ET estimates since canopy resistance is important in controlling ET , especially in the rice crops (Sakuratani and Horie, 1985). However, field measurements of leaf resistance will be hard to do for a larger scale. In this case, the original *FAO 56* reference ET estimation method can be used by applying a fixed canopy resistance (r_c) at 120 sm^{-1} for rice, rather than using the recommended value, 70 sm^{-1} . This finding is in accordance with the findings of previous studies in rice and other agricultural crops (Lecina et al., 2003; Todorovic, 1999; Zhao, 2014). However, this r_c value of 120sm^{-1} is recommended only for the rice crop. For other crops, it is recommended to use the published canopy resistances of the crop of interest cultivated in a similar climatic zone or to measure the leaf resistance in the peak of the crop growing season and use it as an input parameter. •

A drawback of ET_0 estimation by the *56PM* method is its high demands on environmental data (Pereira and Pruitt, 2004; Todorovic et al., 2013). Daily and consecutive inputs for all of the required environmental data may not be available for some regions and under certain conditions. In those cases, Makkink (1957)'s ET_0 estimation method could be a good alternative to *56PM*. Comparing different ET_0 estimation methods with the *56PM* and the modified *56PM* of this study showed that Makkink (1957) method was a good alternative to the *56PM*, especially for rice and agricultural crops.

The *56PM* model needs to multiply the estimated reference crop ET with crop coefficients (K_{cb}). Allen et al. (1998) suggested adjusting the provided crop coefficients according to the climatic condition of the area of interest. However, in some cases it does not work even after

the climatic adjustment since K_{cb} is not only affected by the climatic conditions but also by nutrients, soil water availability, pest and diseases, atypical plant stands, etc. (Hunsaker et al., 2005). Other studies and this study proved that even after the climatic adjustment, the *56PM* recommended K_{cb} value for rice could not represent the actual crop growth very well and leads to over and underestimation of ET (*Figure IV.3*; Bausch and Neale, 1987; Bausch, 1995; Choudhury et al., 2013; Hunsaker, 1999).

The reason could be that the provided K_{cb} value for rice crop was taken from the study on conventional rice crop, which plant height, leaf area index, and above ground biomass are superior to the high yielding rice variety used in this study. Most of the provided crop coefficients in Allen et al. (1998) are mainly based on published literatures before and during that time period of the *56PM* model development and the provided K_{cb} values may not represent the modern high yielding varieties well. Applying the K_{cb} derived from high resolution *NDVI* of rice field delivered better *ET* estimates (*Figure IV.3*, Glenn et al., 2010; Hunsaker et al., 2003; Kamble et al., 2013). The performance of *ET* estimation will be improved if both *NDVI* derived K_{cb} and canopy resistance modification of *56PM* model are applied together.

Previous studies pointed the weakness of the *56PM* type models. Gonzalez-Dugo et al. (2009) compared a satellite *NDVI* based *56PM* type model and a thermal based surface energy balance model. Their works reported that the satellite *NDVI* based *56PM* type model could not represent the actual crop condition due to the over and under estimation of crop coefficients if there is not a reliable data set of rainfall distribution, reference evapotranspiration and soil moisture distribution data over the whole spatial area of interest. However, the use of Unmanned Aerial Vehicle (UAV) derived *NDVI* instead of satellite derived *NDVI* can provide high resolution *NDVI* data which can represent the actual crop growth condition (this study, Gago et al., 2014; Ko et al., 2015) and can provide a reliable crop *ET* estimates. Thus, the *56PM* type models in combination with UAV derived *NDVI* data can still be a good choice for the agricultural crops, especially, in the sense of precision agriculture.

This study is in line with the review comments of Pereira et al. (2014) on the past and future of the *56PM* type models. The need to expend the database of crop coefficients for the new crop varieties is reported practically by comparing the *56PM* provided K_{cb} value for rice and the remotely sensed actual K_{cb} value of high yielding new variety of rice (Chapter 4, Section 4.2.1 and 4.2.2). Moreover, this study also proved the needs to develop more sophisticated K_{cb} curve than the typical four stages K_{cb} curve (initial, crop development, mid-season and late

season) so that the crop coefficients could represent the dynamics and correct estimates of crop growth stages.

7.2 Partitioning Evapotranspiration

Partitioning daily soil evaporation and plant transpiration fluxes by the *56PM* model was along with the partitioning results of $\delta^{18}O$ stable isotopic *ET* partitioning. $\delta^{18}O$ isotopic partitioning method is regarded as direct partitioning approach due to its way of partitioning water fluxes after tracing distinct $\delta^{18}O$ isotopic signals of the soil evaporation and plant transpiration and a useful approach for large scale *ET* partitioning (Dubbert et al., 2013; Kool et al., 2014). On the other hand, due to the needs of timely crop management such as weeding, irrigation, fertilization, chamber-measured $\delta^{18}O$ based *ET* partitioning which needs the permanent installation of soil collars, soil moisture sensors, etc. is still challenging for the large-scale agricultural studies in real agro-ecosystems. However, calibrating and validating the partitioning results of the *56PM* dual crop model with the $\delta^{18}O$ based partitioning output carried out together in a small scale experimental field and apply the model in the real world would be appropriate.

The growing season average *T/ET* of paddy rice in this study is in accordance with the findings of Maruyama and Kuwagata (2010), Sakuratani and Horie (1985) and Wei et al. (2015). *T/ET* of rainfed rice is scarce except the work of Alberto et al. (2014) and *T/ET* of this study is significantly lower than their findings. Crop seasonal average *ET* of this study is lower than most of previous works on rice ecosystem listed in *table (VII-1)* except the *ET* of S. Korean paddy rice system reported by Zhao (2014). The lower crop season average *ET* value of this study and Zhao (2014) may be due to the regional microclimatic differences and crop physiological differences. This study was done under the typical S. Korean monsoon with frequent cloudy days while the other studies were done avoiding most of the monsoon period (*table VII-1*). Moreover, the two Korean paddy rice study with reported lower *ET* used the Japonica rice variety and physiological development of the rice used in this study and the rest was significantly different as the *LAI* of this study was the lowest (*Figure III- 2*, chapter 3) compared to others. Never the less, general *ET* and *T/ET* trends of this study followed the previous reports and are almost the same as the one reported by Zhao (2014).

Table VII-1 Partitioning evapotranspiration of rainfed and paddy rice by different methods

No	Publication	Crop	Irrigation	Study site	Partitioning method			E/ET	T/ET	ET (mmd ⁻¹)	LAI (mm ⁻²)	Planting Time	Crop cycle (Days)
					ET	E	T						
1	Sakuratani and Horie (1985)	Paddy Rice (Indica)	Flooded	Japan	M-lys	Pan	Pan	0.52	0.48	3.98	4.60	May	~130
2	Maruyama and Kuwagata (2010)	Paddy Rice (Indica)	Flooded	Japan	two source model (Kondo and Watababe, 1992)			0.57	0.43	3.78	4.60	April	~130
3	Hossen et al (2012)	Paddy Rice (Indica type <i>Boro rice</i>)	Flooded	Bangladesh	EC	Empirical equation dependent on LAI	0.30	0.70	3.33	5.90	March	~ 100	
		Rainfed rice (Indica type <i>Aman rice</i>)	Rainfed (Total rainfall, 552.80 mm, no irrigation)				0.36	0.64	2.93	4.60	September	~ 100	
4	Alberto et al (2011; 2014)	Paddy Rice (Indica type)	Flooded	The Philippines	EC and 56PM			N/A	N/A	4.29	6.65	June	120
		Rainfed Rice (Indica type)	Sprinkler irrigation (645.9 mm Sprinkler irrigation + 251.9 mm rainfall = 897.8 mm)					0.44	0.56	3.81	4.65	January	120
5	Zhao (2014)	Paddy Rice (Japonica type)	Flooded	S. Korea	EC and empirical equation dependent on LAI			0.62	0.38	2.00	5.80	May	120
6	Wei et al (2015)	Paddy Rice (Indica type)	Flooded	Japan	$\delta^{18}O$			0.20	0.80	N/A	4.50	May	~150
7	This study	Paddy Rice (Indica type)	Flooded	S. Korea	56PM			0.60	0.40	2.00	3.78	April	120
		Rainfed Rice (Japonica type)	Rainfed (Total rainfall, 658.2 mm, no additional irrigation)	S. Korea	$\delta^{18}O$ and 56PM			0.35	0.65	1.16	2.69	April	120

Note: M-lys = micro lysimeter; Pan = Pan evaporation; EC= eddy covariance; 56PM = Penman-Monteith model modified by the FAO of the UN;

$\delta^{18}O = \delta^{18}O$ stable isotope partitioning

Similar to the seasonal trends, daytime water fluxes over the rainfed rice field were also dominated by the transpiration. ft (T/ET calculated based on $\delta^{18}O$) of rainfed rice fluctuated throughout the day but within in the ranged of previous studies, 0.3 to 0.8 (Cavanaugh et al., 2011; Dubbert et al., 2014b, 2013; Wang et al., 2010; Williams et al., 2004). Although $\delta^{18}O$ based partitioning gave the similar results to simulated daily partitioning approach, $\delta^{18}O$ approach gave the robust daytime E and T fluxes and the T/ET variation throughout the day, which support the daily simulation results. Based on the experience of this study, $\delta^{18}O$ approach can perform better if the condensation could be controlled completely in the case of higher humidity condition and if the soil water $\delta^{18}O$ at 0 to 3 cm depth (as recommended by Dubbert et al., 2013) is available and if the leaf water $\delta^{18}O$ is measured in the field. Nevertheless, this study provide a sketch of $\delta^{18}O$ values of source water (rain) and fluxes in the soil-plant-atmosphere continuum of the rainfed rice field cultivated in monsoon 2013 in S. Korea. *Figure (VII-1)* showed the role of crop transpiration fluxes in terms of regional water vapor contribution, which is in accordance with other reports (for example, Jasechko et al., 2013; Shichun et al., 2010; Wang et al., 2014).

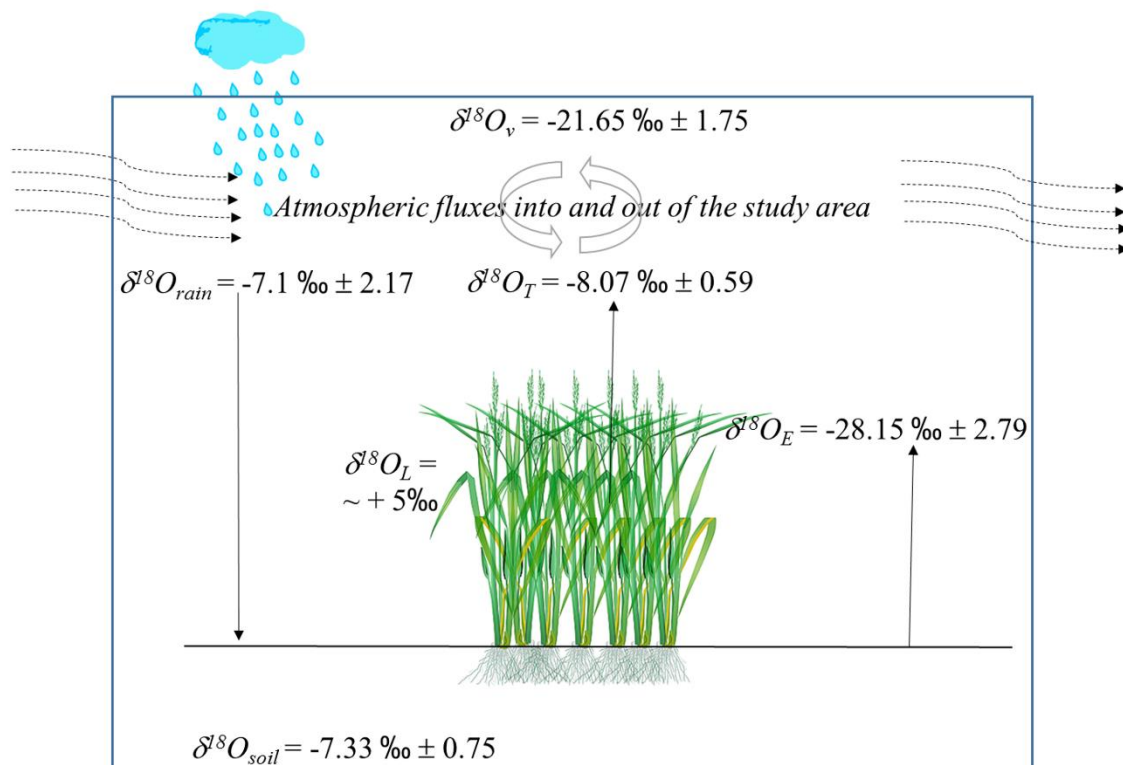


Figure VII-1 $\delta^{18}O$ values of source water (rain) and fluxes in the Soil-Plant-Atmosphere Continuum of the rainfed rice field. $\delta^{18}O_{rain}$ is $\delta^{18}O$ of precipitation; $\delta^{18}O_{soil}$ is $\delta^{18}O$ of soil water; $\delta^{18}O_E$ is $\delta^{18}O$ of soil evaporation; $\delta^{18}O_L$ is $\delta^{18}O$ of bulk leaf water; $\delta^{18}O_T$ is $\delta^{18}O$ of transpiration and δ_v is $\delta^{18}O$ of atmospheric water vapor

7.3 Water use efficiency concepts

Based on the different *WUEs* of the rice measured by different concepts and at different temporal, spatial scales (*Figure VII-2*), *WUEs* can be grouped into two: physiological process based *WUEs* and productivity based *WUEs*. Physiologically defined *WUEs*, which include intrinsic *WUE*, instantaneous *WUE* and ecosystem *WUE*, of rainfed rice was higher than that of paddy rice. On the other hand, productivity based *WUEs*, which include biomass production per transpiration and grain yield per transpiration, paddy rice was higher than that of rainfed rice. Based on the theories and published data sets, Blum (2011, 2009, 2005) pointed the misuse of intrinsic *WUE* (A/g_s) and instantaneous *WUE* (A/T) in the selection of higher water use efficient crop varieties. Tomás et al. (2012) also proved in vineyards that plant water use variability could not be described based on leaf *WUE* analysis. Moreover, as a proxy of the intrinsic *WUE*, $\delta^{13}C$ isotope discrimination ($\Delta^{13}C$) is widely applied in the selection high water use efficient crop varieties (for example, Condon et al., 2004). The relationship between $\Delta^{13}C$ and biomass production and crop yield are often reported for various crops (Cregg and Zhang, 2000; Farquhar et al., 1989; Hall et al., 1994; Monneveux et al., 2007, 2006; Saranga et al., 2004; Sayre et al., 1995; Specht et al., 2001). However, $\Delta^{13}C$, crop yield and agronomic *WUE* do not seem to have a clear relationship since previous studies ranged from no relationship to the positive and negative relationships. On the other hand, time integrated intrinsic *WUE* (A/T) calculated by incorporating the bulk leaf $\Delta^{13}C$ and atmospheric *VPD*, (*Figure VI-6*) could mimic the larger spatial scale *WUEs* including the canopy *WUE* and agronomic *WUE*. But, as reported by Rebetzke et al. (2008a, 2008b) and Sayre et al. (1995), those relationship could be biased by crop phenology, plant height, etc. Thus, care is needed to apply $\Delta^{13}C$ and leaf *WUE* as an indicator in the selection of higher agronomic or plant *WUE* since plant and agronomic *WUE* depends both crop ecophysiology and environmental variations.

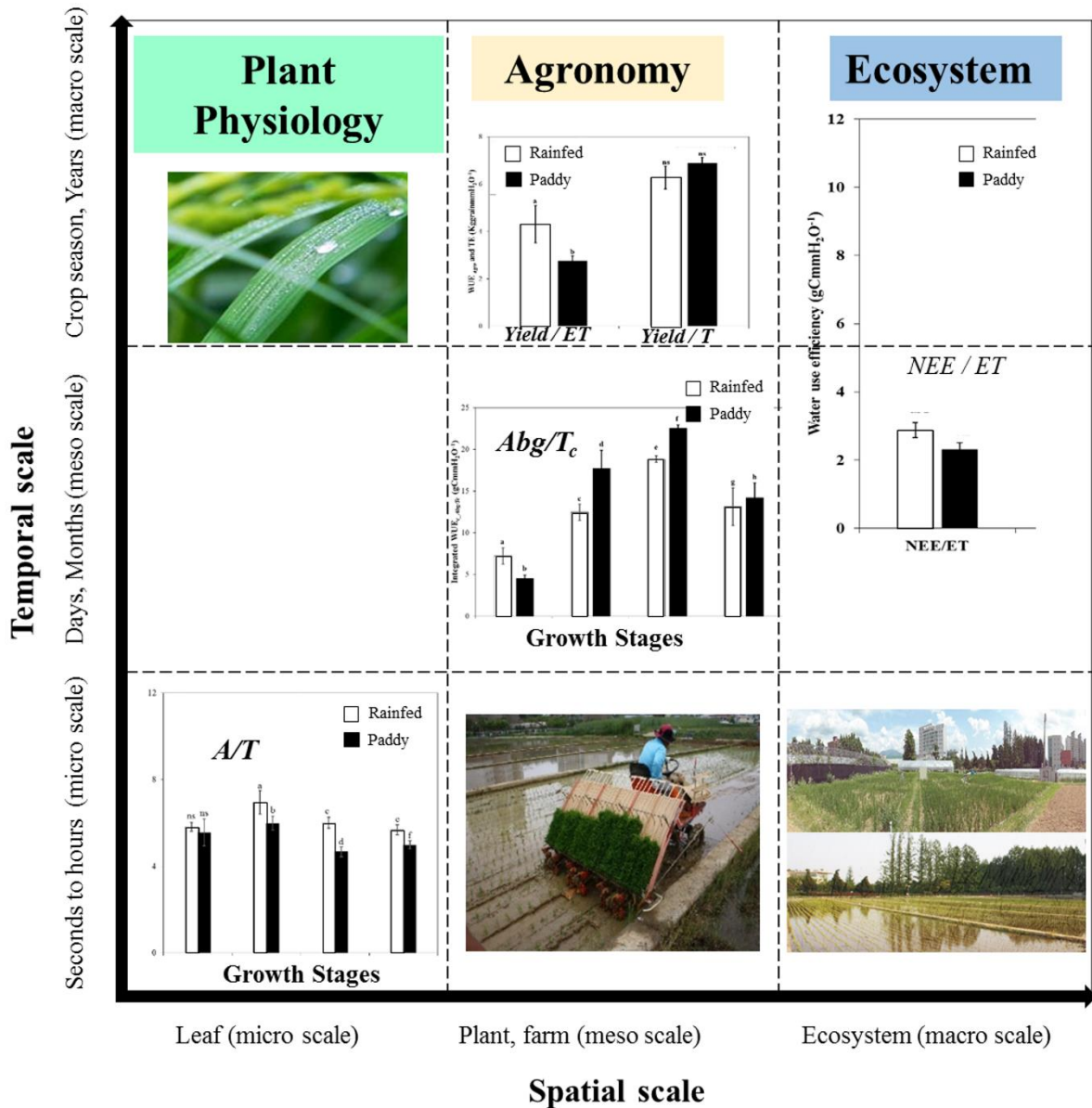


Figure VII-2 Spatial and temporal variation of the different WUEs of rainfed and paddy rice

Definition of ecosystem water use efficiency (WUE_{eco})

As expected, WUE_{eco} and WUE_{agro} (GPP/ET and $Yield/ET$) of rainfed was higher compared to paddy rice (Adekoya et al., 2014; Alberto et al., 2009; Thanawong et al., 2014; Figure VII.4), however a different picture emerged when considering the productive water use and respiratory losses. Generally, WUE_{eco} defined as the ratio of gross primary production to

evapotranspiration ($WUE_{eco} = GPP/ET$), has been estimated for different ecosystems ranging from grasslands to cultivated vegetation without considering the influence of respiratory carbon losses (R_{eco}) (Beer et al., 2009; Reichstein et al., 2002). Although, this yields information on the water use efficiency of plants to fix carbon at the stand level, considering ecosystem respiration losses is crucial to gain an ecosystem perspective (Dubbert et al., 2014b; Huang et al., 2010; Scott et al., 2006; Tallec et al., 2013; Zeri et al., 2013). Partitioning carbon and water fluxes in paddy and rainfed rice revealed the strong influence of R_{eco} over WUE_{eco} . Accordingly, higher GPP/ET in rainfed rice ecosystem was due to higher R_{eco} since rainfed rice had similar GPP to paddy rice but lower net ecosystem fluxes (NEE). Thus, accounting for this difference by considering net ecosystem exchange (NEE/ET) gave a comparable water use efficiencies of both rice production systems.

7.4 More crop per drops

Agricultural production worldwide is highly sensitive to the water scarcity and at the same time accounting for 70 % of the freshwater withdrawals. Increasing heat and drought stress predicted by climate change scenarios may thus strongly impact on the carbon cycling and, hence, the crop productivity, and strongly alter the hydrological cycle, threatening sustainability of current agroecosystems (FAO, 2012; Blanco et al., 2014). Rice production is one of the most water consuming crops and the rice production has huge impacts on the global and regional carbon and water cycling processes (Adekoya et al., 2014; Kim et al., 2013; Lindner et al., 2015). One of the objectives of this study was to compare the carbon and water fluxes between the conventional paddy and water saving rainfed rice, analyzing the distinct contributions of unproductive water losses from soil evaporation and respiratory carbon losses to net ecosystem carbon and water exchange. Quantifying the impact of these distinct irrigation treatments is

specifically important to find an optimal balance between low evaporative and respiratory losses for a sustainable rice production. In the following these trade-offs will be discussed in respect to water use efficiency of the two different rice management systems.

Comparing the paddy and rainfed system under the same climate condition revealed different carbon exchange process of water saving dryland rice and conventional paddy rice clearly (*Figure VII-3*).

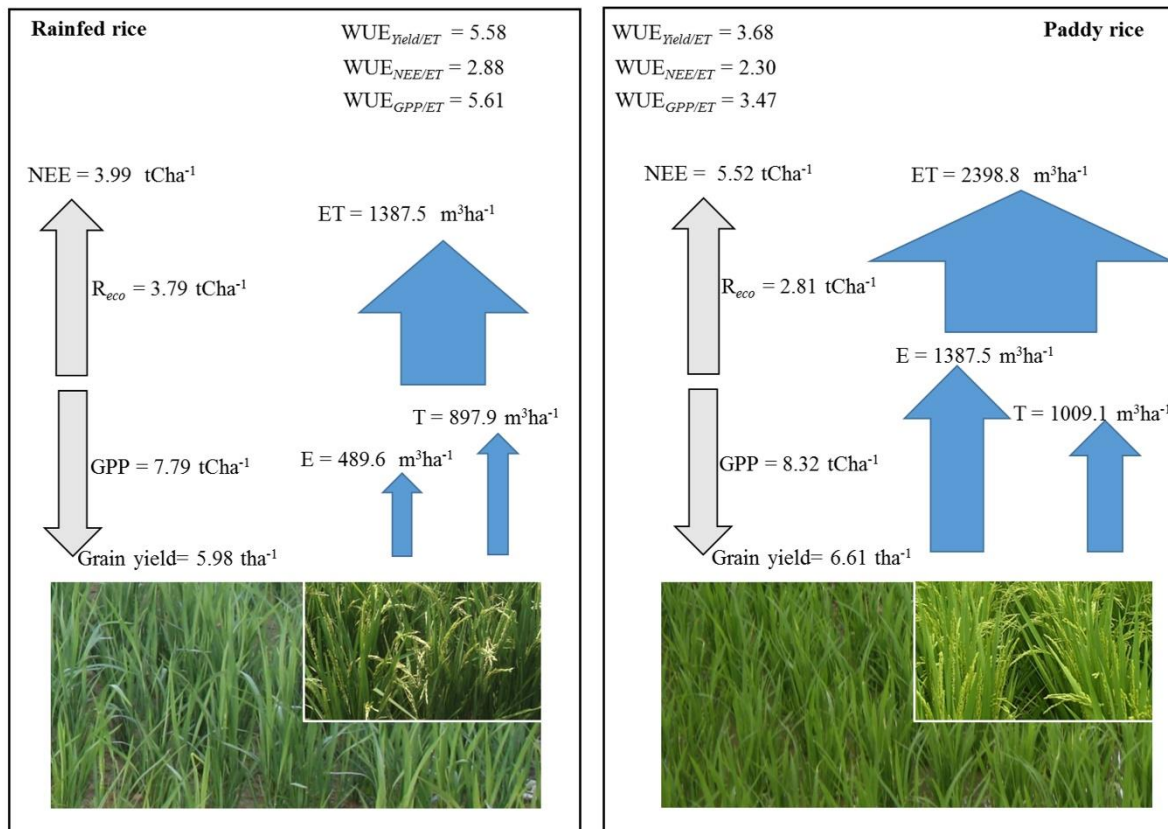


Figure VII-3 Seasonal carbon and water balance of paddy and rainfed rice. Measured and simulated daily gross primary production (*GPP*), net ecosystem exchange (*NEE*), ecosystem respiration (*R_{eco}*), evapotranspiration (*ET*), transpiration (*T*) and grain yields were used in this schematic representation. All flux data and grain yield are mean values (flux data: $n=3 \pm SD$; grain yield: $n=6 \pm SD$). Crop growing season was 120 days (sowing to harvest).

Rainfed rice production had higher R_{eco} (34.88 % higher than paddy) due to its higher soil respiration (see also Alberto et al., 2009; Miyata et al., 2000; Thanawong et al., 2014). On the other hand, paddy rice had higher evaporative water loss, which is regarded as the unproductive water loss. Nevertheless, minimizing the evaporative loss of paddy rice as much as possible, in other words, replacing the conventional paddy rice systems with the water saving and higher water use efficient rice systems, needs to be carefully evaluated. The paddy rice system is the conventional rice production system which can be found in most of the global rice production area (International Rice Research Institute [IRRI], 2002; Seck et al., 2012; Tuong et al., 2005). If most of the paddy system was converted to water saving production system, significantly reduced evaporation per unit production area can raise a question on possible global or regional water cycle changes although it may save the unproductive water losses (Fitzjarrald et al., 2008; Sakai et al., 2004; Zhao et al., 2008). Since the global water and carbon fluxes are coupled by the vegetation, impacts on the water cycle could lead to impacts on the global carbon balance (Hu et al., 2008; Istanbuluoglu et al., 2012; Tian et al., 2011; Williams and Albertson, 2005; Wolf et al., 2011).

Along with the respiratory carbon loss, the unproductive water loss (evaporation; E) considerably affects the water use of rice production. Evaporation (E) influences T by influencing the canopy microclimate (canopy temperature and VPD) which indirectly influences the T/ET , water use, crop growth and yield (Alberto et al., 2009; Balwinder-Singh et al., 2014; Leuning et al., 1994). Because of the maximization of carbon gain per water use along with the available water, the productive water use efficiency (GPP/T and $Yield/T$) of paddy and rainfed rice were almost equal, which means both rice systems had a similar productive water use efficiency and variations in agronomic and ecosystem $WUEs$ were related to the unproductive water losses (i.e., evaporation). The major differences of the amount of evaporation of rainfed and paddy rice occurred before the canopy closure (i.e., until DOY 200

and at the mid of crop development stage). By contrast, the contribution of evaporation to the water fluxes was relatively similar in both production systems, from the end of tillering stage onwards (DOY 200 and onward, *Figure V.5*), when the crop canopy was dense. Overall, the higher WUE_{agro} of rainfed rice was in concert with significantly reduced evaporation but also a slightly decreased grain yield compared to paddy rice.

According to the water scarcity projections based on the socioeconomic assumptions, population density per capita income, climate change scenarios and mitigation options, the frequency of extreme droughts may increase in many regions (Eastern China, India, Western Europe and Middle East) (Arnell and Lloyd-Hughes, 2013; Hejazi et al., 2014), highlighting the change in global hydrologic cycle. Moreover, global annual yield increase rate (current rate = 2.4%) of major agricultural crops (especially, rice, maize, wheat, soybean) should be doubled to meet the projected food demand by 2050 (Alexandratos and Bruinsma, 2012; Ray et al., 2013; Mutayya, et al., 2014). Hence, a choice between the trade-off of paddy rice production with high evaporative losses and methane emissions and rainfed rice with increased respiratory losses and possible impact on grain yield (though this was not significant in this study; Nay-Htoon et al., 2013; Tuong and Bouman, 2003, *Figure III*), depends largely on the regional water availability and precipitation regime. Moreover, the greenhouse gas balance of conventional flooded rice system is still unclear since CH_4 and N_2O emission not only depend on the amount of flooding but also on other factors such as climatic conditions, crop growth, atmospheric CO_2 concentration (Alberto et al., 2014; Wassmann et al., 2000; Groenigen et al., 2011, 2012; Dijkstra et al., 2012), source and rate of fertilizer applied (Berger et al., 2013), inorganic and organic carbon substrate availability for denitrifying bacteria, oxygen availability and bacterial activity (Seo et al., 2013). Traditional flooded paddy rice has high CH_4 and low N_2O emissions while non-flooded rainfed rice shows low CH_4 but high N_2O emissions (Weller

et al., 2014) together with high respiratory CO₂ release, all being relevant greenhouse gases (Xiao et al., 2005).

Under the environmental conditions at the present study location in S. Korea, with abundant monsoon rainfall, the high water consumption of paddy rice presents much less of a concern than high respiratory losses. However, in different climates, such as the Mediterranean, Africa or Middle East, producing rice in a more sustainable management regime considering its impact on the regional hydrological may well outweigh slight impacts on grain yield and higher respiratory losses.

References

- Adekoya, M. a., Liu, Z., Vered, E., Zhou, L., Kong, D., Qin, J., Ma, R., Yu, X., Liu, G., Chen, L., Luo, L., 2014. Agronomic and Ecological Evaluation on Growing Water-Saving and Drought-Resistant Rice (*Oryza sativa* L.) Through Drip Irrigation. *J. Agric. Sci.* 6, 110–119. doi:10.5539/jas.v6n5p110
- Agam, N., Evett, S.R., Tolk, J. a., Kustas, W.P., Colaizzi, P.D., Alfieri, J.G., McKee, L.G., Copeland, K.S., Howell, T. a., Chávez, J.L., 2012. Evaporative loss from irrigated interrows in a highly advective semi-arid agricultural area. *Adv. Water Resour.* 50, 20–30. doi:10.1016/j.advwatres.2012.07.010
- Alberto, M.C.R., Buresh, R.J., Hirano, T., Miyata, A., Wassmann, R., Quilty, J.R., Correa, T.Q., Sandro, J., 2013. Carbon uptake and water productivity for dry-seeded rice and hybrid maize grown with overhead sprinkler irrigation. *F. Crop. Res.* 146, 51–65. doi:10.1016/j.fcr.2013.03.006
- Alberto, M.C.R., Quilty, J.R., Buresh, R.J., Wassmann, R., Haidar, S., Correa, T.Q., Sandro, J.M., 2014. Actual evapotranspiration and dual crop coefficients for dry-seeded rice and hybrid maize grown with overhead sprinkler irrigation. *Agric. Water Manag.* 136, 1–12. doi:10.1016/j.agwat.2014.01.005
- Alberto, M.C.R., Wassmann, R., Hirano, T., Miyata, A., Hatano, R., Kumar, A., Padre, A., Amante, M., 2011. Comparisons of energy balance and evapotranspiration between flooded and aerobic rice fields in the Philippines. *Agric. Water Manag.* 98, 1417–1430. doi:10.1016/j.agwat.2011.04.011
- Alberto, M.C.R., Wassmann, R., Hirano, T., Miyata, A., Kumar, A., Padre, A., Amante, M., 2009. CO₂/heat fluxes in rice fields: Comparative assessment of flooded and non-flooded fields in the Philippines. *Agric. For. Meteorol.* 149, 1737–1750. doi:10.1016/j.agrformet.2009.06.003
- Alexandratos, N., Bruinsma, J., 2012. World agriculture towards 2030/2050: the 2012 revision. *ESA Work. Pap. No. 12-03.*
- Allen, R.G., Pereira, L.S., Raes, D., Smith, M., W, A.B., 1998. Crop evapotranspiration - Guidelines for computing crop water requirements - FAO Irrigation and drainage paper 56. *Irrig. Drain.* 1–15. doi:10.1016/j.eja.2010.12.001
- Allen, R.G., Pruitt, W.O., Wright, J.L., Howell, T.A., Ventura, F., Snyder, R., Itenfisu, D., Steduto, P., Berengena, J., Yrisarry, J.B., Smith, M., Pereira, L.S., Raes, D., Perrier, A., Alves, I., Walter, I., Elliott, R., 2006. A recommendation on standardized surface resistance for hourly calculation of reference ETo by the FAO56 Penman-Monteith method. *Agric. Water Manag.* 81, 1–22. doi:http://dx.doi.org/10.1016/j.agwat.2005.03.007
- Allison, G.B., Barnes, C.J., Hughes, M.W., 1983. The distribution of deuterium and ¹⁸O in dry soils 2. Experimental. *J. Hydrol.* 64, 377–397. doi:http://dx.doi.org/10.1016/0022-1694(83)90078-1

- Arnell, N.W., Lloyd-Hughes, B., 2013. The global-scale impacts of climate change on water resources and flooding under new climate and socio-economic scenarios. *Clim. Change* 122, 127–140. doi:10.1007/s10584-013-0948-4
- Balwinder-Singh, Eberbach, P.L., Humphreys, E., 2014. Simulation of the evaporation of soil water beneath a wheat crop canopy. *Agric. Water Manag.* 135, 19–26. doi:10.1016/j.agwat.2013.12.008
- Barnes, C.J., Allison, G.B., 1983. The distribution of deuterium and ^{18}O in dry soils: 1. Theory. *J. Hydrol.* 60, 141–156. doi:http://dx.doi.org/10.1016/0022-1694(83)90018-5
- Barnes, C.J., Allison, G.B., 1984. The distribution of deuterium and ^{18}O in dry soils: 3. Theory for non-isothermal water movement. *J. Hydrol.* 74, 119–135. doi:http://dx.doi.org/10.1016/0022-1694(84)90144-6
- Bausch, W.C., 1995. Remote sensing of crop coefficients for improving the irrigation scheduling of corn. *Agric. Water Manag.* 27, 55–68. doi:10.1016/0378-3774(95)01125-3
- Bausch, W.C., Neale, C.M.U., 1987. Crop Coefficients Derived from Reflected Canopy Radiation: A Concept. *Am. Soc. Agric. Eng. Trans. TAAEAJ* 30, 703–709.
- Beer, C., Ciais, P., Reichstein, M., Baldocchi, D., Law, B.E., Papale, D., Soussana, J.-F., Ammann, C., Buchmann, N., Frank, D., Gianelle, D., Janssens, I. a., Knohl, A., Köstner, B., Moors, E., Rouspard, O., Verbeeck, H., Vesala, T., Williams, C. a., Wohlfahrt, G., 2009. Temporal and among-site variability of inherent water use efficiency at the ecosystem level. *Global Biogeochem. Cycles* 23, n/a–n/a. doi:10.1029/2008GB003233
- Berger, S., Jang, I., Seo, J., Kang, H., Gebauer, G., 2013. A record of N_2O and CH_4 emissions and underlying soil processes of Korean rice paddies as affected by different water management practices. *Biogeochemistry* 115, 317–332. doi:10.1007/s10533-013-9837-1
- Bhattacharyya, P., Neogi, S., Roy, K.S., Dash, P.K., Nayak, a. K., Mohapatra, T., 2014. Tropical low land rice ecosystem is a net carbon sink. *Agric. Ecosyst. Environ.* 189, 127–135. doi:10.1016/j.agee.2014.03.013
- Bierhuizen, J., Slatyer, R., 1965. Effect of atmospheric concentration of water vapour and CO_2 in determining transpiration-photosynthesis relationships of cotton leaves. *Agric. Meteorol.* 2, 259–270. doi:10.1016/0002-1571(65)90012-9
- Blanco, G., Gerlagh, R., Suh, S., Barrett, J., de Coninck, H.C., Diaz Morejon, C.F., Mathur, R., Nakicenovic, N., Oforu Ahenkora, A., Pan, J., Pathak, H., Rice, J., Richels, R., Smith, S.J., Stern, D.I., Toth, F.L., Zhou, P., 2014. Drivers, Trends and Mitigation, in: Edenhofer, O., Pichs-Madruga, R., Sokona, Y., Farahani, E., Kadner, S., Seyboth, K., Adler, A., Baum, I., Brunner, S., Eickemeier, P., Kriemann, B., Savolainen, J., Schlömer, S., von Stechow, C., Zwickel, T., Minx, J.C. (Eds.), *Climate Change 2014: Mitigation of Climate Change. Contribution of Working Group III to the Fifth Assessment Report of the Intergovernmental Panel on Climate Change*. Cambridge University Press, Cambridge, United Kingdom, Rome, pp. 351–412.

- Blum, a., 2009. Effective use of water (EUW) and not water-use efficiency (WUE) is the target of crop yield improvement under drought stress. *F. Crop. Res.* 112, 119–123. doi:10.1016/j.fcr.2009.03.009
- Blum, A., 2005. Drought resistance, water-use efficiency, and yield potential - Are they compatible, dissonant, or mutually exclusive?, in: *Australian Journal of Agricultural Research*. pp. 1159–1168. doi:10.1071/AR05069
- Blum, A., 2011. Drought resistance - is it really a complex trait? *Funct. Plant Biol.* 38, 753. doi:10.1071/FP11101
- Boast, C.W., Robertson, T.M., 1982. A “Micro-Lysimeter” Method for Determining Evaporation from Bare Soil: Description and Laboratory Evaluation. *Soil Sci. Soc. Am. J.* 46, 689–696. doi:10.2136/sssaj1982.03615995004600040005x
- Bouman, B. a. ., Tuong, T., 2001. Field water management to save water and increase its productivity in irrigated lowland rice. *Agric. Water Manag.* 49, 11–30. doi:10.1016/S0378-3774(00)00128-1
- Bouman, B.A.M., Humphreys, E., Tuong, T.P., Barker, R., 2007. Rice and Water. *Adv. Agron.* doi:10.1016/S0065-2113(04)92004-4
- Bouman, B.A.M., Peng, S., Castañeda, A.R., Visperas, R.M., 2005. Yield and water use of irrigated tropical aerobic rice systems. *Agric. Water Manag.* 74, 87–105. doi:10.1016/j.agwat.2004.11.007
- Bouman, B.A.M., Wopereis, M.C.S., Kropff, M.J., ten Berge, H.F.M., Tuong, T.P., 1994. Water use efficiency of flooded rice fields II. Percolation and seepage losses. *Agric. Water Manag.* 26, 291–304. doi:10.1016/0378-3774(94)90015-9
- Bunnell, F.L., Tait, D.E.N., Flanagan, P.W., 1977. Microbial respiration and substrate weight loss. II. A model of the influences of chemical composition. *Soil Biol. Biochem.* 9, 41–47. doi:10.1016/0038-0717(77)90059-1
- Bunnell, F.L., Tait, D.E.N., Flanagan, P.W., Van Clever, K., 1977. Microbial respiration and substrate weight loss—I. *Soil Biol. Biochem.* 9, 33–40. doi:10.1016/0038-0717(77)90058-X
- Cavanaugh, M.L., Kurc, S.A., Scott, R.L., 2011. Evapotranspiration partitioning in semiarid shrubland ecosystems: a two-site evaluation of soil moisture control on transpiration. *Ecohydrology* 4, 671–681. doi:10.1002/eco.157
- Čermák, J., Deml, M., Penka, M., 1973. A new method of sap flow rate determination in trees. *Biol. Plant.* 15, 171–178. doi:10.1007/BF02922390
- Chapagain, T., Riseman, A., Yamaji, E., 2011. Achieving More with Less Water: Alternate Wet and Dry Irrigation (AWDI) as an Alternative to the Conventional Water Management Practices in Rice Farming. *J. Agric. Sci.* 3, 3–13. doi:10.5539/jas.v3n3p3

- Choi, W.-J., Lee, M.-S., Choi, J.-E., Yoon, S., Kim, H.-Y., 2013. How do weather extremes affect rice productivity in a changing climate? An answer to episodic lack of sunshine. *Glob. Chang. Biol.* 19, 1300–10. doi:10.1111/gcb.12110
- Choudhury B.J., 1987. Relationship between Vegetation Indices, Radiation Absorption, and Net Photosynthesis Evaluated by a Sensitivity Analysis. *Remote Sens. Environ.* 22, 209–233.
- Choudhury, B.J., 1994. Synergism of multispectral satellite observations for estimating regional land surface evaporation. *Remote Sens. Environ.* 49, 264–274. doi:10.1016/0034-4257(94)90021-3
- Choudhury, B.U., Singh, A.K., Pradhan, S., 2013. Estimation of crop coefficients of dry-seeded irrigated rice-wheat rotation on raised beds by field water balance method in the Indo-Gangetic plains, India. *Agric. Water Manag.* 123, 20–31. doi:10.1016/j.agwat.2013.03.006
- Cohen, Y., Fuchs, M., Green, G.C., 1981. Improvement of the heat pulse method for determining sap flow in trees. *Plant. Cell Environ.* 4, 391–397. doi:10.1111/j.1365-3040.1981.tb02117.x
- Cohen, Y., Takeuchi, S., Nozaka, J., Yano, T., 1993. Accuracy of Sap Flow Measurement Using Heat Balance and Heat Pulse Methods. *Agron. J.* 85, 1080–1086. doi:10.2134/agronj1993.00021962008500050023x
- Comprehensive Assessment of Water Management in Agriculture, 2007. *Water for Food, Water for Life: A Comprehensive Assessment of Water Management in Agriculture.* International Water Management Institute.
- Condon, A.G., Richards, R.A., Rebetzke, G.J., Farquhar, G.D., 2004. Breeding for high water-use efficiency. *J. Exp. Bot.* 55, 2447–2460. doi:10.1093/jxb/erh277
- Craig, H., Gordon, L.I., 1965. Deuterium and oxygen 18 variations in the ocean and the marine atmosphere, in: Tongiorgi, E. (Ed.), *Stable Isotopes in Oceanographic Studies and Paleotemperatures.* Consiglio Nazionale Delle Ricerche Laboratori di Geologia Nucleare-Pisa, pp. 9–129.
- Cregg, B., Zhang, J., 2000. Carbon isotope discrimination as a tool to screen for improved drought tolerance. 11th Metrop. Tree Improv. Alliance Conf. 13–20.
- Cruz-Blanco, M., Lorite, I.J., Santos, C., 2014. An innovative remote sensing based reference evapotranspiration method to support irrigation water management under semi-arid conditions. *Agric. Water Manag.* 131, 135–145. doi:10.1016/j.agwat.2013.09.017
- Cuntz, M., Ogée, J., Farquhar, G.D., Peylin, P., Cernusak, L.A., 2007. Modelling advection and diffusion of water isotopologues in leaves. *Plant, Cell Environ.* 30, 892–909. doi:10.1111/j.1365-3040.2007.01676.x
- Dijkstra, F. a, Prior, S. a, Runion, G.B., Torbert, H.A., Tian, H., Lu, C., Venterea, R.T., 2012. Effects of elevated carbon dioxide and increased temperature on methane and nitrous

- oxide fluxes: evidence from field experiments. *Front. Ecol. Environ.* 10, 520–527. doi:10.1890/120059
- Dongmann, G., Nürnberg, H.W., Förstel, H., Wagener, K., 1974. On the enrichment of H₂¹⁸O in the leaves of transpiring plants. *Radiat. Environ. Biophys.* 11, 41–52. doi:10.1007/BF01323099
- Dubbert, M., Cuntz, M., Piayda, A., Maguás, C., Werner, C., 2013. Partitioning evapotranspiration – Testing the Craig and Gordon model with field measurements of oxygen isotope ratios of evaporative fluxes. *J. Hydrol.* 496, 142–153. doi:10.1016/j.jhydrol.2013.05.033
- Dubbert, M., Cuntz, M., Piayda, A., Werner, C., 2014a. Oxygen isotope signatures of transpired water vapor: The role of isotopic non-steady-state transpiration under natural conditions. *New Phytol.* 203, 1242–1252. doi:10.1111/nph.12878
- Dubbert, M., Piayda, A., Cuntz, M., Correia, A.C., Costa E Silva, F., Pereira, J.S., Werner, C., 2014b. Stable oxygen isotope and flux partitioning demonstrates understory of an oak savanna contributes up to half of ecosystem carbon and water exchange. *Front. Plant Sci.* 5, 530. doi:10.3389/fpls.2014.00530
- Duchemin, B., Hadria, R., Erraki, S., Boulet, G., Maisongrande, P., Chehbouni, a., Escadafal, R., Ezzahar, J., Hoedjes, J.C.B., Kharrou, M.H., Khabba, S., Mougenot, B., Olioso, a., Rodriguez, J.-C., Simonneaux, V., 2006. Monitoring wheat phenology and irrigation in Central Morocco: On the use of relationships between evapotranspiration, crops coefficients, leaf area index and remotely-sensed vegetation indices. *Agric. Water Manag.* 79, 1–27. doi:10.1016/j.agwat.2005.02.013
- Ehleringer, J.R., Dawson, T.E., 1992. Water uptake by plants: perspectives from stable isotope composition. *Plant, Cell Environ.* 15, 1073–1082. doi:10.1111/j.1365-3040.1992.tb01657.x
- Farooq, M., Kobayashi, N., Wahid, a., Ito, O., Basra, S.M. a, 2009. Chapter 6 Strategies for Producing More Rice with Less Water. *Adv. Agron.* 101, 351–388. doi:10.1016/S0065-2113(08)00806-7
- Farquhar, G., Richards, R., 1984. Isotopic Composition of Plant Carbon Correlates With Water-Use Efficiency of Wheat Genotypes. *Aust. J. Plant Physiol.* doi:10.1071/PP9840539
- Farquhar, G.D., Ehleringer, J.R., Hubick, K.T., 1989. Carbon Isotope Discrimination and Photosynthesis. *Annu. Rev. Plant Physiol. Plant Mol. Biol.* doi:10.1146/annurev.pp.40.060189.002443
- Fischer, R.A., Turner, N.C., 1978. Plant Productivity in the Arid and Semiarid Zones. *Annu. Rev. Plant Physiol.* doi:10.1146/annurev.pp.29.060178.001425
- Fischer, T., Byerlee, D., Edmeades, G., 2014. Crop yields and global food security. Australian Centre for International Agricultural Research: Canberra.

- Fitzjarrald, D.R., Sakai, R.K., Moraes, O.L.L., Cosme de Oliveira, R., Acevedo, O.C., Czikowsky, M.J., Beldini, T., 2008. Spatial and temporal rainfall variability near the Amazon-Tapajós confluence. *J. Geophys. Res.* 113, G00B11. doi:10.1029/2007JG000596
- Flexas, J., Galmés, J., Gallé, a., Gulías, J., Pou, a., Ribas-Carbo, M., Tomàs, M., Medrano, H., 2010. Improving water use efficiency in grapevines: Potential physiological targets for biotechnological improvement. *Aust. J. Grape Wine Res.* 16, 106–121. doi:10.1111/j.1755-0238.2009.00057.x
- Fuller, D.Q., Qin, L., Zheng, Y., Zhao, Z., Chen, X., Hosoya, L.A., Sun, G.-P., 2009. The domestication process and domestication rate in rice: spikelet bases from the Lower Yangtze. *Science* 323, 1607–1610. doi:10.1126/science.1166605
- Gago, J., Douthe, C., Florez-Sarasa, I., Escalona, J.M., Galmes, J., Fernie, A.R., Flexas, J., Medrano, H., 2014. Opportunities for improving leaf water use efficiency under climate change conditions. *Plant Sci.* 226, 108–119. doi:10.1016/j.plantsci.2014.04.007
- Galmés, J., Conesa, M.A., Ochogavía, J.M., Perdomo, J.A., Francis, D.M., Ribas-Carbó, M., Savé, R., Flexas, J., Medrano, H., Cifre, J., 2011. Physiological and morphological adaptations in relation to water use efficiency in Mediterranean accessions of *Solanum lycopersicum*. *Plant, Cell Environ.* 34, 245–260. doi:10.1111/j.1365-3040.2010.02239.x
- Gitelson, A.A., Peng, Y., Huemmrich, K.F., 2014. Relationship between fraction of radiation absorbed by photosynthesizing maize and soybean canopies and NDVI from remotely sensed data taken at close range and from MODIS 250m resolution data. *Remote Sens. Environ.* 147, 108–120. doi:10.1016/j.rse.2014.02.014
- Glenn, E.P., Nagler, P.L., Huete, A.R., 2010. Vegetation Index Methods for Estimating Evapotranspiration by Remote Sensing. *Surv. Geophys.* 31, 531–555. doi:10.1007/s10712-010-9102-2
- Glenn, E.P., Uete, A.R., Nagler, P.L., Nelson, S.G., 2008. Relationship Between Remotely-sensed Vegetation Indices, Canopy Attributes and Plant Physiological Processes: What Vegetation Indices Can and Cannot Tell Us About the Landscape. *Sensors* 8, 2136–2160. doi:10.3390/s8042136
- Godfray, H.C.J., Beddington, J.R., Crute, I.R., Haddad, L., Lawrence, D., Muir, J.F., Pretty, J., Robinson, S., Thomas, S.M., Toulmin, C., 2010. Food security: the challenge of feeding 9 billion people. *Science* 327, 812–818. doi:10.1126/science.1185383
- Gonzalez-Dugo, M.P., Neale, C.M.U., Mateos, L., Kustas, W.P., Prueger, J.H., Anderson, M.C., Li, F., 2009. A comparison of operational remote sensing-based models for estimating crop evapotranspiration. *Agric. For. Meteorol.* 149, 1843–1853. doi:10.1016/j.agrformet.2009.06.012
- Gordon, L.J., Peterson, G.D., Bennett, E.M., 2008. Agricultural modifications of hydrological flows create ecological surprises. *Trends Ecol. Evol.* 23, 211–219. doi:10.1016/j.tree.2007.11.011

- Goward, S.N., Huemmrich, K.F., 1992. Vegetation canopy PAR absorbance and the normalized difference vegetation index: an assessment using the SAIL model. *Remote Sens. Environ.* 39, 119–140.
- Grafton, R.Q., Williams, J., Jiang, Q., 2015. Food and water gaps to 2050: preliminary results from the global food and water system (GFWS) platform. *Food Secur.* 7, 209–220. doi:10.1007/s12571-015-0439-8
- GRiSP (Global Rice Science Partnership), 2013. Rice almanac. International Rice Research Institute [IRRI], Los Baños (Philippines). doi:10.1093/aob/mcg189
- Gross, B.L., Zhao, Z., 2014. Archaeological and genetic insights into the origins of domesticated rice. *Proc. Natl. Acad. Sci. U. S. A.* 111, 6190–7. doi:10.1073/pnas.1308942110
- Hall, A.E., Richards, R.A., Condon, A.G., Wright, G.C., Farquhar, G.D., 1994. Carbon isotope discrimination and plant breeding. *Plant Breed. Rev.* 12, 81–113.
- Harrold, L.L., Peters, D.B., Dreibelbis, F.R., McGuinness, J.L., 1959. Transpiration Evaluation of Corn Grown on a Plastic-Covered Lysimeter. *Soil Sci. Soc. Am. J.* 23, 174–178. doi:10.2136/sssaj1959.03615995002300020027x
- Hejazi, M.I., Edmonds, J., Clarke, L., Kyle, P., Davies, E., Chaturvedi, V., Wise, M., Patel, P., Eom, J., Calvin, K., 2014. Integrated assessment of global water scarcity over the 21st century under multiple climate change mitigation policies. *Hydrol. Earth Syst. Sci.* 18, 2859–2883. doi:10.5194/hess-18-2859-2014
- Hu, Z., Yu, G., Fu, Y., Sun, X., Li, Y., Shi, P., Wang, Y., Zheng, Z., 2008. Effects of vegetation control on ecosystem water use efficiency within and among four grassland ecosystems in China. *Glob. Chang. Biol.* 14, 1609–1619. doi:10.1111/j.1365-2486.2008.01582.x
- Hu, Z., Yu, G., Zhou, Y., Sun, X., Li, Y., Shi, P., Wang, Y., Song, X., Zheng, Z., Zhang, L., Li, S., 2009. Partitioning of evapotranspiration and its controls in four grassland ecosystems: Application of a two-source model. *Agric. For. Meteorol.* 149, 1410–1420. doi:10.1016/j.agrformet.2009.03.014
- Huang, X., Hao, Y., Wang, Y., Cui, X., Mo, X., Zhou, X., 2010. Partitioning of evapotranspiration and its relation to carbon dioxide fluxes in Inner Mongolia steppe. *J. Arid Environ.* 74, 1616–1623. doi:10.1016/j.jaridenv.2010.07.005
- Huang, X., Kurata, N., Wei, X., Wang, Z.-X., Wang, A., Zhao, Q., Zhao, Y., Liu, K., Lu, H., Li, W., Guo, Y., Lu, Y., Zhou, C., Fan, D., Weng, Q., Zhu, C., Huang, T., Zhang, L., Wang, Y., Feng, L., Furuumi, H., Kubo, T., Miyabayashi, T., Yuan, X., Xu, Q., Dong, G., Zhan, Q., Li, C., Fujiyama, A., Toyoda, A., Lu, T., Feng, Q., Qian, Q., Li, J., Han, B., 2012. A map of rice genome variation reveals the origin of cultivated rice. *Nature* 490, 497–501. doi:10.1038/nature11532
- Hunsaker, D., Barnes, E., Clarke, T., Fitzgerald, G., Pinter Jr, P., 2005. Cotton irrigation scheduling using remotely sensed and FAO-56 basal crop coefficients. *Trans. ASAE* 48, 1395–1407.

- Hunsaker, D.J., 1999. Basal crop coefficients and water use for early maturity cotton. *Trans. ASAE* 42, 927–936 ST – Basal crop coefficients and water us.
- Hunsaker, D.J., Pinter, P.J., Barnes, E.M., Kimball, B.A., 2003. Estimating cotton evapotranspiration crop coefficients with a multispectral vegetation index. *Irrig. Sci.* 22, 95–104. doi:10.1007/s00271-003-0074-6
- Hussain, S., Peng, S., Fahad, S., Khaliq, A., Huang, J., Cui, K., Nie, L., 2014. Rice management interventions to mitigate greenhouse gas emissions: a review. *Environ. Sci. Pollut. Res. Int.* doi:10.1007/s11356-014-3760-4
- Iizumi, T., Yokozawa, M., Nishimori, M., 2011. Probabilistic evaluation of climate change impacts on paddy rice productivity in Japan. *Clim. Change* 107, 391–415. doi:10.1007/s10584-010-9990-7
- International Rice Research Institute [IRRI], 2002. Water-wise rice production. Proceedings of the International Workshop on Water-wise Rice Production, 8-11 April 2002. International Rice Research Institute [IRRI], Los Baños, the Philippines.
- International Rice Research Institute [IRRI], 2014. Rice growing area and global rice crop calander database [WWW Document].
- Istanbulluoglu, E., Wang, T., Wedin, D.A., 2012. Evaluation of ecohydrologic model parsimony at local and regional scales in a semiarid grassland ecosystem 142, 121–142. doi:10.1002/eco
- Jasechko, S., Sharp, Z.D., Gibson, J.J., Birks, S.J., Yi, Y., Fawcett, P.J., 2013. Terrestrial water fluxes dominated by transpiration. *Nature* 496, 347–50. doi:10.1038/nature11983
- Kamble, B., Kilic, A., Hubbard, K., 2013. Estimating crop coefficients using remote sensing-based vegetation index. *Remote Sens.* 5, 1588–1602. doi:10.3390/rs5041588
- Katerji, N., Rana, G., 2006. Modelling evapotranspiration of six irrigated crops under Mediterranean climate conditions. *Agric. For. Meteorol.* 138, 142–155. doi:http://dx.doi.org/10.1016/j.agrformet.2006.04.006
- Kelliher, F.M., Leuning, R., Raupach, M.R., Schulze, E.D., 1995. Maximum conductances for evaporation from global vegetation types. *Agric. For. Meteorol.* 73, 1–16. doi:10.1016/0168-1923(94)02178-M
- Kim, H.K., Nakai, N., 1988. Isotopic compositions of precipitations and groundwaters in South Korea. *J. Geol. Soc. Korea* 24, 37– 46 (in Korean with English abstract).
- Kim, H.-Y., Ko, J., Kang, S., Tenhunen, J., 2013. Impacts of climate change on paddy rice yield in a temperate climate. *Glob. Chang. Biol.* 19, 548–62. doi:10.1111/gcb.12047
- Ko, J., Jeong, S., Yeom, J., Kim, H., Ban, J.-O., Kim, H.-Y., 2015. Simulation and mapping of rice growth and yield based on remote sensing. *J. Appl. Remote Sens.* 9, 96067. doi:10.1117/1.JRS.9.096067

- Ko, J., Kim, H., Jeong, S., An, J., Choi, G., Kang, S., Tenhunen, J., 2014. Potential impacts on climate change on paddy rice yield in mountainous highland terrains. *J. Crop Sci. Biotechnol.* 17, 117–126. doi:10.1007/s12892-013-0110-x
- Ko, J., Maas, S.J., Mauget, S., Piccinni, G., Wanjura, D., 2006. Modeling water-stressed cotton growth using within-season remote sensing data. *Agron. J.* 98, 1600–1609. doi:10.2134/agronj2005.0284
- Kool, D., Agam, N., Lazarovitch, N., Heitman, J.L.L., Sauer, T.J.J., Ben-Gal, a., 2014. A review of approaches for evapotranspiration partitioning. *Agric. For. Meteorol.* 184, 56–70. doi:10.1016/j.agrformet.2013.09.003
- Kovach, M.J., Sweeney, M.T., McCouch, S.R., 2007. New insights into the history of rice domestication. *Trends Genet.* 23, 578–587. doi:10.1016/j.tig.2007.08.012
- Kudo, Y., Noborio, K., Shimoozono, N., Kurihara, R., 2014. The effective water management practice for mitigating greenhouse gas emissions and maintaining rice yield in central Japan. *Agric. Ecosyst. Environ.* 186, 77–85. doi:10.1016/j.agee.2014.01.015
- Kuglitsch, F.G., Reichstein, M., Beer, C., Carrara, A., Ceulemans, R., Granier, A., Janssens, I.A., Koestner, B., Lindroth, A., Loustau, D., Matteucci, G., Montagnani, L., Moors, E.J., Papale, D., Pilegaard, K., Rambal, S., Rebmann, C., Schulze, E.D., Seufert, G., Verbeeck, H., Vesala, T., Aubinet, M., Bernhofer, C., Foken, T., Grünwald, T., Heinesch, B., Kutsch, W., Laurila, T., Longdoz, B., Miglietta, F., Sanz, M.J., Valentini, R., 2008. Characterisation of ecosystem water-use efficiency of european forests from eddy covariance measurements. *Biogeosciences Discuss.* 5, 4481–4519. doi:10.5194/bgd-5-4481-2008
- Lecina, S., Martínez-Cob, A., Pérez, P.J., Villalobos, F.J., Baselga, J.J., 2003. Fixed versus variable bulk canopy resistance for reference evapotranspiration estimation using the Penman-Monteith equation under semiarid conditions. *Agric. Water Manag.* 60, 181–198. doi:10.1016/S0378-3774(02)00174-9
- Lee, J., Worden, J., Koh, D.C., Yoshimura, K., Lee, J.E., 2013. A seasonality of δD of water vapor (850-500 hPa) observed from space over Jeju Island, Korea. *Geosci. J.* 17, 87–95. doi:10.1007/s12303-013-0003-5
- Lee, K., Grundstein, A., Wenner, D., Choi, M., Woo, N., Lee, D., 2003. Climatic controls on the stable isotopic composition of precipitation in Northeast Asia. *Clim. Res.* 23, 137–148. doi:10.3354/cr023137
- Lee, K.-S., Kim, J.-M., Lee, D.-R., Kim, Y., Lee, D., 2007. Analysis of water movement through an unsaturated soil zone in Jeju Island, Korea using stable oxygen and hydrogen isotopes. *J. Hydrol.* 345, 199–211. doi:10.1016/j.jhydrol.2007.08.006
- Lee, K.S., Kim, Y., 2007. Determining the seasonality of groundwater recharge using water isotopes: A case study from the upper North Han River basin, Korea. *Environ. Geol.* 52, 853–859. doi:10.1007/s00254-006-0527-3

- Leuning, R., Condon, A.G., Dunin, F.X., Zegelin, S., Denmead, O.T., 1994. Rainfall interception and evaporation from soil below a wheat canopy. *Agric. For. Meteorol.* 67, 221–238. doi:10.1016/0168-1923(94)90004-3
- Li Liu, Lee, G.-A., Leping Jiang, Juzhong Zhang, 2007. Evidence for the early beginning (c. 9000 cal. BP) of rice domestication in China: a response. *The Holocene* 17, 1059–1068. doi:10.1177/0959683607085121
- Li, Y.-L., Tenhunen, J., Mirzaei, H., Hussain, M.Z., Siebicke, L., Foken, T., Otieno, D., Schmidt, M., Ribeiro, N., Aires, L., Pio, C., Banza, J., Pereira, J., 2008. Assessment and up-scaling of CO₂ exchange by patches of the herbaceous vegetation mosaic in a Portuguese cork oak woodland. *Agric. For. Meteorol.* 148, 1318–1331. doi:10.1016/j.agrformet.2008.03.013
- Linares, O.F., 2002. African rice (*Oryza glaberrima*): history and future potential. *Proc. Natl. Acad. Sci. U. S. A.* 99, 16360–16365. doi:10.1073/pnas.252604599
- Linderson, M.L., Mikkelsen, T.N., Ibrom, a., Lindroth, a., Ro-Poulsen, H., Pilegaard, K., 2012. Up-scaling of water use efficiency from leaf to canopy as based on leaf gas exchange relationships and the modeled in-canopy light distribution. *Agric. For. Meteorol.* 152, 201–211. doi:10.1016/j.agrformet.2011.09.019
- Lindner, S., Otieno, D., Lee, B., Xue, W., Arnhold, S., Kwon, H., Huwe, B., Tenhunen, J., 2015. Carbon dioxide exchange and its regulation in the main agro-ecosystems of Haean catchment in South Korea. *Agric. Ecosyst. Environ.* 199, 132–145. doi:10.1016/j.agee.2014.09.005
- Lloyd, J., Taylor, J. a., 1994. On the Temperature Dependence of Soil Respiration. *Funct. Ecol.* 8, 315. doi:10.2307/2389824
- Lobell, D.B., Field, C.B., 2007. Global scale climate–crop yield relationships and the impacts of recent warming. *Environ. Res. Lett.* 2, 014002. doi:10.1088/1748-9326/2/1/014002
- Lobell, D.B., Schlenker, W., Costa-Roberts, J., 2011. Climate trends and global crop production since 1980. *Science* 333, 616–620. doi:10.1126/science.1204531
- Londo, J.P., Chiang, Y.-C., Hung, K.-H., Chiang, T.-Y., Schaal, B. a, 2006. Phylogeography of Asian wild rice, *Oryza rufipogon*, reveals multiple independent domestications of cultivated rice, *Oryza sativa*. *Proc. Natl. Acad. Sci.* 103, 9578–9583. doi:10.1073/pnas.0603152103
- Long, S.P., Ainsworth, E.A., Leakey, A.D.B., Ort, D.R., No, J., 2006. Food for Thought : Lower-Than- 312, 1918–1922.
- López-Urrea, R., Martín de Santa Olalla, F., Fabeiro, C., Moratalla, A., 2006. Testing evapotranspiration equations using lysimeter observations in a semiarid climate. *Agric. Water Manag.* 85, 15–26. doi:10.1016/j.agwat.2006.03.014
- Luo, L.J., 2010. Breeding for water-saving and drought-resistance rice (WDR) in China. *J. Exp. Bot.* doi:10.1093/jxb/erq185

- Luo, Z., Wang, E., Sun, O.J., 2010. Soil carbon change and its responses to agricultural practices in Australian agro-ecosystems: A review and synthesis. *Geoderma*. doi:10.1016/j.geoderma.2009.12.012
- Maas, S.J., 1993a. Parameterized Model of Gramineous Crop Growth: I. Leaf Area and Dry Mass Simulation. *Agron. J.* 85, 348. doi:10.2134/agronj1993.00021962008500020034x
- Maas, S.J., 1993b. Parameterized Model of Gramineous Crop Growth: II. Within-Season Simulation Calibration. *Agron. J.* 85, 354. doi:10.2134/agronj1993.00021962008500020035x
- Majoube, M., 1971. Oxygen-18 and Deuterium Fractionation between Water and Steam. *J. Chem. Phys.* 68, 1423–1436.
- Makkink, G.F., 1957. Testing the Penman formula by means of lysimeters. *J. Inst. Water Eng.* 11, 277–288.
- Maruyama, A., Kuwagata, T., 2010. Coupling land surface and crop growth models to estimate the effects of changes in the growing season on energy balance and water use of rice paddies. *Agric. For. Meteorol.* 150, 919–930. doi:10.1016/j.agrformet.2010.02.011
- Medrano, H., Flexas, J., Galmés, J., 2009. Variability in water use efficiency at the leaf level among Mediterranean plants with different growth forms. *Plant Soil* 317, 17–29. doi:10.1007/s11104-008-9785-z
- Medrano, H., Pou, A., Tomás, M., Martorell, S., Gulias, J., Flexas, J., Escalona, J.M., 2012. Average daily light interception determines leaf water use efficiency among different canopy locations in grapevine. *Agric. Water Manag.* 114, 4–10. doi:10.1016/j.agwat.2012.06.025
- Medrano, H., Tomás, M., Martorell, S., Flexas, J., Hernández, E., Rosselló, J., Pou, A., Escalona, J.-M., Bota, J., 2015. From leaf to whole-plant water use efficiency (WUE) in complex canopies: limitations of leaf WUE as a selection target. *Crop J.* 3, 220–228. doi:10.1016/j.cj.2015.04.002
- Meehl, G. a, Stocker, T.F., 2007. Global climate projections, in: Solomon, S., Qin, D., Manning, M., Chen, Z., Marquis, M., Averyt, K.B., Tignor, M., Miller, H.L. (Eds.), *Contribution of Working Group I to the Fourth Assessment Report of the Intergovernmental Panel on Climate Change, 2007*. Cambridge University Press, Cambridge, United Kingdom, pp. 748–845.
- Merlivat, L., 1978. Molecular diffusivities of H₂¹⁶O, HD¹⁶O, and H₂¹⁸O in gases. *J. Chem. Phys.* 69, 2864. doi:10.1063/1.436884
- Miyata, A., Leuning, R., Denmead, O.T., Kim, J., Harazono, Y., 2000. Carbon dioxide and methane fluxes from an intermittently flooded paddy field. *Agric. For. Meteorol.* 102, 287–303. doi:10.1016/S0168-1923(00)00092-7

- Mo, X., Liu, S., Lin, Z., Zhao, W., 2004. Simulating temporal and spatial variation of evapotranspiration over the Lushi basin. *J. Hydrol.* 285, 125–142. doi:10.1016/j.jhydrol.2003.08.013
- Mo, X.G., Liu, S.X., Lin, Z.H., Guo, R.P., 2009. Regional crop yield, water consumption and water use efficiency and their responses to climate change in the North China Plain. *Agric. Ecosyst. Environ.* 134, 67–78. doi:DOI 10.1016/j.agee.2009.05.017
- Mohanty, S., Wassmann, R., Nelson, A., Moya, P., Jagadish, S.V.K., 2013. Rice and climate change: significance for food security and vulnerability, in: *IRRI Discussion Paper Series No. 49*. International Rice Research Institute, Los Baños (Philippines), p. 14.
- Molina, J., Sikora, M., Garud, N., Flowers, J.M., Rubinstein, S., Reynolds, A., Huang, P., Jackson, S., Schaal, B. a, Bustamante, C.D., Boyko, A.R., Purugganan, M.D., 2011. Molecular evidence for a single evolutionary origin of domesticated rice. *Proc. Natl. Acad. Sci. U. S. A.* 108, 8351–8356. doi:10.1073/pnas.1104686108
- Monneveux, P., Rekika, D., Acevedo, E., Merah, O., 2006. Effect of drought on leaf gas exchange, carbon isotope discrimination, transpiration efficiency and productivity in field grown durum wheat genotypes. *Plant Sci.* 170, 867–872. doi:10.1016/j.plantsci.2005.12.008
- Monneveux, P., Sheshshayee, M.S., Akhter, J., Ribaut, J.-M., 2007. Using carbon isotope discrimination to select maize (*Zea mays* L.) inbred lines and hybrids for drought tolerance. *Plant Sci.* doi:10.1016/j.plantsci.2007.06.003
- Monteith, J.L., 1965. Evaporation and environment. *Symp. Soc. Exp. Biol.* 19, 205–234.
- Monteith, J.L., 1972. Solar radiation and productivity in tropical ecosystems. *J. Appl. Ecol.* 9, 747–766. doi:10.2307/2401901
- Monteith, J.L., 1981. Evaporation and surface temperature. *Q. J. R. Meteorol. Soc.* 107, 1–27. doi:10.1002/qj.49710745102
- Morison, J.I.L., Baker, N.R., Mullineaux, P.M., Davies, W.J., 2008. Improving water use in crop production. *Philos. Trans. R. Soc. Lond. B. Biol. Sci.* 363, 639–658. doi:10.1098/rstb.2007.2175
- Mostafa, H., Fujimoto, N., 2014. Water saving scenarios for effective irrigation management in Egyptian rice cultivation. *Ecol. Eng.* doi:10.1016/j.ecoleng.2014.04.005
- Nash, J.E., Sutcliffe, J.V., 1970. River flow forecasting through conceptual models part I — A discussion of principles. *J. Hydrol.* 10, 282–290. doi:10.1016/0022-1694(70)90255-6
- Nay-Htoon, B., Tung Phong, N., Schlüter, S., Janaiah, A., 2013. A water productive and economically profitable paddy rice production method to adapt water scarcity in the Vu Gia-Thu Bon river basin, Vietnam. *J. Nat. Resour. Dev.* 03, 58–65. doi:10.5027/jnrd.v3i0.05

- Nie, L., Peng, S., Chen, M., 2012. Aerobic rice for water-saving agriculture . A review To cite this version : 32, 411–418. doi:10.1007/s13593-011-0055-8
- Nishimura, S., Yonemura, S., Minamikawa, K., Yagi, K., 2015. Seasonal and diurnal variations in net carbon dioxide flux throughout the year from soil in paddy field. *J. Geophys. Res. Biogeosciences* n/a–n/a. doi:10.1002/2014JG002746
- Nishimura, S., Yonemura, S., Sawamoto, T., Shirato, Y., Akiyama, H., Sudo, S., Yagi, K., 2008. Effect of land use change from paddy rice cultivation to upland crop cultivation on soil carbon budget of a cropland in Japan. *Agric. Ecosyst. Environ.* 125, 9–20. doi:10.1016/j.agee.2007.11.003
- Osmond, C.B., Bjorkman, O., Anderson, D.J., 1980. *Physiological processes in plant ecology. Toward a synthesis with Atriplex.* Springer Verlag.
- Otieno, D., Lindner, S., Muhr, J., Borcken, W., 2012. Sensitivity of peatland herbaceous vegetation to vapor pressure deficit influences net ecosystem CO₂ exchange. *Wetlands* 32, 895–905. doi:10.1007/s13157-012-0322-8
- Pape, L., Ammann, C., Nyfeler-Brunner, a., Spirig, C., Hens, K., Meixner, F.X., 2009. An automated dynamic chamber system for surface exchange measurement of non-reactive and reactive trace gases of grassland ecosystems. *Biogeosciences* 6, 405–429. doi:10.5194/bg-6-405-2009
- Pathak, H., Li, C., Wassmann, R., 2005. Greenhouse gas emissions from Indian rice fields: calibration and upscaling using the DNDC model. *Biogeosciences Discuss.* doi:10.5194/bgd-2-77-2005
- Payero, J.O., Irmak, S., 2013. Daily energy fluxes, evapotranspiration and crop coefficient of soybean. *Agric. Water Manag.* 129, 31–43. doi:10.1016/j.agwat.2013.06.018
- Peng, S., Huang, J., Sheehy, J.E., Laza, R.C., Visperas, R.M., Zhong, X., Centeno, G.S., Khush, G.S., Cassman, K.G., 2004. Rice yields decline with higher night temperature from global warming. *Proc. Natl. Acad. Sci. U. S. A.* 101, 9971–9975. doi:10.1073/pnas.0403720101
- PENMAN, H.L., 1948. Natural evaporation from open water, bare soil and grass. *Proc. R. Soc. London. Ser. A Math. Phys. Sci.* 193, 120–145. doi:10.1098/rspa.1948.0037
- Pereira, A.R., Pruitt, W.O., 2004. Adaptation of the Thornthwaite scheme for estimating daily reference evapotranspiration. *Agric. Water Manag.* 66, 251–257. doi:10.1016/j.agwat.2003.11.003
- Pereira, L.S., Allen, R.G., Smith, M., Raes, D., 2014. Crop evapotranspiration estimation with FAO56: Past and future. *Agric. Water Manag.* 147, 4–20. doi:10.1016/j.agwat.2014.07.031
- Pereira, L.S., Cordery, I., Iacovides, I., 2012. Improved indicators of water use performance and productivity for sustainable water conservation and saving. *Agric. Water Manag.* 108, 39–51. doi:10.1016/j.agwat.2011.08.022

- Peters, D.B., Russell, M.B., 1959. Relative Water Losses by Evaporation and Transpiration in Field Corn. *Soil Sci. Soc. Am. J.* 23, 170–173. doi:10.2136/sssaj1959.03615995002300020026x
- Pielke, R.A., Adegoke, J.O., Chase, T.N., Marshall, C.H., Matsui, T., Niyogi, D., 2007. A new paradigm for assessing the role of agriculture in the climate system and in climate change. *Agric. For. Meteorol.* 142, 234–254. doi:10.1016/j.agrformet.2006.06.012
- Pittelkow, C.M., Adviento-borbe, M.A., Hill, J.E., Six, J., Kessel, C. Van, Linn, B.A., 2013. Agriculture, Ecosystems and Environment Yield-scaled global warming potential of annual nitrous oxide and methane emissions from continuously flooded rice in response to nitrogen input. *Agriculture, Ecosyst. Environ.* 177, 10–20. doi:10.1016/j.agee.2013.05.011
- Priestley, C.H.B., Taylor, R.J., 1972. On the Assessment of Surface Heat Flux and Evaporation Using Large-Scale Parameters. *Mon. Weather Rev.* 100, 81–92. doi:10.1175/1520-0493(1972)100<0081:OTAOSH>2.3.CO;2
- R Core Team, 2014. R: A language and environment for statistical computing. R Found. Stat. Comput. Vienna, Austria URL <http://www.R-project.org/>.
- Rana, G., Katerji, N., Mastrorilli, M., El Moujabber, M., 1994. Evapotranspiration and canopy resistance of grass in a Mediterranean region. *Theor. Appl. Climatol.* 50, 61–71. doi:10.1007/BF00864903
- Ray, D.K., Gerber, J.S., Macdonald, G.K., West, P.C., 2015. Climate variation explains a third of global crop yield variability. *Nat. Commun.* 6, 1–9. doi:10.1038/ncomms6989
- Ray, D.K., Mueller, N.D., West, P.C., Foley, J. a, 2013. Yield Trends Are Insufficient to Double Global Crop Production by 2050. *PLoS One* 8, e66428. doi:10.1371/journal.pone.0066428
- Rebetzke, G.J., Condon, A.G., Farquhar, G.D., Appels, R., Richards, R.A., 2008a. Quantitative trait loci for carbon isotope discrimination are repeatable across environments and wheat mapping populations. *Theor. Appl. Genet.* 118, 123–137. doi:10.1007/s00122-008-0882-4
- Rebetzke, G.J., Van Herwaarden, A.F., Jenkins, C., Weiss, M., Lewis, D., Ruuska, S., Tabe, L., Fettell, N.A., Richards, R.A., 2008b. Quantitative trait loci for water-soluble carbohydrates and associations with agronomic traits in wheat. *Aust. J. Agric. Res.* 59, 891–905. doi:10.1071/AR08067
- Reichstein, M., Falge, E., Baldocchi, D., Papale, D., Aubinet, M., Berbigier, P., Bernhofer, C., Buchmann, N., Gilmanov, T., Granier, A., Grunwald, T., Havrankova, K., Ilvesniemi, H., Janous, D., Knohl, A., Laurila, T., Lohila, A., Loustau, D., Matteucci, G., Meyers, T., Miglietta, F., Ourcival, J.-M., Pumpanen, J., Rambal, S., Rotenberg, E., Sanz, M., Tenhunen, J., Seufert, G., Vaccari, F., Vesala, T., Yakir, D., Valentini, R., 2005. On the separation of net ecosystem exchange into assimilation and ecosystem respiration: review and improved algorithm. *Glob. Chang. Biol.* 11, 1424–1439. doi:10.1111/j.1365-2486.2005.001002.x

- Reichstein, M., Tenhunen, J.D., Rouspard, O., Ourcival, J.-M., Rambal, S., Dore, S., Valentini, R., 2002. Ecosystem respiration in two Mediterranean evergreen Holm Oak forests: drought effects and decomposition dynamics. *Funct. Ecol.* 16, 27–39. doi:10.1046/j.0269-8463.2001.00597.x
- Ritchie, J.T., 1972. Model for predicting evaporation from a row crop with incomplete cover. *Water Resour. Res.* doi:10.1029/WR008i005p01204
- Rizza, F., Ghashghaie, J., Meyer, S., Matteu, L., Mastrangelo, A.M., Badeck, F.W., 2012. Constitutive differences in water use efficiency between two durum wheat cultivars. *F. Crop. Res.* 125, 49–60. doi:10.1016/j.fcr.2011.09.001
- Running, S.W., Nemani, R.R., Heinsch, F.A., Zhao, M., Reeves, M., Hashimoto, H., 2004. A Continuous Satellite-Derived Measure of Global Terrestrial Primary Production. *Bioscience* 54, 547. doi:10.1641/0006-3568(2004)054[0547:ACSMOG]2.0.CO;2
- Sakai, R.K., Fitzjarrald, D.R., Moraes, O.L.L., Staebler, R.M., Acevedo, O.C., Czikowsky, M.J., Silva, R. Da, Brait, E., Miranda, V., 2004. Land-use change effects on local energy, water, and carbon balances in an Amazonian agricultural field. *Glob. Chang. Biol.* 10, 895–907. doi:10.1111/j.1529-8817.2003.00773.x
- SAKURATANI, T., 1981. A Heat Balance Method for Measuring Water Flux in the Stem of Intact Plants. *J. Agric. Meteorol.* 37, 9–17. doi:10.2480/agrmet.37.9
- Sakuratani, T., Horie, T., 1985. Studies on evapotranspiration from crops: (1) On seasonal changes, varietal differences and evapotranspiration of paddy rice. *J. Agric. Meteorol.* 41, 45–55.
- Saranga, Y., Jiang, C.X., Wright, R.J., Yakir, D., Paterson, A.H., 2004. Genetic dissection of cotton physiological responses to arid conditions and their inter-relationships with productivity. *Plant, Cell Environ.* 27, 263–277. doi:10.1111/j.1365-3040.2003.01134.x
- Sayre, K.D., Acevedo, E., Austin, R.B., 1995. Carbon isotope discrimination and grain yield for three bread wheat germplasm groups grown at different levels of water stress. *F. Crop. Res.* doi:10.1016/0378-4290(94)00105-L
- Scott, R.L., Huxman, T.E., Cable, W.L., Emmerich, W.E., 2006. Partitioning of evapotranspiration and its relation to carbon dioxide exchange in a Chihuahuan Desert shrubland. *Hydrol. Process.* 20, 3227–3243. doi:10.1002/hyp.6329
- Seck, P.A., Diagne, A., Mohanty, S., Wopereis, M.C.S., 2012. Crops that feed the world 7: Rice. *Food Secur.* doi:10.1007/s12571-012-0168-1
- Sellers, P.J., 1985. Canopy reflectance, photosynthesis and transpiration. *Int. J. Remote Sens.* 6, 1335–1372. doi:10.1080/01431168508948283
- Seo, J., Jang, I., Gebauer, G., Kang, H., 2013. Abundance of Methanogens, Methanotrophic Bacteria, and Denitrifiers in Rice Paddy Soils. *Wetlands* 34, 213–223. doi:10.1007/s13157-013-0477-y

- Shaw, R.H., 1959. Water Use from Plastic-covered and Uncovered Corn Plots. *Agron. J.* 51, 172–173. doi:10.2134/agronj1959.00021962005100030015x
- Shichun, Z., Xuefa, W., Jianlin, W., Guirui, Y., Xiaomin, S., 2010. *Acta Ecologica Sinica* The use of stable isotopes to partition evapotranspiration fluxes into evaporation and transpiration. *Acta Ecol. Sin.* 30, 201–209. doi:10.1016/j.chnaes.2010.06.003
- Shuttleworth, W.J., Wallace, J.S., 1985. Evaporation from sparse crops-an energy combination theory. *Q. J. R. Meteorol. Soc.* 111, 839–855. doi:10.1002/qj.49711146910
- Smith, P., Martino, D., Cai, Z., Gwary, D., Janzen, H., Kumar, P., McCarl, B., Ogle, S., O'Mara, F., Rice, C., Scholes, B., Sirotenko, O., 2007. Agriculture, in: Metz, B., Davidson, O.R., Bosch, P.R., Dave, R., Meyer, L.A. (Eds.), *Climate Change 2007: Mitigation. Contribution of Working Group III to the Fourth Assessment Report of the Intergovernmental Panel on Climate Change*. Cambridge University Press, Cambridge, United Kingdom and New York, NY, USA.
- Specht, J.E., Chase, K., Macrander, M., Graef, G.L., Chung, J., Markwell, J.P., Germann, M., Orf, J.H., Lark, K.G., 2001. Soybean response to water: A QTL analysis of drought tolerance. *Crop Sci.* 41, 493–509.
- Steduto, P., Hsiao, T.C., 1998. Maize canopies under two soil water regimes: II. Seasonal trends of evapotranspiration, carbon dioxide assimilation and canopy conductance, and as related to leaf area index. *Agric. For. Meteorol.* 89, 185–200. doi:http://dx.doi.org/10.1016/S0168-1923(97)00084-1
- Steduto, P., Katerji, N., Puertos-Molina, H., Ünü, M., Mastrorilli, M., Rana, G., 1997. Water-use efficiency of sweet sorghum under water stress conditions gas-exchange investigations at leaf and canopy scales. *F. Crop. Res.* 54, 221–234. doi:10.1016/S0378-4290(97)00050-6
- Steduto, P., Todorovic, M., Calciandro, A., Rubino, P., 2003. Daily reference evapotranspiration estimates by the Penman-Monteith equation in Southern Italy. Constant vs. variable canopy resistance. *Theor. Appl. Climatol.* 74, 217–225. doi:10.1007/s00704-002-0720-6
- Talleg, T., Béziat, P., Jarosz, N., Rivalland, V., Ceschia, E., 2013. Crops' water use efficiencies in temperate climate: Comparison of stand, ecosystem and agronomical approaches. *Agric. For. Meteorol.* 168, 69–81. doi:10.1016/j.agrformet.2012.07.008
- Tanner, C.B., Jury, W.A., 1976. Estimating Evaporation and Transpiration from a Row Crop during Incomplete Cover1. *Agron. J.* 68, 239–243. doi:10.2134/agronj1976.00021962006800020007x
- Thanawong, K., Perret, S.R., Basset-Mens, C., 2014. Eco-efficiency of paddy rice production in Northeastern Thailand: a comparison of rain-fed and irrigated cropping systems. *J. Clean. Prod.* 73, 204–217. doi:10.1016/j.jclepro.2013.12.067
- Tian, H., Lu, C., Chen, G., Xu, X., Liu, M., Ren, W., Tao, B., Sun, G., Pan, S., Liu, J., 2011. Climate and land use controls over terrestrial water use efficiency in monsoon Asia. *Ecohydrology* 4, 322–340. doi:10.1002/eco.216

- Todorovic, M., 1999. Single-Layer Evapotranspiration Model with Variable Canopy Resistance. *J. Irrig. Drain. Eng.* doi:10.1061/(ASCE)0733-9437(1999)125:5(235)
- Todorovic, M., Karic, B., Pereira, L.S., 2013. Reference evapotranspiration estimate with limited weather data across a range of Mediterranean climates. *J. Hydrol.* 481, 166–176. doi:10.1016/j.jhydrol.2012.12.034
- Tolk, J. a., Howell, T. a., Steiner, J.L., Krieg, D.R., Schneider, a. D., 1995. Role of transpiration suppression by evaporation of intercepted water in improving irrigation efficiency. *Irrig. Sci.* 16, 89–95. doi:10.1007/BF00189165
- Tomás, M., Medrano, H., Pou, a., Escalona, J.M., Martorell, S., Ribas-Carbó, M., Flexas, J., 2012. Water-use efficiency in grapevine cultivars grown under controlled conditions: Effects of water stress at the leaf and whole-plant level. *Aust. J. Grape Wine Res.* 18, 164–172. doi:10.1111/j.1755-0238.2012.00184.x
- Tuong, T.P., Bhuiyan, S.I., 1999. Increasing water-use efficiency in rice production: Farm-level perspectives. *Agric. Water Manag.* 40, 117–122. doi:10.1016/S0378-3774(98)00091-2
- Tuong, T.P., Bouman, B. a. M., Mortimer, M., 2005. More Rice, Less Water-Integrated Approaches for Increasing Water Productivity in Irrigated Rice-Based Systems in Asia. *Plant Prod. Sci.* 8, 231–241. doi:10.1626/pp.s.8.231
- Tuong, T.P., Bouman, B.A.M., 2003. Rice Production in Water-scarce Environments, in: J.W. Kijne; R. Barker and D. Molden (Ed.), *Water Productivity in Agriculture: Limits and Opportunities for Improvement*. pp. 53–67.
- Van Groenigen, K.J., Osenberg, C.W., Hungate, B. a, 2011. Increased soil emissions of potent greenhouse gases under increased atmospheric CO₂. *Nature* 475, 214–216. doi:10.1038/nature10176
- Van Groenigen, K.J., van Kessel, C., Hungate, B. a., 2012. Increased greenhouse-gas intensity of rice production under future atmospheric conditions. *Nat. Clim. Chang.* 3, 288–291. doi:10.1038/nclimate1712
- Van Halsema, G.E., Vincent, L., 2012. Efficiency and productivity terms for water management: A matter of contextual relativism versus general absolutism. *Agric. Water Manag.* 108, 9–15. doi:10.1016/j.agwat.2011.05.016
- VanLoocke, A., Twine, T.E., Zeri, M., Bernacchi, C.J., 2012. A regional comparison of water use efficiency for miscanthus, switchgrass and maize. *Agric. For. Meteorol.* 164, 82–95. doi:10.1016/j.agrformet.2012.05.016
- Ventura, F., Spano, D., Duce, P., Snyder, R.L., 1999. An evaluation of common evapotranspiration equations. *Irrig. Sci.* 18, 163–170. doi:10.1007/s002710050058
- Von Caemmerer, S., Farquhar, G.D., 1981. Some relationships between the biochemistry of photosynthesis and the gas exchange of leaves. *Planta* 153, 376–387. doi:10.1007/BF00384257

- Walker, G.K., 1984. Evaporation from wet soil surfaces beneath plant canopies. *Agric. For. Meteorol.* 33, 259–264. doi:[http://dx.doi.org/10.1016/0168-1923\(84\)90075-3](http://dx.doi.org/10.1016/0168-1923(84)90075-3)
- Wang, L., Caylor, K.K., Villegas, J.C., Barron-Gafford, G. a., Breshears, D.D., Huxman, T.E., 2010. Partitioning evapotranspiration across gradients of woody plant cover: Assessment of a stable isotope technique. *Geophys. Res. Lett.* 37, 1–7. doi:[10.1029/2010GL043228](https://doi.org/10.1029/2010GL043228)
- Wang, L., Good, S.P., Caylor, K.K., 2014. Global synthesis of vegetation control on evapotranspiration partitioning. *Geophys. Res. Lett.* 41, 6753–6757. doi:[10.1002/2014GL061439](https://doi.org/10.1002/2014GL061439)
- Wang, X.F., Yakir, D., 2000. Using stable isotopes of water in evapotranspiration studies. *Hydrol. Process.* 14, 1407–1421. doi:[10.1002/1099-1085\(20000615\)14:8<1407::AID-HYP992>3.0.CO;2-K](https://doi.org/10.1002/1099-1085(20000615)14:8<1407::AID-HYP992>3.0.CO;2-K)
- Wang, Z.Y., Xu, Y.C., Li, Z., Guo, Y.X., Wassmann, R., Neue, H.U., Lantin, R.S., Buendia, L. V., Ding, Y.P., Wang, Z.Z., 2000. A four-year record of methane emissions from irrigated rice fields in the Beijing region of China. *Nutr. Cycl. Agroecosystems* 58, 55–63. doi:[10.1023/A:1009878115811](https://doi.org/10.1023/A:1009878115811)
- Wassmann, R., Lantin, R.S., Neue, H.U., Buendia, L. V, Corton, T.M., Lu, Y., 2000. Characterization of methane emissions from rice fields in Asia . III . Mitigation options and future research needs 23–36. doi:[10.1023/A:1009874014903](https://doi.org/10.1023/A:1009874014903)
- Wei, Z., Yoshimura, K., Okazaki, A., Kim, W., Liu, Z., Yokoi, M., 2015. Partitioning of evapotranspiration using high-frequency water vapor isotopic measurement over a rice paddy field. *Water Resour. Res.* 51, 3716–3729. doi:[10.1002/2014WR016737](https://doi.org/10.1002/2014WR016737)
- Weller, S., Kraus, D., Ayag, K.R.P., Wassmann, R., Alberto, M.C.R., Butterbach-Bahl, K., Kiese, R., 2014. Methane and nitrous oxide emissions from rice and maize production in diversified rice cropping systems. *Nutr. Cycl. Agroecosystems*. doi:[10.1007/s10705-014-9658-1](https://doi.org/10.1007/s10705-014-9658-1)
- Werner, C., Badeck, F., Brugnoli, E., Cohn, B., Cuntz, M., Dawson, T., Gessler, A., Ghashghaie, J., Grams, T.E.E., Kayler, Z., Keitel, C., Lakatos, M., Lee, X., Máguas, C., Ogée, J., Rascher, K.G., Schnyder, H., Siegwolf, R., Unger, S., Welker, J., Wingate, L., Zeeman, M.J., 2011. Linking carbon and water cycles using stable isotopes across scales: progress and challenges. *Biogeosciences Discuss.* 8, 2659–2719. doi:[10.5194/bgd-8-2659-2011](https://doi.org/10.5194/bgd-8-2659-2011)
- West, T.O., Marland, G., 2002. A synthesis of carbon sequestration, carbon emissions, and net carbon flux in agriculture: comparing tillage practices in the United States. *Agric. Ecosyst. Environ.* 91, 217–232. doi:[10.1016/S0167-8809\(01\)00233-X](https://doi.org/10.1016/S0167-8809(01)00233-X)
- Williams, C.A., Albertson, J.D., 2005. Contrasting short- and long-timescale effects of vegetation dynamics on water and carbon fluxes in water-limited ecosystems. *Water Resour. Res.* 41, n/a–n/a. doi:[10.1029/2004WR003750](https://doi.org/10.1029/2004WR003750)
- Williams, D.G., Cable, W., Hultine, K., Hoedjes, J.C.B., Yopez, E. a., Simonneaux, V., Er-Raki, S., Boulet, G., De Bruin, H. a R., Chehbouni, a., Hartogensis, O.K., Timouk, F.,

2004. Evapotranspiration components determined by stable isotope, sap flow and eddy covariance techniques. *Agric. For. Meteorol.* 125, 241–258. doi:10.1016/j.agrformet.2004.04.008
- Wolf, S., Eugster, W., Potvin, C., Buchmann, N., 2011. Strong seasonal variations in net ecosystem CO₂ exchange of a tropical pasture and afforestation in Panama. *Agric. For. Meteorol.* 151, 1139–1151. doi:10.1016/j.agrformet.2011.04.002
- Xiao, Y., Xie, G., Lu, C., Ding, X., Lu, Y., 2005. The value of gas exchange as a service by rice paddies in suburban Shanghai, PR China. *Agric. Ecosyst. Environ.* 109, 273–283. doi:10.1016/j.agee.2005.03.016
- Yakir, D., Sternberg, L. da S.L., 2000. The use of stable isotopes to study ecosystem gas exchange. *Oecologia* 123, 297–311. doi:10.1007/s004420051016
- Yakir, D., Sternberg, L.D.S.L., 2000. The use of stable isotopes to study ecosystem gas exchange. *Oecologia*. doi:10.1007/s004420051016
- Yan, X., Ohara, T., Akimoto, H., 2003. Development of region-specific emission factors and estimation of methane emission from rice fields in the East , Southeast and South Asian countries. *Glob. Chang. Biol.* 9, 237–254.
- Yao, Z., Du, Y., Tao, Y., Zheng, X., Liu, C., Lin, S., Butterbach-Bahl, K., 2014. Water-saving ground cover rice production system reduces net greenhouse gas fluxes in an annual rice-based cropping system. *Biogeosciences* 11, 6221–6236. doi:10.5194/bg-11-6221-2014
- Yoshida, S., 1981. Fundamentals of rice crop science. *Int. Rice Res. Inst.*
- Zeri, M., Hussain, M.Z., Anderson-Teixeira, K.J., DeLucia, E., Bernacchi, C.J., 2013. Water use efficiency of perennial and annual bioenergy crops in central Illinois. *J. Geophys. Res. Biogeosciences* 118, 581–589. doi:10.1002/jgrg.20052
- Zhang, S., Wen, X., Wang, J., Yu, G., Sun, X., 2010. The use of stable isotopes to partition evapotranspiration fluxes into evaporation and transpiration. *Acta Ecol. Sin.* 30, 201–209. doi:10.1016/j.chnaes.2010.06.003
- Zhao, P., 2014. Ecosystem-atmosphere exchange of carbon dioxide and water vapour in typical East-Asian croplands. University of Bayreuth.
- Zhao, X., Huang, Y., Jia, Z., Liu, H., Song, T., Wang, Y., Shi, L., Song, C., Wang, Y., 2008. Effects of the conversion of marshland to cropland on water and energy exchanges in northeastern China. *J. Hydrol.* 355, 181–191. doi:10.1016/j.jhydrol.2008.03.019
- Zhou, M.C., Ishidaira, H., Hapuarachchi, H.P., Magome, J., Kiem, A.S., Takeuchi, K., 2006. Estimating potential evapotranspiration using Shuttleworth Wallace model and NOAA-AVHRR NDVI data to feed a distributed hydrological model over the Mekong River basin. *J. Hydrol.* 327, 151–173. doi:10.1016/j.jhydrol.2005.11.013

- Ziemer, R.R., 1979. Evaporation and transpiration. *Rev. Geophys.* 17, 1175–1186. doi:10.1029/RG017i006p01175
- Zimmermann, U., Ehhalt, D., Muennich, K.O., 1967. SOIL-WATER MOVEMENT AND EVAPOTRANSPIRATION: CHANGES IN THE ISOTOPIC COMPOSITION OF THE WATER., in: Conference on Isotopes in Hydrology. IAEA, Vienna, Vienna, pp. 567–585.
- Zou, J., Huang, Y., Jiang, J., Zheng, X., Sass, R.L., 2005. A 3-year field measurement of methane and nitrous oxide emissions from rice paddies in China: Effects of water regime, crop residue, and fertilizer application. *Global Biogeochem. Cycles* 19, n/a–n/a. doi:10.1029/2004GB002401

List of publication

Peer Reviewed

(1) A water productive and economically profitable paddy rice production method to adapt water scarcity in the Vu Gia-Thu Bon river basin, Vietnam (Published 2013)

Nay-Htoon, Bhone; Nguyen Tung Phong; Sabine Schlüter ; Aldas Janaiah.

J. Nat. Resour. Dev. 03, 58–65. doi:10.5027/jnrd.v3i0.05

(2) Flux partitioning reveals trade-off between water and carbon loss of paddy and rainfed rice (*Oryza sativa* L.)

Nay-Htoon, Bhone; Xue, Wei; Dubbert, Maren; Lindner, Steve; Cuntz, Matthias; Ko, Jonghan; Tenhunen, John ; Werner, Christiane

(Submitted to Agriculture and Forest Meteorology; Under Review)

(3) Tracing the allocation of water in rainfed rice ecosystem by partitioning evapotranspiration of rainfed rice (*Oryza Sativa* L.)

Nay-Htoon, Bhone; Xue, Wei; Dubbert, Maren; Cuntz, Matthias; Ko, Jonghan, Tenhunen, John; Werner, Christiane

(In preparation)

(4) Nutritional and developmental influences on components of rice crop light use efficiency

Wie Xue; **Bhone Nay-Htoon**; Steve Lindner; Maren Dubbert; Dennis Otieno; Jonghan Ko; Hiroyuki Muraoka; Christiane Werner; John Tenhunen; Peter Harley

(Submitted to Agricultural and Forest Meteorology; Under Review)

(5) Differentiations in paddy versus rainfed rice in factors influencing carbon gain, water use and grain yield in monsoon region South Korea

Wei Xue; **Bhone Nay-Htoon**; Maren Dubbert; Jonghan Ko; Christiane Werner; John Tenhunen

(In preparation)

(6) Comparing CO₂ exchange and productivity of transplanted paddy and direct seeded rainfed rice production system in S. Korea

Lindner, Steve, Xue, Wei, **Nay-Htoon, Bhone**, Choi, Jinsil, Ege, Yannic, Lichtenwald, Nikolas, Fischer, Fabian, Ko, Jonghan, Werner, Christiane, Tenhunen, John, Otieno, Dennis

(In preparation)

Conference contribution

(1) Partitioning Evapotranspiration of rainfed dryland rice (*Oryza Sativa* L) based on the stable oxygen isotope ratio of evaporative fluxes

Nay-Htoon, B; Dubbert, M; Ko, J.; Werner, C.

Asiaflux Workshop 2013, Seoul, South Korea. (Talk)

(2) Seasonal and spatial variations of water use efficiency of rice (*Oryza Sativa*): from the leaf to the ecosystem

Nay-Htoon, Bhone; Xue, Wei; Dubbert, Maren; Lindner, Steve; Tenhunen, John; Ko, Jonghan; Werner, Christiane

Asiaflux Workshop 2014, International Rice Research Institute, the Philippines. (Talk)

(3) Water use efficiency and productive water loss of rice (*Oryza Sativa*): partitioning seasonal water and carbon fluxes of paddy and rainfed rice

Nay-Htoon, Bhone; Xue, Wei; Dubbert, Maren; Lindner, Steve; Tenhunen, John; Ko, Jonghan; Werner, Christiane

BayCEER Workshop 2014, University of Bayreuth. (Talk)

(4) Seasonal and spatial variations of carbon and water fluxes of rice (*Oryza Sativa*)

Nay-Htoon, Bhone; Xue, Wei; Dubbert, Maren; Lindner, Steve; Tenhunen, John; Ko, Jonghan; Werner, Christiane

Biogeomon 2014 Conference, University of Bayreuth. (Poster)

(5) Carbon and water cycling in flooded and rainfed rice (*Oryza Sativa*) ecosystem: Disentangling agronomical and ecological aspects of water use efficiency

Nay-Htoon, Bhone; Xue, Wei; Dubbert, Maren; Lindner, Steve; Cuntz, Matthias; Ko, Jonghan, Tenhunen, John; Werner, Christiane

European Geoscience Union Assembly 2015, Vienna, Australia (Poster)

(6) Tracing the allocation of water in rainfed rice ecosystem by partitioning evapotranspiration of rainfed rice (*Oryza Sativa* L.)

Nay-Htoon, Bhone; Xue, Wei; Dubbert, Maren; Cuntz, Matthias; Ko, Jonghan, Tenhunen, John; Werner, Christiane

European Geoscience Union Assembly 2015, Vienna, Australia (Poster)

(7) Bottom-up biophysical mechanisms responsible for inter-seasonal variations of ecosystem carbon and water fluxes in rice crop

Wei Xue; **Bhone Nay-Htoon**; Jonghan Ko; Christiane Werner; John Tenhunen

Workshop on the ecosystem carbon/water cycling research in the changing climate, April 2015, NIES, Tsukuba, Japan (Talk)

Theses

(1) Effects of different substrate on acclimatization of medicinal orchid, *Dendrobium fimbriatum* invitro seedlings

Nay-Htoon, Bhone

Bachelor thesis submitted to the Yezin Agricultural University, Myanmar. Submitted in 2007.

(2) Direct seeded and water saving summer rice productions

Nay-Htoon, Bhone, et al.

Bachelor graduation term paper submitted to the Yezin Agricultural University, Myanmar. Submitted in 2007.

(3) Modelling Economically Profitable and Higher Water Productive Paddy Rice Production Practices to Adapt Water Scarcity in Vu Gia-Thu Bon Riber Basin, Vietnam

Nay-Htoon, Bhone

M.Sc. thesis submitted to the ITT of Fh. Köln. Submitted in 2012)

Curriculum Vitae

Name : Bhone Nay-Htoon
Born : 03.04.1987
Nationality : Myanmar (Burmese)
Contact : bhonene@gmail.com / +49 01577 1983559 / +95 9 9 7206 7232

Education

2012 : M.Sc. (Fh. Köln)
2007 : B.Agr.Sc. (Yezin Agricultural University, Myanmar)
2003 : State Matriculation Exam certificate (equivalent to Highschool Final)

Research and work experiences

2014- 2015 : Scientific Assistant at the Department of Agroecosystem Research
2012 –2015 : Member of TERRECO project of the BayCEER, University of Bayreuth
2011-2012 : Member, LuCCi project of the ITT of Fh. Köln. Did parts of M.Sc. study and thesis in Vietnam
2009-2010 : Junior Agronomist
Welthungerhilfe Myanmar, Bogalay office.
2008-2009 : Agricultural trainer
Golden plain agricultural cooperative society Ltd., Yangon, Myanmar
2007-2008 : Assistant farm manager
Model contract farm, Nawaday Sugarmill, Pyay, Myanmar.

Versicherungen und Erklärungen

(8 S. 2 Nr. 6 PromoO)

Hermit erkläre ich mich damit einverstanden, das die elektronische Fassung meiner Dissertation unter Wahrung meiner Urheberrechte und des Datenschutzes einer gesonderten Überprüfung hinsichtlich der eigenständigen Anfertigung der Dissertation unterzogen werden kann.

(8 S. 2 Nr. 8 PromoO)

Hermit erkläre ich eidesstattlich, dass ich die Dissertation selbständig verfasst und keine anderen als die von mir angegebenen Quellen und Hilfsmittel benutzt habe.

(8 S. 2 Nr. 9 PromoO)

Ich habe die Dissertation nicht bereits zur Erlangung eines akademischen Grades anderweitig eingereicht und habe auch nicht bereits diese oder eine gleichartige Doktorprüfung endgültig nicht bestanden.

(8 S. 2 Nr. 10 PromoO)

Hermit erkläre ich, dass ich keine Hilfe von gewerbliche Promotionsberatern bzw. –vermittlern in Anspruch genommen habe und auch künftig nicht nehmen werde.

Ort, Datum, Unterschrift